Check for updates

Advanced Healthcare Materials

ADVANCED HEALTHCARE MATERIALS
www.advhealthmat.de

REVIEW OPEN ACCESS

Laser-Assisted Processing and Modification of Bioactive Glasses: A Review

Antonio Riveiro[1,2,3] | Mario González-Quintas[1] | Mónica Fernández-Arias[1,3,4] | Jesús del Val[1] | Félix Quintero[1,3,4] | Rafael Comesaña[1,2,3] | Fernando Lusquiños[1,3,4] | Julian R. Jones[5] | Juan Pou[1,3,4]

[1]LaserON, CINTECX, University of Vigo, Vigo, Spain | [2]Materials Engineering, Applied Mechanics and Construction Department, E.E.I., University of Vigo, Vigo, Spain | [3]Galicia Sur Health Research Institute (IIS Galicia Sur), Vigo, Spain | [4]Applied Physics Department, E.E.I., University of Vigo, Vigo, Spain | [5]Department of Materials, Imperial College London, London, UK

Correspondence: Antonio Riveiro (ariveiro@uvigo.gal) | Juan Pou (jpou@uvigo.es)

Received: 22 July 2025 | **Revised:** 9 March 2026 | **Accepted:** 16 March 2026

Keywords: bioactive glass | laser-assisted additive manufacturing | laser processing | laser surface engineering

ABSTRACT

Bioactive glasses and lasers have followed a relatively similar path. Lasers and bioactive glasses began their journey in the second half of last century. It was in 1960 when Dr. Theodore H. Maiman constructed the first laser and fascinated the world with that marvellous ray. It was in 1967 when a young associate professor, Larry L. Hench, was addressed by a colonel returned from Vietnam, that asked him about developing a material that could help his soldiers recover from severe bone injuries. Two years later, the first bioactive material, the Bioglass, was launched. From there, the development of lasers and bioactive glasses has been extraordinaire. From the very first laser, the red ruby laser, different types of lasers in terms of wavelength, power, mode of functioning, etc. have been developed during the last decades. In a similar way, starting with the 45S5 silicate-based Bioglass many different bioactive glass formulations, including distinct active ions have been explored. This paper attempts to provide insight into these points of interaction, where the application of different types of lasers on distinct formulations of bioactive glass has allowed the transformation of bioactive glass for use as coatings, as three-dimensional implants, or the production of nanofibers.

1 | Introduction

1.1 | Bioactive Glasses and Their Relevance

Bioactive glasses are a class of biomaterials developed in the late 1960s to overcome the limitations of traditional materials, particularly their poor ability to form strong biological bonds with tissues [1, 2]. Since the development of the first bioactive silicate glass, many other bioactive compositions have been produced, not only within the silica-based family but also in alternative systems such as borate and phosphate glasses. [3]. Bioactive glasses stand out for their ability to interact with biological tissues, particularly bone, to promote healing and regeneration [4]; however, they also find applications in soft tissues [5]. They bond easily with hard and soft tissues without showing the classical fibrous tissue formation exhibited by metals and polymers. The key of their bioactivity lies in the surface reactions occurring when exposed to physiological fluids [6, 7]. In this situation, bioactive glasses degrade in contact with fluids [7]. The degradation rate strongly depends on the composition of the bioactive glass, measured in terms of the network connectivity [3, 8, 9]. Through a series of surface reactions, a hydroxyapatite-like layer, a compound similar to the mineral component of bone, is formed onto these glasses [7, 10]. This layer makes easier the cell attachment, proliferation and tissue integration [11, 12]. As the bioactive glasses degrade, they release different ions which can trigger different cell reactions

This is an open access article under the terms of the Creative Commons Attribution-NonCommercial License, which permits use, distribution and reproduction in any medium, provided the original work is properly cited and is not used for commercial purposes.
© 2026 The Author(s). *Advanced Healthcare Materials* published by Wiley-VCH GmbH

[1–3]. In consequence, bioactive glasses are excellent platforms to be doped with therapeutic ions which can stimulate the cellular activity, and be relevant, for example, to promote angiogenesis [13], osteogenesis [14], or also to promote the antibacterial activity [15] (see the review papers [16–18] for more information on the biological response to therapeutical ions released by bioactive glasses).

With these advantages, bioactive glasses have found a substantial number of medical applications, for example, in orthopedics, craniomaxillofacial surgery or dentistry [19]. Applications in these fields include their utilization as bone defect fillers [20], in the treatment of dentin hypersensitivity [21] or in wound dressings [5]; however, emerging applications beyond these traditional uses are constantly provided, such as in cartilage regeneration [22], coatings for metallic implants [23], or as a part of bioinks [24].

1.2 | Relevance of Processing Technologies for Transforming Bioactive Glasses

Bioactive glasses are very versatile, and customizable for biomedical purposes; however, their processing and transformation is also a key step to expand and offer new and innovative solutions for complex clinical challenges. Typically, these materials are produced by two main methods: melt-quenching method or the sol-gel process [25]. As they are synthesized, bioactive glasses are transformed to suit the necessities for specific applications. For example, they are used in particulate form for bone filling applications [20]. The application of conventional processing and transformation technologies, such as casting, grinding, melt-spinning, etc. strongly restricts the potential final formats of glasses, and in consequence their potential applications. By using these conventional methods, only bulky parts with a low complex geometry, particles, or fibers (with diameters up to micrometric size) are possible to be produced. More recent processing technologies, such as additive manufacturing, electrospinning, or foaming technologies among others can be of interest. They let us explore potential and novel applications, such as tailored implants for personalized medicine, porous scaffolds for bone tissue engineering, fibers for wound healing, or nanoparticles for drug delivery applications [26, 27].

1.3 | Relevance of Lasers for Processing Bioactive Glasses

Among the wide range of available processing and transformation techniques, laser-based methods stand out as particularly unique and highly attractive for application to bioactive glasses. Lasers not only enable conventional operations such as cutting, drilling, or coating, but also allow the development of novel and distinctive processes that are not achievable with other technologies [28]. Lasers can be used for precise shaping and surface modification of bioactive glasses. Laser ablation can create intricate patterns, enhance surface roughness, or improve the bonding of bioactive glass coatings on implants [29, 30]. Laser-assisted additive manufacturing (e.g., selective laser melting) is also employed to fabricate complex 3D scaffolds for bone tissue engineering [31]. Laser technology offers unique advantages as compared to other techniques for processing and transforming bioactive glasses (see Table 1) [32, 33]. Notice that these properties are general and should be particularized for each process. Technology competitors for each laser technique may show distinct advantages which can be relevant for the type of processing (e.g. simplicity, operational costs, etc.) and the final biomedical application. It is important to highlight that, although laser technology provides general advantages over many conventional manufacturing methods (discussed below), these advantages should be interpreted with caution, since each laser-based process must be evaluated individually. The specific benefits and limitations should be assessed in relation to the specific competing technologies available for the intended application (coating, surface texturing, additive manufacturing, etc.), as these may offer advantages (such as simplicity or lower operational costs, etc.) that may become relevant.

TABLE 1 | Advantages/disadvantages of using lasers for processing bioactive glasses.

Advantages	Disadvantages
High precision	High costs
No contact	Thermal stresses
Localized heating	Specialized Training
High versatility in processes, materials, and geometries	
High processing speed	
High efficiency	
Customization	
Minimal waste	

Laser technology stands out for its high precision as the deposition of energy is highly localized [34]. This could be of interest for creating intricate micro-or nano-designs, such as for complex scaffolds, or surface modifications aimed to promote cell adhesion and tissue integration. Moreover, as the deposition of energy is localized, the thermal damage of the surrounding materials is minimized.

Another advantage of laser processes is their high efficiency. Laser processes typically are performed at very large processing speeds with minimal wastage of materials to be processed. For example, processing speeds in laser cutting, can reach several meters per minute, and the waste of material is restricted to kerfs with typical dimensions in the micrometric range [35, 36].

Laser processing is a non-contact technique. In this way, the risk of damage (critical when processing brittle materials such as bioactive glasses), contamination of the processed part (crucial for biomedical materials, where sterility and structural integrity should be guaranteed), and tool wear is reduced, negligible or suppressed.

The versatility of laser technology for processing bioactive glasses, as in other materials, is very wide. One tool can be used for multiple processes, conventional (such as laser cutting, drilling, or ablation) or unconventional (such as laser spinning [37]).

21922659, 2026, 20, Downloaded from https://advanced.onlinelibrary.wiley.com/doi/10.1002/adhm.202503610 by Julian Jones - Cochraneitalia , Wiley Online Library on [06/08/2026]. See the Terms and Conditions (https://onlinelibrary.wiley.com/terms-and-conditions) on Wiley Online Library for rules of use; OA articles are governed by the applicable Creative Commons License

Also, one tool is suitable for many potential materials, e.g. different glass systems (such as silicate, phosphate or borate bioactive glasses), and for simple or complex geometries (planar or three-dimensional).

Finally, a key advantage of laser technology for biomedical applications of bioactive glasses is the possibility of customization. Laser processing enables the precise modification or fabrication of patient-specific implants and devices with controlled geometries, thereby supporting truly individualized medical solutions.

As with other processing and transformation technologies, laser-based methods also present certain limitations, particularly when producing glass components or coatings. As noticed in Table 1 the most relevant disadvantages associated with laser technologies are the higher costs (of equipment and maintenance), and the potential generation of thermal stresses in laser treated samples which can lead to surface or sub-surface cracking. In both cases, the impact can be moderated as typical costs of laser technology have been substantially reduced in recent years. On the other hand, thermal stresses, with a very deleterious impact in brittle materials such as bioactive glasses, can also be reduced by adjusting the processing parameters (see Section 2.2). Then, these can be minimized or even suppressed. Minor disadvantages of these processing technologies are related to the requirement of specialized training for technicians and personnel using this technology. However, in general, advantages related to laser technology greatly overcome all these disadvantages.

In summary, laser technology excels in precision, versatility, and customization, making it ideal for complex or personalized biomedical applications; then, this technology has great potential for the laser surface transformation (e.g. laser surface engineering) and manufacturing of novel and new bioactive glass products (such as bioactive glass nanofibers and nanoparticles); however, to the best of the authors' knowledge, the current literature lacks any critical review of the state of the art regarding the use of lasers for transforming bioactive glasses or producing new bioactive glass–based products.

In this paper, we review the major applications of laser technology in the synthesis and processing of bioactive glass products. First, we have summarized the optical response of bioactive glasses to the laser radiation (both, in the linear and non-linear regimes) and the main laser-induced phenomena occurring during laser materials processing of bioactive glasses. Their introduction is crucial for understanding the particularities of laser processing of bioactive glasses, as the optical response determines the optimum laser source and the laser-induced phenomena impose limitations and challenges (but also can provide new opportunities) for processing these materials. Next, we have reviewed the most relevant research works dealing with the surface engineering of bioactive glasses (production of thin and thick coatings by laser cladding or Pulsed Laser Deposition (PLD); laser texturing or structuring), additive manufacturing of bioactive glass parts (produced by Selective Laser Sintering (SLS)/ Selective Laser Melting (SLM) and other laser-based methods), as well as the synthesis of bioactive glass-derived nanomaterials.

2 | Optical Properties and Laser-Induced Phenomena During Laser Processing of Bioactive Glasses

2.1 | Absorption of Laser Radiation by Bioactive Glasses

Glass has been used since ancient times for its optical properties, largely because silica is transparent in the visible spectrum. However, this transparency becomes a disadvantage in laser materials processing, where low absorption of the laser radiation limits energy deposition. Since the first step in any laser-based processing technique is the absorption (and, in most cases, the subsequent thermalization) of the laser energy by the material, selecting an appropriate laser wavelength for the specific process is crucial.

The absorption of laser radiation in glasses can be classified into linear and non-linear regimes, depending on whether the absorption coefficient is independent of the optical intensity or varies with it. Both regimes have been exploited, and find application during laser processing of bioactive glasses.

2.1.1 | Linear Absorption

The linear absorption of laser radiation in glasses mainly depends on their chemical composition and on the laser wavelength. Most oxide glasses are highly transparent across a broad spectral range (see Figure 1a), typically from ∼200–300 nm in the ultraviolet (UV) to ∼2–3.5 μm in the infrared (IR) regions of the spectrum [38]. Within this interval, their transparency usually exceeds 80%, resulting in very low absorption. At shorter or longer wavelengths (such as those produced by excimer or CO_2 lasers), light can couple more efficiently into the material. Absorption in the UV–visible range is governed by electronic transitions, whereas in the mid-infrared (≈2–14 μm) it is dominated by vibrational transitions [25].

The optical properties of glasses are highly sensitive to factors such as composition, impurities, degree of crystallinity, point defects, inclusions, bubbles, temperature, and even the manufacturing process, which affects surface quality [39]. Once radiation is absorbed, it is rapidly thermalized, leading to heating, melting, evaporation, or even plasma formation within the interaction zone. Further details can be found in specialized references such as [40, 41].

2.1.1.1 | UV Absorption. Even transparent bioactive glasses cannot transmit laser radiation at wavelengths shorter than a threshold called ultraviolet edge. For silica glass this cutoff is located at ∼ 160 nm; however, this value is an orientation as it is modified by the glass composition, impurities or defects. It was noticed that presence of Fe^{3+}, Cr^{3+}, and Ti^{3+} ions shift this value into the visible (Vis) range [39]. A similar observation is found with the increment of the alkali content [44]. Moreover, defects and impurities can also induce absorption bands located in the UV to Vis regions of the spectrum. For example, oxygen deficiency is related to absorption bands located in the UV region (λ∼190 – 250 nm), while impurities (often related to transition

21922659, 2026, 20, Downloaded from https://advanced.onlinelibrary.wiley.com/doi/10.1002/adhm.202503610 by Julian Jones - Cochraneitalia , Wiley Online Library on [06/08/2026]. See the Terms and Conditions (https://onlinelibrary.wiley.com/terms-and-conditions) on Wiley Online Library for rules of use; OA articles are governed by the applicable Creative Commons License

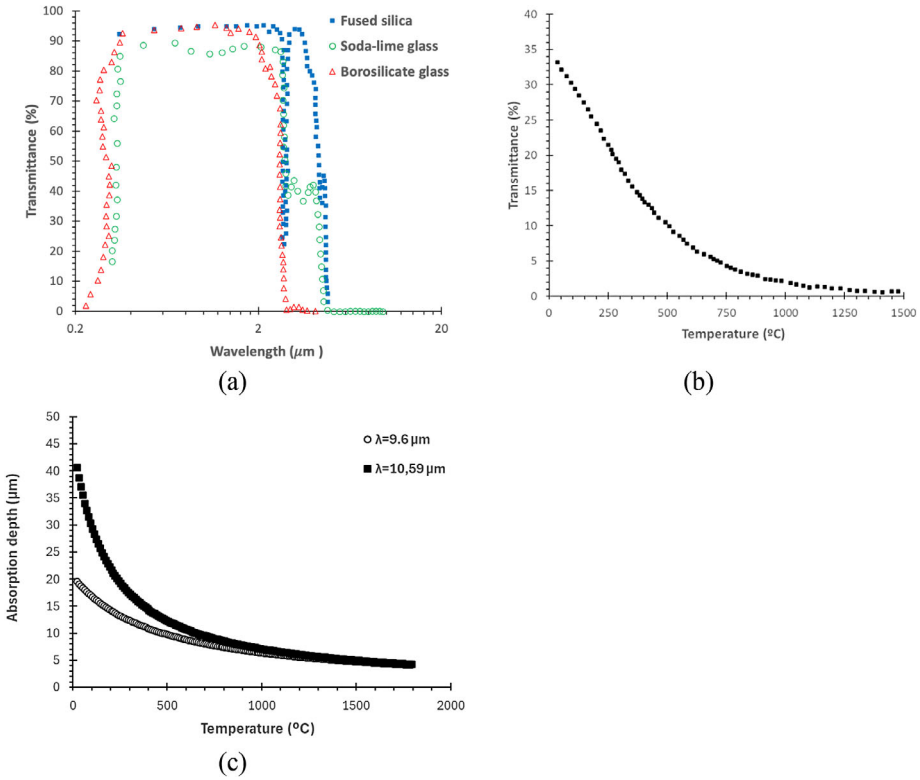


FIGURE 1 | (a) Transmission spectra for some common glasses. Data extracted from Ref. [42]. (b) Variation of the transmittance with the temperature for fused silica at $\lambda = 10.6$ μm. Data extracted from Ref. [43]. (c) Absorption depth for fused silica glass at $\lambda = 9.6$ and 10.6 μm calculated using the expression $\delta = \lambda/4\pi k$ (where λ is the laser wavelength, and k is the extinction coefficient of the glass). Data from the extinction coefficient were extracted from Ref. [43].

metals ions) give wide absorption bands extending from UV to Vis wavelengths.

2.1.1.2 | IR Absorption. In the IR part of the spectrum, silica glasses are opaque for wavelengths larger than 3.5–5 μm. For these glasses, the absorption takes place in a very thin outer layer of the surface. Typically, the absorption depth is around 10–40 μm for CO_2 laser radiation (10.6 μm) at room temperature [45, 46]. The major absorption bands of oxide glasses in the IR region occur at approximately 9.0–9.5 μm (asymmetric stretching vibration of Si–O–Si bridges), ~12.5 μm (symmetric stretching vibration of Si–O–Si), and ~21–25 μm (O–Si–O bending modes) [47]. For laser-based materials processing, only the first two bands are technologically relevant, as they lie close to the operating wavelengths of industrial CO and CO_2 laser sources.

2.1.1.3 | Influence of the Temperature. The optical properties of glasses change significantly with temperature, a factor that becomes critical during laser materials processing -particularly in low-power laser surface treatments such as laser texturing, where maximizing absorption is essential. McLachlan and Meyer demonstrated that the transmittance of fused silica drops sharply with increasing temperature (Figure 1b), falling from about 30% at room temperature to nearly zero above 1000°C [43]. Consequently, laser absorption rises, but the optical absorption depth decreases. As shown in Figure 1c, this depth contracts to roughly 5 μm at temperatures approaching 1800°C, largely independent of the laser wavelength. It is also observed that absorption is stronger at the surface for long-wavelength laser radiation, whereas shorter wavelengths penetrate deeper into the material. In this latter case, absorption shifts from being predominantly superficial to more volumetric.

2.1.2 | Non-Linear Absorption

Non-linear absorption phenomena can also take place during laser processing. This depends on the laser intensity, since the optical transparency of the material changes with this parameter [48]. These mechanisms enable the modification of the surface or bulk of bioactive glasses using laser wavelengths for which the material shows no linear absorption (e.g. using Vis laser sources). In such cases, energy is deposited by promoting electrons from the valence band to the conduction band [49]. Laser radiation can therefore be absorbed even at wavelengths where the glass is normally transparent, through laser-induced optical breakdown. This breakdown is driven by non-linear processes such as multi-photon absorption and avalanche ionization [50]. The intensities required for optical breakdown in glasses are typically on the order of 10^{13} W/cm^2 (e.g., $>2.8 \times 10^{13}$ W/cm^2 for soda-lime glass and $>1.0 \times 10^{13}$ W/cm^2 for fused silica) [51]. Such high intensities are readily achieved in ultrashort-pulse laser processing using picosecond or femtosecond sources [52].

Because these mechanisms are strongly non-linear, absorption occurs only within the focal volume (on the order of μm^3). As a result, laser processes relying on non-linear absorption exhibit high spatial selectivity, and can be very interesting for micro-machining or the precise treatment of the surface of bioactive glasses.

21922659, 2026, 20, Downloaded from https://advanced.onlinelibrary.wiley.com/doi/10.1002/adhm.202503610 by Julian Jones - Cochraneitalia , Wiley Online Library on [06/08/2026]. See the Terms and Conditions (https://onlinelibrary.wiley.com/terms-and-conditions) on Wiley Online Library for rules of use; OA articles are governed by the applicable Creative Commons License

2.1.2.1 | Avalanche Ionization. In transparent materials such as bioactive glasses, valence electrons are strongly bound and their ionization potential exceeds the photon energy of the laser. However, a small population of free "seed" electrons (typically in the range of 10^8–10^{10} cm^{-3}) is always present due to impurities, lattice defects [53], or thermal ionization [54]. When a seed electron interacts with the laser field, it can gain sufficient kinetic energy to ionize a bound electron via impact. This impact ionization produces two low-energy free electrons. Repetition of this cascade leads to an exponential rise in electron density, forming a plasma once the critical density is reached. At that point, the material becomes absorbing and the free electrons efficiently transfer laser energy to the lattice through collisions. Avalanche ionization is known to dominate laser-induced breakdown for pulse durations longer than ~100 fs [55]. For shorter pulses, photoionization mechanisms prevail, although multiphoton absorption can still generate the seed electrons that initiate the avalanche process [50].

2.1.2.2 | Photoionization. Photoionization corresponds to the direct promotion of electrons to the conduction band by the laser field [49] occurring through two main regimes depending on the laser frequency and intensity: multiphoton absorption and tunneling ionization [56]. At high photon frequencies, multiphoton absorption dominates, whereby an electron absorbs n photons simultaneously when the total energy ($nh\vartheta$) exceeds the bandgap (E_g) of the material [57]. At lower frequencies and sufficiently strong fields, tunneling ionization becomes predominant, as the laser field distorts the potential barrier and reduces the effective bandgap, enabling electrons to tunnel from the valence to the conduction band [49, 58]. Both processes are described by Keldysh theory [59], which predicts the dominant mechanism through the Keldysh parameter γ: multiphoton absorption for $\gamma > 1.5$, tunneling for $\gamma < 1.5$, and a mixed regime when $\gamma \approx 1.5$.

2.2 | Laser Induced Phenomena During Laser Irradiation of Bioactive Glasses

In addition to the well-known laser-induced phenomena occurring during laser materials processing (vaporization, recoil pressure, etc.) [60], laser processing of bioactive glasses shows some associated specific phenomena, in particular: crystallization, and thermal stresses.

2.2.1 | Crystallization

Crystallization of glass involves the transformation of amorphous glass into a crystalline state [25]. This is relevant in bioactive glasses as crystallization compromises severely the bioactivity [61] and the degradation rate [62].

In general, crystallization is considered undesirable in bioactive glasses because it alters their dissolution behavior and reduces their bioactivity. Crystallized glasses typically dissolve more slowly, and the formation of hydroxycarbonate apatite (HCA) in SBF is delayed when immersed into SBF, then, producing a noticeable retardation of in-vitro bioactivity [63]. Surface crystallization can also impair biological response by inhibiting protein adsorption and inducing unfavorable protein conformations for cell attachment, thereby limiting adhesion and spreading [64]. However, these effects depend strongly on composition and should be studied. In phosphate-rich glasses, crystallization may be beneficial because it can generate phosphate phases (including apatite) that are inherently bioactive, as noted by Brauer [3]. Moreover, as highlighted by Montazerian et al. [65], controlled crystallization can be deliberately used to enhance the mechanical properties of bioactive glasses and to modulate their reactivity, dissolution rate, and overall durability.

During laser processing, crystallization occurs when the temperature of the laser-irradiated region reaches temperatures higher than the glass transition (typically in the range of T_g = 500–600°C in bioactive silicate glasses) or crystallization ((typically in the range of T_g = 700–900°C in bioactive silicate glasses)) temperature [25, 66, 67]. Notice that heat dissipates very fast from the interaction region by conduction to the bulk [68, 69]. In consequence, high interaction times, and the utilization of continuous wave (CW) lasers (lasers that deliver a constant amount of energy along time), would be expected to be suitable for laser-induced crystallization in glass; however, it has been demonstrated that many other laser sources can be used. Laser-induced crystallization in glass was demonstrated using pulsed laser sources: such as nanosecond- and even femtosecond laser sources (nanosecond lasers are laser sources that deliver the energy in a pulsed manner along time, being the pulse duration in the nanosecond range; whereas femtosecond lasers are similar pulsed lasers but with the duration of the pulses in the femtosecond range) [70]. The only requirement when using pulsed sources is that time between pulses should be shorter than that required to avoid a substantial cooling due to heat diffusion from the interaction region (typically, in the order of ns for fs-laser processing of high thermal diffusive materials such as gold [71]; for bioactive glasses is expected a higher time). Notice that using fs-laser sources laser-induced crystallization can be performed into the bulk of glass parts [72], in contrast to using CW laser sources where the typical absorption takes place only in the surface [66]. In this way, heat is only accumulated into the focal volume, and the fs laser processing of glass is considered a highly space selective process.

Laser-induced crystallization has not been studied or exploited in bioactive glasses, but it has been observed in some laser processes involving bioactive glasses (see Figure 2), such as in selective laser sintering [73, 74] and in laser cladding [75]. The influence of laser-induced crystallization on the bioactivity, ion release, and overall biological performance of bioactive glasses remains largely unexplored. This approach offers a promising route to tailor, either locally or at the macroscale, key properties such as mechanical behavior, reactivity, dissolution rate, and consequently the release of therapeutic ions into the biological environment.

2.2.2 | Thermal Stresses

During laser processing of bioactive glasses large stresses and strains of thermal nature can appear. Thermal stresses arise due to the large thermal gradients in the laser irradiated region. Laser irradiation induces the sudden thermal expansion of the irradiated material (tensile stresses); as the laser beam moves, the

21922659, 2026, 20, Downloaded from https://advanced.onlinelibrary.wiley.com/doi/10.1002/adhm.202503610 by Julian Jones - Cochraneitalia , Wiley Online Library on [06/08/2026]. See the Terms and Conditions (https://onlinelibrary.wiley.com/terms-and-conditions) on Wiley Online Library for rules of use; OA articles are governed by the applicable Creative Commons License

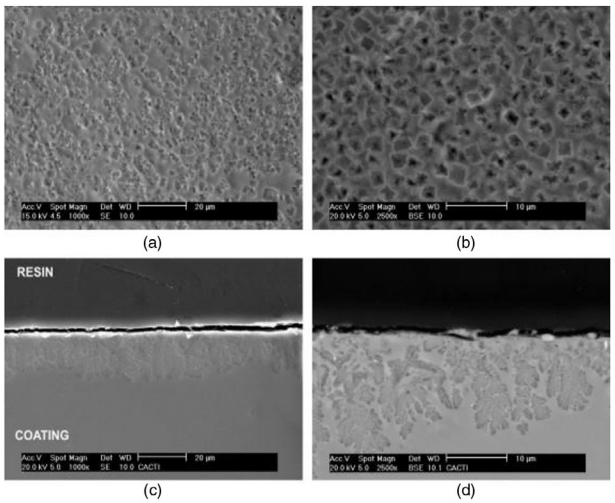


FIGURE 2 | (a) SE- and (b) BSE-SEM micrographs of the surface of a S520 bioactive glass coating produced laser cladding showing partial crystallization. (c) SE- and (d) BSE-SEM images of the cross section showing that crystallization is restricted to the surface of such coatings. Images extracted from Ref. [75] and reprinted with kind permission of Elsevier.

irradiated material suffers also a dramatic temperature reduction and consequently a contraction (compressive stresses) takes place [76]. Notice that the laser irradiated volume is constrained by the surrounding cooler material [77]. This expansion and contraction (cycle of tensile / compressive stress) tend to induce the cracking (surface and subsurface cracking) of the irradiated area. Furthermore, in glasses, the thermal gradients across the laser-irradiated region are usually very large due to the low thermal conductivity of the material; then, stresses are even higher than those found during laser processing of materials with higher thermal conductivity, e.g. metals. This is also aggravated by the brittle nature of glasses. On the other hand, thermal stresses can lead to distortions. Planification and control of the laser scanning pattern was found to reduce (at some extent) these thermal stresses and the final distortion during laser-additively manufactured parts [78].

Thermal stresses can be determined by using the thermoelasticity theory [77]; however, their determination using analytical theories is restricted to very simple cases. In order to determine them in more realistic scenarios, FEM simulations have been developed [79].

The temporal evolution of this thermal field is controlled at a large extent by the laser pulse temporal profile [80]. In this way, processing in pulsed mode provides a more complex thermal and stress field than in CW mode.

The formation of cracks due to thermal stresses during laser irradiation can be estimated by evaluating the hoop stress, which is the dominant stress component responsible for cracking. This stress reaches its maximum at the edge of the irradiated zone (i.e., at radius r = a, where a is the beam radius). For a Gaussian laser beam, the maximum hoop stress can be approximated as $\sigma_{max} \sim \alpha E T_0$ where α is the coefficient of linear thermal expansion, E is the Young's modulus, and T_0 is the peak temperature at the center of the laser spot [81, 82]. For the 45S5 bioactive glass (Young's modulus E = 78 GPa [83] and coefficient of linear thermal expansion $\alpha = 14–15 \times 10^{-6}\ K^{-1}$ [84]) and a maximum temperature of 2000°C (typically found during CO_2 laser irradiation of glass using a spot of 4.5 mm in radius and a low laser power P = 50 W [82]), a value for the hoop stress of $\sigma_{max} \sim 218\ MPa$ is found. This stress is comparable, i.e. in the same order of magnitude, than the tensile strength of 45S5 bioactive glass fibers ($\sigma \approx$ 82-340 MPa according to Refs. [85, 86]). From this calculation we cannot state that cracking is going to happen due to thermal stress, but it is an indication of the possibility of cracking during laser processing. Furthermore, experimental evidence supports this estimation. Wu et al. [87] determined that stresses generated by laser heating correlates with the coefficient of linear thermal expansion. In this way, glasses with high values of linear thermal expansion coefficient tend to generate micro-cracks more easily. From this point of view, phosphate glasses would crack easier than silicate and borate bioactive glasses, as the phosphate glasses have a higher linear thermal expansion coefficient [88].

Laser induced thermal stress can be negative as they can produce cracks reducing the strength of the treated workpiece but also can be positive. Some laser processing techniques use them to cut very precisely glass workpieces, e.g. using laser cutting with the controlled fracture technique [89], or to remove a continuous strip of glass by laser peeling technique [76]. This approach to cutting or machining glasses has not yet been explored for bioactive glasses, and it may open the door to producing custom-shaped bioactive glass components.

2.3 | Some Remarks on the Laser Sources for Processing Bioactive Glasses

Selecting an appropriate laser source for processing bioactive glasses requires the consideration of several factors, including the absorption characteristics of the material, the spatial and temporal selectivity needed for the process, the efficiency of the laser system, and the associated investment and operating costs. Table 2 summarizes the main laser sources suitable for processing bioactive glasses.

From the standpoint of laser-energy absorption by glasses, the most suitable sources include CO_2, CO, and UV lasers (such as excimer lasers or modern frequency-quadrupled fiber lasers). As discussed in Section 2.1.1, absorption is highest in the UV and far-IR regions of the spectrum. However, since the introduction of ultrafast laser systems (ps and fs pulses), these sources have gained significant popularity because of their high spatial and temporal selectivity of energy deposition, which is particularly attractive in applications such as microfluidics [90, 91] or optical applications [57, 92]. Their effectiveness benefits from nonlinear absorption processes, as explained in Section 2.1.2. It is worth noting that CO_2 and CO lasers are generally more energy-efficient than UV excimer sources. Another interesting option for efficient UV processing is the use of frequency-tripled (THG) Nd:YAG or Nd:YVO_4 lasers.

Beyond the efficiency with which the material thermalizes the absorbed laser radiation, spatial resolution is another key factor when selecting a laser source. Smaller focal-spot sizes

21922659, 2026, 20, Downloaded from https://advanced.onlinelibrary.wiley.com/doi/10.1002/adhm.202503610 by Julian Jones - Cochraneitalia , Wiley Online Library on [06/08/2026]. See the Terms and Conditions (https://onlinelibrary.wiley.com/terms-and-conditions) on Wiley Online Library for rules of use; OA articles are governed by the applicable Creative Commons License

TABLE 2 | Laser sources used or suitable for laser processing of bioactive glasses. Type of emitted laser radiation (spectral region and operation mode), wavelength, approximated wall-plug efficiency.

Laser source	Region	Wavelength (nm)	CW/Pulsed	Wall-plug efficiency (%)
F_2 (excimer)	UV	157	Pulsed	1.5–2 [94]
ArF (excimer)	UV	193	Pulsed	1.5–2 [94]
KrF (excimer)	UV	248	Pulsed	1.5–2 [94]
Fiber (FHG)	UV	266	CW/Pulsed	
XeCl (excimer)	UV	308	Pulsed	1.5–2 [94]
Nd:YVO_4 or Nd:YAG (THG)	UV	355	Pulsed	<10 [95]
Nd:YVO_4 or Nd:YAG (SHG)	Vis	532	Pulsed	<10 [96]
Ti:sapphire	Vis-IR	680–1100	Pulsed (ultrashort)	<5 [97]
Nd:YAG	IR	1064	Pulsed	<20 [94]
Nd:YVO_4	IR	1064	Pulsed	<20 [98]
Fiber	IR	1030–1080	Pulsed	30–40 [94]
CO	IR	5500	Pulsed	10–15 [99, 100]
CO_2	IR	9300, 9600, 10600	CW/Pulsed	5–20 [94]

Abbreviations: FHG: Fourth harmonic generation; SHG: second harmonic generation; THG: Third harmonic generation.

(and therefore finer definition) are achieved when using shorter wavelengths, such as those provided by Vis or UV lasers (as the diameter of the focal spot is proportional to the wavelength $d_{spot} \propto \lambda$ [93]). High spatial selectivity can also be obtained with ultrafast laser sources, since absorption is largely confined to the focal volume where the light intensity is greatest.

3 | Laser Surface Engineering

Bioactive glasses are too brittle to be used as structural materials in load-bearing applications (e.g. dental root implant). The low fracture toughness and strength limit the use of bulk glasses to non-load-bearing implants such as filler material in bone defects, to reconstruct the middle ear and in small bone replacement. To overcome this problem, one alternative is to coat a metallic material with good mechanical properties, such as titanium alloys (e.g. Ti6Al4V [101] or Ti6Al7Nb [102]), with a layer of bioactive glass. The coating provides the bone bonding characteristics, while the metal provides the mechanical properties.

Different coatings techniques have been applied, such as sputtering [103] enameling [104], electrophoresis [105], sol-gel [106], or plasma spray [107]; however, the main problems associated to these techniques are related to the poor adhesion strength of the coating, or the substrate specificity of techniques as sol-gel, and electrophoresis. In this sense, laser surface engineering has solved some of these problems.

A major classification of the bioactive glass coatings can be done in terms of the thickness of the coated layer. In this sense, the coatings produced using a laser beam (or other coating techniques) can be ranged in two groups: (a) thin (thickness in the micrometer and submicrometer ranges), and (b) thick (thickness in the order of hundred micrometers to mm) coatings. Based on this criteria, bioactive glass coatings on different materials are studied separately in the following sections. Finally, a last section of the possibilities of laser to modify the topography of bioactive glass surfaces is introduced.

3.1 | Thick Coatings Produced by Laser Cladding

3.1.1 | Description of the Technique

Laser cladding is a comprehensive technique that utilizes laser technology, computer-aided design and manufacturing, robotics, sensors and control systems, to produce a coating of a certain material on a given substrate. Laser cladding was developed by Prof. Willian M. Steen during the 1980s while working at Imperial College London (UK) [108, 109]. In its beginnings, laser cladding technology was used for metallurgical applications in which the coating had to provide the substrate with improved wear resistance, corrosion resistance or erosion resistance properties. Laser cladding has demonstrated several advantages in the metallurgical field such as the following [28]:

- controlled shape of the clad within certain limits
- localized heating which reduces thermal distortion and the size of the heat-affected zone
- flexibility of the process
- controlled levels of dilution
- smooth surface finish, near isotropic mechanical properties, fine quench microstructures and good fusion bonding
- minimum surface preparation required
- high deposition rate.

In the biomedical field, the rationale for using this technique is to enhance the biocompatibility of the underlying substrate. In the case of bioactive glass coatings, the goal is to promote a faster and more effective osseointegration (i.e., greater bone apposition)

21922659, 2026, 20, Downloaded from https://advanced.onlinelibrary.wiley.com/doi/10.1002/adhm.202503610 by Julian Jones - Cochraneitalia , Wiley Online Library on [06/08/2026]. See the Terms and Conditions (https://onlinelibrary.wiley.com/terms-and-conditions) on Wiley Online Library for rules of use; OA articles are governed by the applicable Creative Commons License

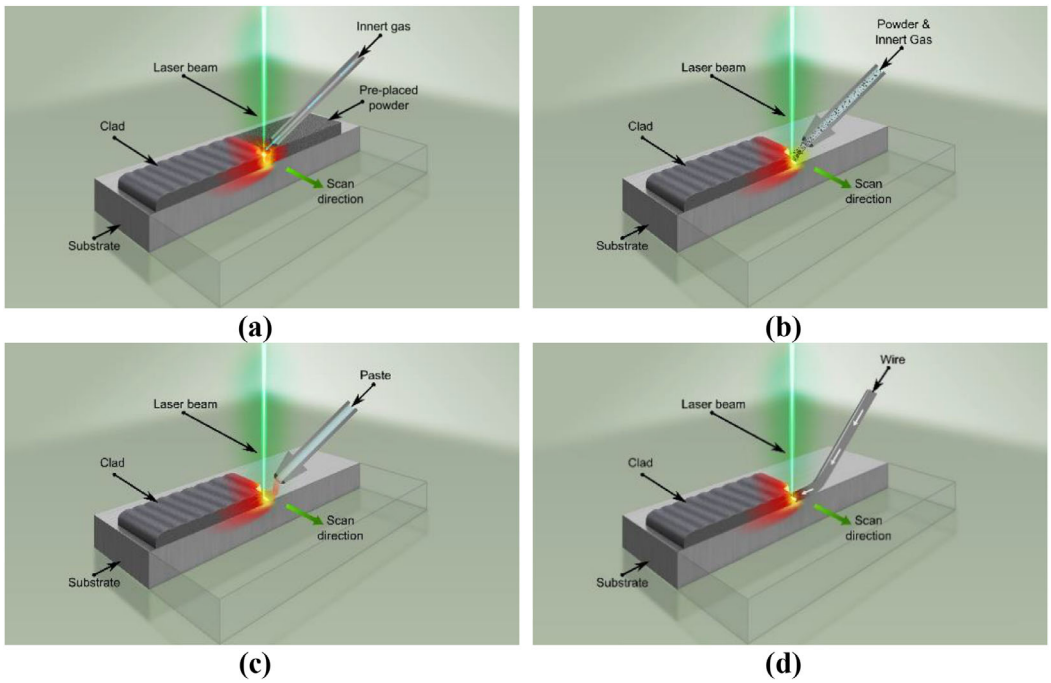


FIGURE 3 | Potential modalities of the laser cladding technique to produce bioactive glass coatings: (a) preplaced powder (two-step), (b) powder injection (one-step), (c) paste (one-step), (d) wire feed (one-step).

once the implant comes into contact with the surrounding bone tissue.

In general terms we can distinguish two modalities to carry out the laser cladding technique: A two-step process, also called pre-deposited laser cladding; and one-step process.

In the two-step process, the first phase entails the application of a precursor material layer to the substrate before the laser beam is scanned over its surface. In the second phase, the interaction of the laser beam with the surface causes both the precursor layer and the substrate surface to melt (see Figure 3a).

In the one-step procedure, an additive substance is incorporated into the molten pool created by the laser on the substrate. The precursor material may be delivered in several forms: fluidized powder injection (Figure 3b), paste (Figure 3c), and wire-fed (Figure 3d).

Among the various alternatives, powder injection has proven to be the most versatile, robust, and efficient method for supplying the precursor material necessary for the laser cladding process. In this approach, the energy emitted by the laser is utilized to melt a thin layer of the substrate, while the particles can be melted through their interaction with the laser beam or upon reaching the melting pool created on the substrate. A relative motion between the substrate and the laser/powder jet facilitates the formation of a single clad track and overlapping these tracks results in extensive area coverage. To avoid oxidation in the interaction zone during laser processing, an inert shielding gas (typically argon or nitrogen) is introduced. A rapid quenching occurs when the molten pool moves away from the area irradiated by the laser. Consequently, the result is a coating applied to the surface of the metallic substrate.

3.1.2 | Laser Cladding of Bioactive Glass Coatings

The research group led by Prof. Yli-Urpo at the University of Turku, in Finland used the two step laser cladding technique for coating titanium implants with bioactive glass through a technique involving preplaced precursor materials [110, 111]. The procedure involves roughening the surface through sand blasting and the application of bioactive glass powder blasting. Subsequently, the implant undergoes dip-coating by being immersed in a suspension of fine particles of 1–98 bioactive glass suspended in ethanol. Following this, the implant is extracted from the solution and allowed to dry. The concluding step entails scanning the implant surface with a low power CO_2 laser (merely 6–8 W) to melt the glass onto the rough titanium surface. It is evident that the extremely low laser power density achieved on the implant surface is insufficient to melt the outer layer of the implant; thus, the coating is merely secured due to the significant surface roughness.

Kuo et al. followed the two-step approach to coat Ti6Al4V substrates by means of a Nd:YAG laser delivering higher optical power (400 to 800 W) [112]. They started by spraying an emulsion of 45S5 bioglass in a water-based organic solvent. Under the processing conditions used, the coating lost the intrinsic bioactivity of the 45S5 bioglass due to Al migration from the substrate to the coating. Three primary factors contributed to the significant dilution of the substrate: first, the thickness of the pre-deposited layer; second, the specific composition of the bioactive glass; and third the laser irradiance (power density) applied. Laser cladding using pre-deposited powder is viable solely with a thin preplaced layer, so that the laser energy is able to melt a thin layer of the substrate. Usually, excessive heating takes place resulting in a extensive dilution, mixing the coating with the substrate, causing the loosening of the bioactive properties of the precursor glass.

21922659, 2026, 20, Downloaded from https://advanced.onlinelibrary.wiley.com/doi/10.1002/adhm.202503610 by Julian Jones - Cochraneitalia , Wiley Online Library on [06/08/2026]. See the Terms and Conditions (https://onlinelibrary.wiley.com/terms-and-conditions) on Wiley Online Library for rules of use; OA articles are governed by the applicable Creative Commons License

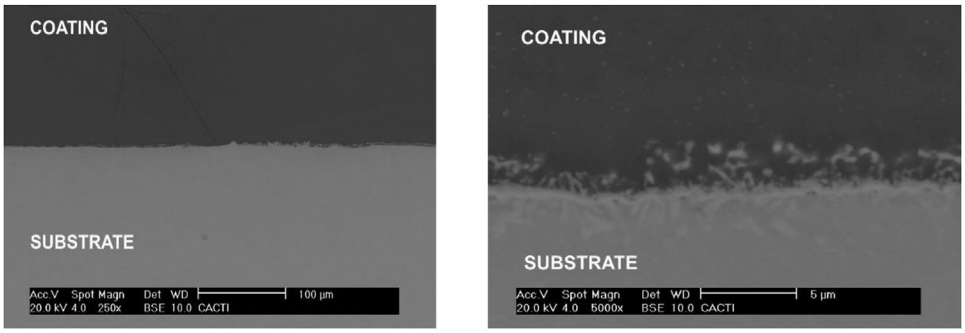


FIGURE 4 | Cross section of bioactive glass coating on Ti6Al4V titanium alloy produced by laser cladding. (a) Low magnification image showing the homogeneity of the coating; (b) detail of the coating-to-substrate interface, showing the formation of TiP (lighter particles). Extracted from Ref. [75] with kind permission of Elsevier.

Moreover, the 45S5 bioglass exhibits a limited operational range and necessitates an exact energy input to facilitate glass flow without causing overheating.

An alternative approach to improve the coating-to-substrate adhesion while ensuring the preservation of the bioactive properties of glass, is to use the one step laser cladding process injecting the precursor material as a jet of fluidized bioactive glass powder. Our group used this method to coat Ti6Al4V implants by a bioactive coating in the SiO_2-Na_2O-CaO-P_2O_5-K_2O system [75, 113–115]. Figure 4 shows a S520 bioactive glass coating applied on Ti6Al4V using a Nd:YAG laser. Overall, the coatings are uniform and with a homogeneous composition. Partial devitrification can be observed in the most superficial region of the coating due to the slower cooling rate experienced in this zone. Furthermore, TiP formation can be observed at the interface between the coating and the substrate due to the partial dilution taking place. This confirms the metallurgical bond between the coating and the substrate. In any case, the irradiance (laser power density) applied in the process must be precisely controlled so that it is not excessive and an alloy of the precursor material with the titanium substrate is obtained, instead of a proper coating [116].

The appropriateness of bioactive glasses is typically determined by their bioactivity levels [7]. The reduction in network connectivity of silicate-based BGs, accomplished through chemical modification, has enabled the enhancement of osteoconductive and osteoinductive characteristics while maintaining elevated resorbability. However, when applying the laser cladding technique, it is essential to consider additional properties, including rheological characteristics. Although the cooling rates that the material undergoes remain moderate, the circumstances differ significantly from those of glass casting, allowing for nucleation and crystal growth to occur. Bioactive glasses (BGs) with elevated bioactivity are susceptible to phase separation and devitrification as a result of diminished network connectivity [117].

For use in laser cladding, it is preferable to select bioactive glasses with compositions that present increased glass processing windows, i.e. higher temperature range between the glass softening point and the flow point. There exists an inverse relationship between the bioactivity of the glass and the width of the processing window in relation to the connectivity of the silica network; consequently, the selected glass formulation must achieve a compromise between bioactivity and the laser processing window. The Hruby (Hr) parameter has been suggested as a means to quantify the processing window; this parameter connects the stability of the glass vitreous state with the tendency for crystallization [118, 119]. Table 3 collects different glass compositions used for the laser cladding technique. Most of these glasses were developed for the production of fibers, showing a gentle change of viscosity with the temperature.

The thermal evolution of the precursor powder material during the laser cladding process is influenced by various factors, including processing speed, the temperature of the underlying material, the mass flow of precursor powder, and the flows of carrier and assist gases [123]. An uncontrolled heterogeneous thermal cycle can result in an undesirable heterogeneous microstructure in the processed component, potentially leading to failure as a consequence of thermal shock.

The relevance of substrate preheating and optimization of the working head scanning path in the laser cladding of bioactive glass was pointed out by Krzyzanowski et al. [124]. Cracking susceptibility in laser-cladded bioactive glass mainly results from the high transient thermal stresses generated during the first deposited layer and from thermal interactions between adjacent tracks. Preheating the substrate and the progressive heat accumulation in subsequent layers (during the production of multi-layered coatings) reduce cooling rates and stress peaks, significantly improving the resistance of the coating to cracking.

The laser cladding technique has been primarily used to apply a coating (in this case, bioactive glass) to a metallic substrate (e.g., titanium or Ti6Al4V in biomedical applications). However, as Baino et al. demonstrated [121, 122], the laser cladding technique can also be used on ceramic substrates. They produced bioactive glass coatings on Al_2O_3/ZrO_2 ceramic acetabular cups intended for hip joint prostheses (see Figure 5). The coatings were applied through a two-step laser cladding process. An initial layer of S57A7 inert glass is applied prior to the outer S50B2 bioactive glass layer. This S57A7 glass layer serves as a bonding bridge between the bioactive coating and the substrate, improving interfacial stability.

21922659, 2026, 20, Downloaded from https://advanced.onlinelibrary.wiley.com/doi/10.1002/adhm.202503610 by Julian Jones - Cochraneitalia , Wiley Online Library on [06/08/2026]. See the Terms and Conditions (https://onlinelibrary.wiley.com/terms-and-conditions) on Wiley Online Library for rules of use; OA articles are governed by the applicable Creative Commons License

TABLE 3 | Composition (mol%) of bioactive glasses used in laser cladding.

Designation	SiO_2	CaO	Na_2O	P_2O_5	K_2O	B_2O_5	*Hr*	References
45S5	46.1	26.9	24.4	2.6	—	—	0.28	[75, 113–115]
S520	52.0	18.0	20.9	2.0	7.1	—	0.39	[75, 120]
S50B2	50.0	35.0	7.0	6.0	—	2.0	0.37	[121, 122]
1-98	53.0	22.0	6.0	2.0	11.0	1.0	0.48	[110, 111]



FIGURE 5 | (a) S57A7 glass interlayer coating by laser cladding on a ceramic acetabular cup. (b) Detail of the final layer of S50B2 laser clad layer. *Source:* Baino et al. [121], with permission from Springer Nature.

Despite the thermal loads that bioactive glasses undergo during the laser cladding process, their bioactivity has not been compromised. As demonstrated by Comesaña et al. [75], the S520 bioactive glass coatings obtained by laser cladding exhibit a bioactivity level similar to that of the precursor powder. Following a one-day immersion in simulated body fluid (SBF), a distinctive silica-rich layer is formed, indicated by the absence of Si–O·2NBO peaks in the Fourier Transform Infrared analyses taken at the surface. After nine days of immersion in SBF, a biologic-like apatite layer was observed covering the entire coating surface [75].

Similar behavior was observed in the case of the S50B2 bioactive glass coatings produced by laser cladding on ceramic acetabular cups [121, 122]. These coatings demonstrated a strong capacity for apatite formation in vitro, exhibiting characteristic average Ca/P ratios indicative of calcium deficient apatite. Furthermore, biological assessments involving osteoblast-like cells and mesenchymal stem cells (MSCs) indicated excellent biocompatibility.

The bioactive glass coatings produced by the two-step laser cladding method, exhibited a similar ability to form apatite in SBF when compared to the precursor 1–98 bioactive glass material [110, 111]. These coatings were applied to pure Ti cylindrical implants and subsequently tested in vivo within the femoral epicondyle of rabbits. Histological analysis conducted after eight weeks indicated that the laser coated surfaces have significantly more bone surrounding the surface of the implant than those of bare metal and NaOH-treated Ti surfaces (see Figure 6).

Based on the studies conducted to date on producing thick bioactive glass coatings by laser cladding, it can be stated that the resulting coatings show good adhesion to the substrate and satisfactory performance in both in vitro and in vivo evaluations. Among potential applications, selective coating of load-bearing joint implants appears to be the most promising avenue for the use of this technique. Nevertheless, further research is required to enable the successful transfer of this technology from laboratory-scale demonstrations to the commercial manufacture of bone implants. Additional in vitro and in vivo studies on laser-cladded surfaces are needed to better understand their interaction with biological tissues. Long term studies to determine the mechanical stability and integrity of the coating are required.

3.1.3 | Comparative Analysis of Laser Cladding for Producing Thick Bioactive Glass Coatings

Table 4 summarizes the main characteristics of some techniques used to produce thick bioactive glass coatings. As shown, laser cladding offers significant advantages compared with alternative methods such as thermal spraying and sol–gel dip coating, particularly in terms of precision, compositional control, and versatility. Laser cladding offers a precise control of the melt pool and coating geometry, allowing the deposition of relatively thick and well-adhered coatings with limited dilution of the substrate. As a result, the bonding of coatings produced by laser cladding is generally higher than in thermal spraying or sol-gel dip coating. Moreover, this technique offers a good control of the thickness of the coating, ranging this from several hundred of

21922659, 2026, 20, Downloaded from https://advanced.onlinelibrary.wiley.com/doi/10.1002/adhm.202503610 by Julian Jones - Cochraneitalia , Wiley Online Library on [06/08/2026]. See the Terms and Conditions (https://onlinelibrary.wiley.com/terms-and-conditions) on Wiley Online Library for rules of use; OA articles are governed by the applicable Creative Commons License

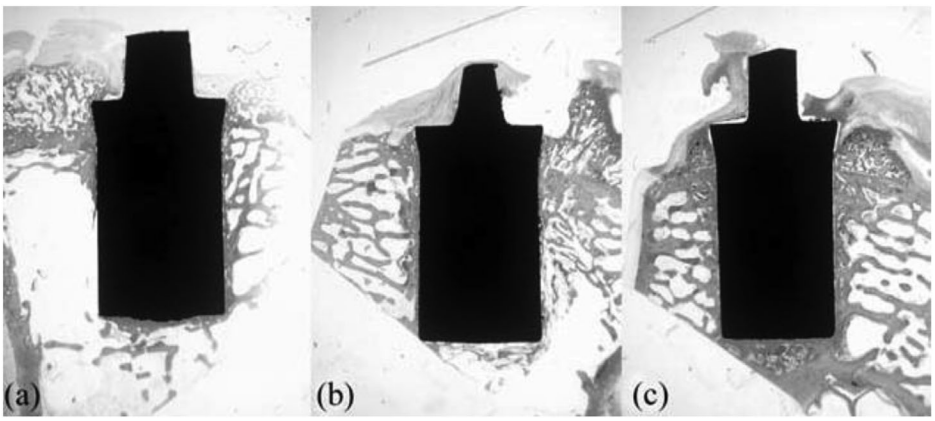


FIGURE 6 | Histological slices of Ti implants after implantation in the femur of New Zealand white rabbit. (a) Bare Ti implant, (b) NaOH-treated implant, (c) implant coated by laser cladding with preplaced 1–98 bioactive glass. *Source:* Moritz et al. [111], Figure 8 [p. 800]/with permission from Springer Nature.

TABLE 4 | Comparison of different technologies for producing glass coatings.

Feature	Laser cladding	Plasma spraying	Sol-Gel dip coating
Precision	High	Moderate	Moderate
Contact	Non-contact	Non-contact	Contact: substrate dipping required
Versatility	High	Moderate	Moderate
Speed/Efficiency	Fast	Fast	Fast
Material Waste	Minimal	Moderate	Minimal
Cost	High: equipment and maintenance	High	Low: simple equipment
Material Limitations	Problem with thermal stress	Restricted to sprayable materials	Not possible to produce sol-gel glasses with any arbitrary composition
Specialized Training	High	Moderate	Low

micrometers up to the millimeter scale in a single step, which is significantly higher than the thicknesses commonly achieved by sol–gel dip coating. Another advantage of laser cladding is the possibility of producing coatings with tailored composition, e.g. the fabrication of graded coatings [125]. This possibility has been demonstrated with enameling technique [126, 127], but it has not been explored with laser cladding (e.g. producing coatings of glasses with different resorbability). However, despite these advantages, several limitations must be considered. The main drawbacks of laser cladding are related to the relatively high capital investment and operational costs of the equipment, as well as the complexity of process optimization. Furthermore, the rapid heating and cooling cycles inherent to laser processing can generate steep thermal gradients that may induce residual stresses and promote crack formation in brittle materials such as bioactive glasses. Additionally, the high processing temperatures involved during the process may lead to partial crystallization of the initially amorphous bioactive glass used as precursor material. Preheating of the substrate and controlling the temperature of the glass part can alleviate this problem but makes the process more complex.

In contrast, thermal spraying techniques are generally more suitable for large-area coatings and industrial-scale production; however, they often produce coatings with relatively high porosity and weaker coating–substrate bonding. Similarly, sol–gel dip coating represents a simple and cost-effective approach that provides excellent compositional homogeneity and allows the preservation of the amorphous structure of the glass, but it typically yields much thinner coatings and often requires multiple coating and heat-treatment steps to achieve sufficient thickness.

3.2 | Thin Coatings Produced by Pulsed Laser Deposition (PLD)

3.2.1 | Description of the Technique

Pulsed-laser deposition (PLD) has gained a great attention over the past decades for its ease of use and success in depositing very different materials [128, 129]. This technique relies on the absorption of the pulsed laser radiation by a target material, and the consequent formation of a plume of evaporated material after its ablation (see Figure 7a) [130]. The evaporated materials mainly consist of highly excited and ionized species, but clusters and particles are also present [131]. The vapors forming the plasma plume are collected on a substrate placed at a short distance from the target (typically 2–10 cm), and a film is produced (see

21922659, 2026, 20, Downloaded from https://advanced.onlinelibrary.wiley.com/doi/10.1002/adhm.202503610 by Julian Jones - Cochraneitalia , Wiley Online Library on [06/08/2026]. See the Terms and Conditions (https://onlinelibrary.wiley.com/terms-and-conditions) on Wiley Online Library for rules of use; OA articles are governed by the applicable Creative Commons License

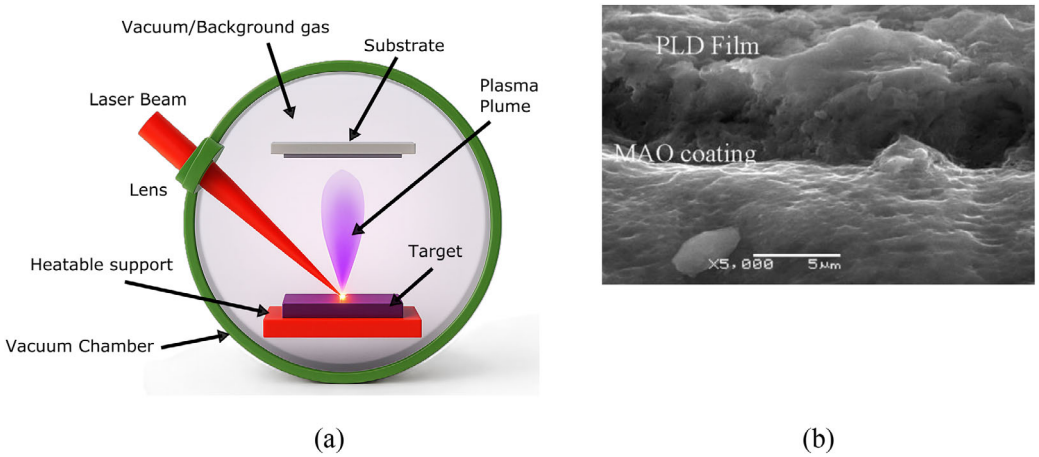


FIGURE 7 | (a) Schematic representation of a PLD setup. (b) Bioactive glass thin film produced over a Ti substrate (Extracted from Ref. [137] with kind permission of Elsevier).

Figure 7b) [132]. This laser-induced evaporation produces a plume of material with a stoichiometry similar to the target; therefore, it is possible to produce films with the same composition as the target [133]. This is a consequence of the congruent evaporation of the target, irrespectively of the boiling point of their constituents. Controlling the energy deposited on the target material (by the laser fluence and the number of pulses), it is possible to control the degree of ablation/evaporation and then the thickness of the film deposited over a substrate. Thin films or coatings produced by PLD show a strong bonding of the coating with substrate, low residual stress in the coating, and controlled roughness of the surface [130].

For producing bioactive glass coatings, the target is usually a pellet produced from pressed glass particles (with the desired composition) and subsequently sintered. Bulk glass monoliths could also be used.

PLD is typically performed in a vacuum chamber to control the processing atmosphere. The process can be performed under vacuum conditions (from ultrahigh vacuum up to the mbar range) or with a background gas [131]. Vacuum is performed by turbomolecular and backing pumps [134].

The main problem of this technique is the splashing or the particulates deposition on the films because of sub-surface boiling, exfoliation, or due to recoil pressure [133]. Despite the simplicity of this technique, many complex mechanisms and physical phenomena are involved [135]. Main parameters in PLD are: laser wavelength, pulse energy, pulse duration, gas composition and pressure in the deposition chamber, type of the target, and temperature of substrate [133, 136].

3.2.2 | Processing Parameters

Utilization of PLD to produce thin film coatings of bioactive glass with desired composition has been demonstrated in many different research works from more than two decades ago [138]. PLD is an alternative to other techniques used to produce bioactive glass coatings such as plasma spraying [139], sputtering [140], sol–gel [141] and electrophoresis deposition [142]. PLD offers great advantages for producing bioactive glass films, such as: being a non-contact technique, absence of contamination (very relevant for biomedical applications), stoichiometric coating composition, possibility of processing high-melting point materials as glasses, or a good control over the crystallinity of the glass film [143, 144].

PLD of bioactive glass films can be performed, as summarized in Table 5 using different laser sources from those reported in Section 2.3; however, it is apparent that UV radiation is one the more efficient wavelengths due to the optical response of glass. Glasses are quite transparent to the laser radiation in the visible, and near IR regions of the spectrum (as seen in Section 2.1); then, a significant absorption can occur only after the laser induces a superficial modification (defects, microcracks, etc) during the processing with these wavelengths. This explains the high ablation threshold (3.5 J/cm^2) observed during the processing with the Nd:YAG laser [145]. Coatings produced by PLD are in the micrometer range of thickness, but this value mainly depends on the laser fluence used during the process [146–148]. In general, increasing the laser fluence produces thicker films [130].

Bioactive glass coatings produced by PLD are in general highly uniform, but some small droplets embedded in a continuous matrix are occasionally observed [146]. Macroscopic particles with spherical shape and size around 0.1 μm have been observed in some cases [148]. Depending on the laser fluence and the target composition, some atomic species, but also microscopic particles ranging from 0.1 to 1 μm are generated during PLD [149].

Main relevant parameters used to control the PLD process are the laser fluence, temperature of the substrate, relative position of target with respect to substrate, ant type of processing atmosphere and pressure. Their influence during processing of bioactive glasses are as follows.

3.2.2.1 | Laser Fluence. The bioactive glass deposition rate, and then, the thickness of the coating produced by PLD is strongly dependent on the laser fluence [145, 148]. This parameter also influences the surface morphology, but the chemical structure of the film remains almost unaltered.

21922659, 2026, 20, Downloaded from https://advanced.onlinelibrary.wiley.com/doi/10.1002/adhm.202503610 by Julian Jones - Cochraneitalia , Wiley Online Library on [06/08/2026]. See the Terms and Conditions (https://onlinelibrary.wiley.com/terms-and-conditions) on Wiley Online Library for rules of use; OA articles are governed by the applicable Creative Commons License

TABLE 5 | Bioactive glass coatings obtained by PLD.

References	Target designation	Target composition (wt.%)	Substrate	Distance target – substrate (mm)	Laser source (Wavelength)	Fluence range (J/cm^2)	Repetition rate (Hz)	Temp. (°C)	Pressure (mbar)
[145]	Bioglass 45S5	(at.%) Na 38.31, Ca 21.21, Si 36.37, P 4.11	Ti4Al		Nd:YAG (1064 nm)	0.5–14	10	Room	Vacuum (10^{-4})
[150]	Bioglass 45S5	53% SiO_2, 20% CaO, 23% Na_2O, 4% P_2O_5	Ti6Al4V		ArF (193 nm)	1.41	10	Room	Vacuum (10^{-3})
			c-Si (100)						
[151]	Bioglass 45S5		c-Si (100)		ArF (193 nm)	—			
[146]	Bioglass 45S5		Ti6Al4V		Nd:YAG SHG (532 nm)	9			
[148]	Silicate glass	42% SiO_2, 20% Na_2O, 10% K_2O, 20% CaO, 3% P_2O_5, 5% MgO	Si, Ti	35	ArF (193 nm)	0.2-6	10	25-500	Vacuum (10^{-5})
[152]	Silicate glass	42% SiO_2, 20% Na_2O, 10% K_2O, 20% CaO, 3% P_2O_5, 5% MgO	Si (1 1 1)	35	ArF (193 nm)	4.2	10	200	Vacumm ($6.5{\cdot}10^{-4}$), Ar, Si_2H_6/Ar, NH_3/Ar (0.12-1.18)
[153]	Silicate glass	(42%–59%) SiO_2, (20%–10%) Na_2O, (10%–5%) K_2O, (20%–15%) CaO, (3%–0%) P_2O_5, (5%–2%) MgO, (3%–0%) B2O3	Ti		ArF (193 nm)	4.2	10	200	
[154]	Silicate glass	SiO2 57%, CaO 15%, Na2O 11%, MgO 8.5%, P2O5 6%, and K2O 3%	Ti	40	KrF (248 nm)	2	2	400–550	Films deposited in O_2 atm. at 5–15 Pa
[155]	Bioglass 45S5	53% SiO_2, 20% CaO, 23% Na_2O, 4% P_2O_5	Ti6Al4V	55 (incidence angle 45°)	ArF (248 nm)	5	10	20–200-500	Vacuum ($8.5\ 10^{-5}$)
[156]	Silicate glass	57 – 61% SiO2	Ti gr4	40 (incidence angle 45°)	KrF (248 nm)	6.6	2	400	O_2 (0.13)
[157]	Phosphate glass	P2O5–Nb2O5–CaO-(CaF2) system	Ti	30	Nd:YAG THG (532 nm)		10		Vacuum ($3{\cdot}10^{-6}$)
[158]	Silicate (13-93) & Borate (13-93B3) glasses	(5.5 Na_2O, 11.1 K_2O, 4.6 MgO, 18.5 CaO, 3.7 P_2O_5, 56.6 SiO_2) and (5.5 Na_2O, 11.1 K_2O, 4.6 MgO, 18.5 CaO, 3.7 P_2O_5, 56.6 B_2O_3)	Si (100) and Ti	20 (incidence angle 45°)	Nd:YAG SHG (532 nm)	12	10		Vacuum (10^{-4})

21922659, 2026, 20, Downloaded from https://advanced.onlinelibrary.wiley.com/doi/10.1002/adhm.202503610 by Julian Jones - Cochraneltalia , Wiley Online Library on [06/08/2026]. See the Terms and Conditions (https://onlinelibrary.wiley.com/terms-and-conditions) on Wiley Online Library for rules of use; OA articles are governed by the applicable Creative Commons License

3.2.2.2 | Temperature of Substrate. The temperature of the substrate is another parameter affecting the PLD process. Bonding configuration is largely impacted by the temperature. Using infrared spectroscopy, small variations in the amount of Si−O−NBO(s) were observed as a function of the temperature of the substrate. These were associated to a network rearrangement due to changes in the surface mobility of the ablated products during the growth process of the glass film [148].

Notice that an excessive temperature (>200°C) leads to some crystallization of the bioactive glass films [154]; this affects negatively the biocompatibility.

3.2.2.3 | Relative Position Between the Target and Substrate. The position of the substrate with regard to the plume greatly influences the surface structure of the coating. It was observed that a more uniform morphology was obtained when the substrate is placed vertical and parallel to the target [147]. Moreover, an optimum separation between target and substrate was determined to be 10 cm during the coating of a Ti6Al4V substrate with 45S5 bioactive glass [147].

3.2.2.4 | Processing Atmosphere. The atmosphere (chemical nature and pressure) of the process also has an impact on the characteristics and bioactivity of the bioactive glass films. In general, atmospheres for the production of bioactive glass coatings are an inert or a reactive gas [159]. An oxidant atmosphere (H_2O, N_2O or Ar) reduces the amount of Si–O–NBO groups in the film. A mixture of disilane/argon was seen to inhibit the formation of Si–O–NBO groups in the film [152]. The reactive silicon resulting from the photodissociated species of the disilane molecule can trap the atomic oxygen in the ablation plume. This generates SiOxHy products, which are finally incorporated in the glass film. Therefore, the depletion of the oxygen in the ablation plume prevents the formation of Si–O–NBO groups in the film. On the other hand, the presence of an ammonia atmosphere (at low pressures, 0.05 mbar) favors the formation of Si–O–NBO groups [152, 160]. This occurs because the presence of H radical (formed during the decomposition of the ammonia) in the plume avoids the saturation of the Si–O–NBO groups ablated from the target.

3.2.2.5 | Pressure. The pressure in the vacuum chamber was also noticed to be a relevant parameter affecting the growth rate of the bioactive glass film. It was determined a reduction (in some cases linear [159], but in others exponential) with the total pressure (using argon as background gas) in the chamber [160]. This behavior was attributed to the disruption of the plasma plume dynamics due to the deceleration of the ablated species by the atmosphere (i.e. the ablated species decelerate more because of a higher number of collisions with molecules of the background gas).

The increment of the pressure promotes the formation of carbonates and reduces the amount of non-bridging oxygen sites (Si-O-NBO) in the film. This reduction comprises the biological response of the film because they are responsible for their bioactivity. Finally, the pressure also has an impact on the quantity and shape of the particulate formed on the surface of the films. Quantity of particles increases with the pressure as this parameter affects the mechanisms of generation particles [159].

3.2.3 | Properties of the Coatings

3.2.3.1 Chemistry Bioactive glass coatings with different composition can be produced by PLD. Silicate-based [148, 151], but also, phosphate-based [157], or borate-based [158] bioactive glass coatings were produced. More recently, it has been also demonstrated the possibility of producing bioactive glass films doped with therapeutic ions, such as: Nb [157], Cu [161], Mn [162], Mg [137], Sr [163], Eu, and Ag [164].

Compositional characterization using semi-quantitative EDS analyses show that bioactive glass coatings produced by PLD on different substrates have the same composition as the target [145, 150]. PLD can transfer the complex stoichiometry from the glass to the coating; however, some inhomogeneities are found along the film. Films retain an amorphous structure, as demonstrated by means of X-ray diffraction (unless a too excessive temperature is applied to the substrate, crystallization is avoided).

These coatings are easily aged as a consequence of the exposure to atmospheric moisture [151]. This is expected as they degrade in contact with body fluids. Degradation is noticeable higher as compared to the bulk counterpart due to the reduced thickness of these films. The atmospheric moisture promotes the leaching out of Na^+, P^{+5}, Ca^{+2} ions during the first weeks to exposure, and the formation of a hydrated silica gel in the surface of the coating. Another observed ageing effect is the formation of carbonates due to the reaction with the CO_2 of the atmosphere. To avoid these ageing effects and preserve stable and unaltered the bioactive properties of these coatings the best option is the soaking of the coatings in alcohol. These aging effects also have an impact on the hardness of the deposited film. Using a microhardness tester (Vickers indenter), the evolution of the hardness along the depth of a 45S5 bioactive glass coatings (3.7 um thick) deposited onto a Ti6Al4V substrate was determined [146]. A hardness around 0.5 GPa was measured in the hydrated layer; however, this value increases to 3.8 GPa in the non-hydrated layer. Then, the hydration due to the contact of the film with the atmosphere reduces the mechanical properties of the glassy film.

3.2.3.2 Adhesion The adhesion of the bioactive glass coatings to the substrate is high, although, sand-blasting was observed to improve it [147]. An adhesion strength of 15.5 MPa was determined by a scratch test in a 45S5 bioactive glass film deposited onto a Ti6Al4V substrate [146]. Same parameter was determined by means of a pull-off test in similar coatings. Values in a range of 5.5–17 MPa were obtained. Bioactive glass coatings were also introduced in functionally graded coatings in order to increase the adherence of a hydroxyapatite layer to the substrate and to improve the crystallinity of this apatite layer [144, 165].

3.2.4 | Biological (Bioactivity, In Vitro, and In Vivo) Response of the Coatings

Bioactive glass coatings were produced in different substrates, mainly on titanium and alloys [150], silicon [151], or silicon carbide [166]. In all of these cases, it was confirmed the good in-vitro bioactivity of these coated-substrates with a bioactive glass film [167, 168]. These coatings exhibit a clear bioactive character. A CaP and SiO_2–rich layers are clearly observed after 72 h of

21922659, 2026, 20, Downloaded from https://advanced.onlinelibrary.wiley.com/doi/10.1002/adhm.202503610 by Julian Jones - Cochraneitalia , Wiley Online Library on [06/08/2026]. See the Terms and Conditions (https://onlinelibrary.wiley.com/terms-and-conditions) on Wiley Online Library for rules of use; OA articles are governed by the applicable Creative Commons License

immersion in SBF [153, 166]; however, the nature of the substrate has a definite influence on the bioactivity of the coating. It was observed that coating different substrates (such as silicon and titanium) with a layer of the same bioactive glass, induces a different response under immersion in SBF solution [169]. In the case of coating titanium substrates, the apatite nucleation is delayed, probably, due to the formation of new chemical species, and the presence of titanium oxides. On the other hand it was observed that a layer with a minimum thickness of 30 um is required to produce to promote the CaP formation [169]. Bioactive silicate-glass coatings with a higher silica content were observed to be more resistant to corrosion and slower in apatite formation while immersed into SBF solution, as expected [156, 170].

In vitro cell tests also corroborated the excellent biocompatibility of the coated surfaces. Bioactive glass coatings produced by PLD shown a very large cell adhesion and proliferation as compared to uncoated surfaces [168, 171, 172]. This biocompability is observed to be higher for bioactive glass films with lower silica content [171].

The bioactive glass coatings produced by PLD have been also characterized in-vivo. Different research works demonstrated that they develop the same reaction pattern as in vitro, and an apatite-like layer is formed by the coating and the living tissue [153]. Moreover, titanium substrates coated with bioactive glass films produced by PLD were shown not to elicit any inflammatory response on the surrounding tissues [153]. These tests also show that new bone growth easily on this type of coatings [172]. No signs of inflammation, infection, or suppuration were not detected in coated implants [172]; however, more in-vivo tests, especially involving a long term evaluation of the performance of the coated implants are required to totally understand the interaction with the biological environment and evaluate the stability of the coating.

Finally, we should mention that PLD offers the possibility to produce precise patterns of bioactive glass coatings on implants. The production of such patterns with bioactive materials has been observed to be a very interesting way to study cell-cell interactions [173] or to study e.g. cell adhesion and spreading [174]. The main advantage in this case is the possibility to produce precise patterns of thin-bioactive glass coatings with good spatial resolution using masks.

3.2.5 | Comparative Analysis of PLD for Producing Thin Bioactive Glass Coatings

Different techniques have been used for producing thin bioactive glass coatings; however, PLD is probably the technique most widely studied [127, 175]. As shown in Table 6, PLD offers excellent stoichiometric transfer from the target to the film, which is particularly advantageous for producing thin coatings of multicomponent materials such as bioactive glasses; however, it generally suffers from limited scalability, relatively small deposition rate, and the possible formation of particulates or droplets on the film surface. On the other hand, magnetron sputtering provides good control of film thickness, relatively high deposition rates, and excellent uniformity over large substrate areas, making it suitable for both research and industrial-scale coating processes [175]. Nevertheless, maintaining the exact target composition in the deposited film may be challenging due to preferential sputtering effects. Ion beam sputtering produces very dense, smooth, and high-quality films with precise thickness control and strong adhesion, but it typically has low deposition rates and higher equipment complexity, which limits its scalability [103].

3.3 | Laser Texturing of Bioactive Glass Surfaces

3.3.1 | Description of the Technique

The surface texture characteristics of implants determine their bioactivity. A high-specific surface area in bioactive glasses promotes a higher release of Si^{+} and Ca^{2+} ions, and more Si-OH groups in their surface, which ultimately induces a higher nucleation rate of apatite and consequently a higher bioactivity [176, 177]. On the other hand, a higher surface area also helps protein adsorption which has a very important effect on the cell adhesion, proliferation and differentiation [178]. In consequence, it was observed that rough bioactive glass surfaces may be beneficial in-vivo, as it may increase the bone formation at the tissue-implant interface [179]. Due to the relevance of the surface topography several techniques to produces rough bioactive glass surfaces, such as sintering glass particles [180], chemical etching [180, 181] or laser texturing [30, 182–184] have been studied. Among them, laser texturing offers many advantages and possibilities over the rest of the methods, namely, low mechanical damage, low contamination (as there is no mechanical contact with the part), high efficiency, high spatial precision, high replicability, possibility of producing very complex structures, etc. [185].

Laser texturing is performed by focusing a laser beam onto the material's surface. Laser energy is absorbed and thermalized by the surface, leading to melting or vaporization (see Figure 8a). In this way, material can be removed by the ablation or the displacement of the melted material (by the effect of the recoil pressure induced by an intense vaporization) [186]. Using laser texturing, we can create both regular and irregular patterns - such as grooves, dimples, and bumps- on surfaces of different materials, geometry an application [187–191].

Laser texturing can be produced using different laser sources as those reported in Section 2.3. Using CW or pulsed lasers (ms-, and ns-lasers) thermal mechanisms dominate and melting is clear along the treated areas. Using ultrashort laser sources (ps- or fs-lasers) this thermal affectation is avoided and similar textures but without a relevant heat-affected zone [192]. In this way, cleaner surfaces can be produced. On the other hand, surface patterns can be produced using UV, Vis or IR laser sources. As noticed in Section 2, if CW or pulsed lasers are used, maximum absorption is produced in the UV or IR regions of the spectrum for the bioactive glasses. If ultrashort laser sources are used even in the Vis range of the spectrum glasses can be treated as non-linear processes are involved.

3.3.2 | Laser Texturing of Bioactive Glass Surfaces

Laser texturing of bioactive glass surfaces was demonstrated on 45S5, ICIE16 or phosphate glasses using CO_2 [184], ns- [183], and

21922659, 2026, 20, Downloaded from https://advanced.onlinelibrary.wiley.com/doi/10.1002/adhm.202503610 by Julian Jones - Cochraneitalia , Wiley Online Library on [06/08/2026]. See the Terms and Conditions (https://onlinelibrary.wiley.com/terms-and-conditions) on Wiley Online Library for rules of use; OA articles are governed by the applicable Creative Commons License

TABLE 6 | Comparison of different technologies for producing thin glass coatings.

Feature	PLD	Ion beam sputtering	RF magnetron sputtering
Stoichiometry control	Excellent	Very good	Good
Film density	Moderate–high	Very high	High
Surface roughness	Moderate (droplets possible)	Very low	Low
Deposition rate	Low–moderate	Very low	Moderate
Large-area scalability	Poor	Poor–moderate	Excellent
Equipment cost	Moderate–high	Very high	High

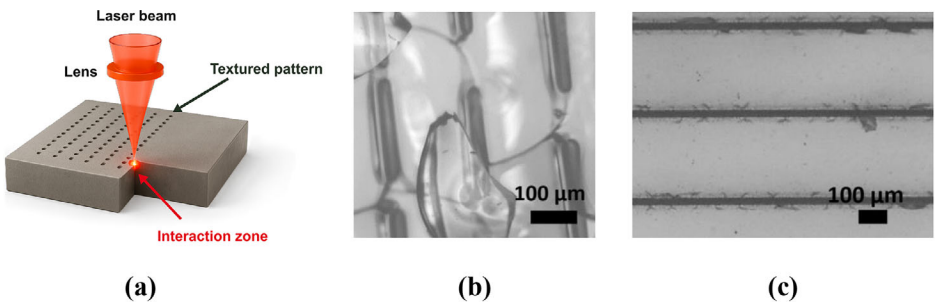


FIGURE 8 | (a) Schematic of laser texturing process. (b) CO_2 and (c) fs laser texturing of 45S5 bioactive glass.

fs-lasers [182, 184]. By using a CO_2 or a ns-laser, roughening of surfaces is produced by their melting/evaporation. Thermal effects are clear and typically induces many microcracks of thermoelastic nature along the treated area (see Figure 8b) [184]. In order to avoid this drawback, ultrashort laser processing, where non-thermal mechanisms are present, is an excellent option [184]. Using a fs-laser it is possible to produce cleaner microfeatures (see Figure 8c). After laser texturing, roughness in the treated area is increased. Roughness depends on the amount of energy deposited; then, processing parameters such as laser power (or better, irradiance), scanning speed, overlapping between scans, pulse frequency, focus spot diameter, etc. determines the degree of surface modification.

A clear effect after texturing in most of the materials is the modification of the wetting properties of treated surfaces [193, 194]. González-Quintas et al. reported a reduction in the wettability of 45S5 (contact angle: base material- 39.9°, laser treated- 63.2°) and ICIE16 (contact angle: base material- 36°, laser treated- 59.1°) bioactive glass surfaces after CO_2 laser texturing. This reduction in wettability was not observed for fs-laser processing [184].

Bioactivity of laser textured surfaces was evaluated in vitro. The apatite formation in laser treated bioactive glass surfaces was not substantially modified. Only it was observed for CO_2 laser-treated surfaces, at short term, a delay in the silica-rich layer formation and apatite precipitation. This effect can be related to crystallization induced by the thermal processes induced by CO_2 laser processing. After soaking in SBF laser textured samples it was observed that the roughness maintains in the long term [184]. This is result is relevant as macroscopic features control the anchorage and mechanical stability of implants.

Antibacterial properties of bioactive glass surfaces were increased after laser texturing while the bioactivity was not affected [182]. This antibacterial effect was attributed to several causes: (1) reduction of bacteria attachment with the roughness, (2) high pH environment (as calcium hydroxide was detected in treated areas). This effect is relevant to avoid biofilm formation.

Laser texturing of bioactive glasses is a very simple process which offers many opportunities, but as noted, it should be evaluated in more detail from a biological point of view. Short- and long-term in-vitro and in-vivo performance of textured surfaces should be evaluated more in-depth to understand the response of cells and tissues to laser textured bioactive glass surfaces. As soon as more information is obtained, this technology could be easily transferred into the market for the surface functionalization of bioactive glass surfaces (e.g. for texturing bioglass middle ear prosthesis [195]) as can be easily integrated into any production chain.

3.3.3 | Comparative Analysis of Different Surface Modification Techniques of Bioactive Glass Surfaces

Laser texturing of bioactive glass surfaces is the most widely explored technique to modify the surface of bioactive glasses. Laser texturing offers a highly precise and versatile approach for modifying the surfaces of bioactive glasses and metallic implants, enabling the fabrication of micro- and nanoscale hierarchical structures without the need for masks or templates. Compared with mechanical milling [179] or chemical etching [180, 181], laser texturing provides superior control over feature geometry and nanoscale resolution, while avoiding tool wear or uncontrolled chemical reactions [182–184]. Plasma or ion beam treatments can also achieve fine-scale surface modification, but these techniques are limited by low throughput and high equipment complexity. The main limitations of laser texturing are its relatively high equipment cost and the potential for thermal effects, such as

21922659, 2026, 20, Downloaded from https://advanced.onlinelibrary.wiley.com/doi/10.1002/adhm.202503610 by Julian Jones - Cochraneitalia , Wiley Online Library on [06/08/2026]. See the Terms and Conditions (https://onlinelibrary.wiley.com/terms-and-conditions) on Wiley Online Library for rules of use; OA articles are governed by the applicable Creative Commons License

TABLE 7 | Comparison of different technologies for modifying the surface topography of bioactive glass surfaces.

Technique	Advantages	Disadvantages
Laser texturing	– High precision and repeatability – Mask-free, flexible design – Production of hierarchical micro/nano structures – Localized treatment (bulk material unaltered)	– High equipment cost – Thermal effects (production of microcracks or residual stresses)
Mechanical texturing	– Simple and widely available – Low operational cost	– Limited to production of controlled microscale features – Tool wear and debris generation
Chemical etching	– Can produce high surface roughness – Relatively low cost	– Difficult to produce complex patterns – Environmental/handling hazards – Low control of uniformity and geometry

residual stresses or microcracking, particularly relevant on brittle materials such as bioactive glasses. Despite these challenges, laser texturing is especially attractive for biomedical applications that require localized, high-precision surface modifications to enhance cell response, wettability, or antibacterial properties (Table 7).

3.4 | Linking Processing Parameters to Biological Outcomes During Laser Surface Engineering of Bioactive Glasses

In laser-based processing, biological outcomes such as bioactivity, cytocompatibility, osteointegration, and stability are mainly determined by a small number of material characteristics controlled by the processing conditions [4, 27]:

- amorphous versus crystalline character (thermal history),
- surface area and micro/nanotopography,
- interfacial chemistry and dilution (particularly for coatings on metals)
- ageing/stability of highly reactive films.

The relationships between laser processing parameters, induced structural modifications, and biological outcomes for laser processed bioactive glasses in surface engineering are summarized in Table 8. The evidence highlights that biological performance is not an intrinsic property of the glass composition alone, but a process-dependent outcome governed by crystallinity, interfacial chemistry, dilution effects, surface topography, and ageing behavior. Therefore, decoding the direct influence of processing parameters with the biological outcome is not simple and constitutes a real challenge which could be solved in the future, for example, by means of machine learning methods or other computational tools [196]. Notice that similar processing parameters (e.g. laser power, processing speed, pulse frequency, etc.) could produce contrary effects, from the point of view of the biological response, depending on the specific laser process. In general, identical processing parameters may result in different biological outcomes depending on whether the manufacturing approach is subtractive or additive.

In laser cladding, irradiance and interaction time control dilution and interdiffusion [112, 114], which can lead to loss of intrinsic bioactivity (e.g., Al migration from Ti6Al4V substrate into the 45S5 coatings) [112]. In pulsed laser deposition (PLD), substrate temperature controls crystallization, which has been linked to reduced biocompatibility when excessive temperatures are applied [154]. Ageing effects in PLD films under atmospheric moisture represent a stability limitation that should be considered together with biological performance [146, 151]. In laser texturing, thermal processing can induce microcracks [176, 178], whereas ultrafast regimes reduce thermal damage and enable cleaner features, with demonstrated relevance for bacterial adhesion control on 45S5 [182, 184].

4 | Synthesis of Nanomaterials or Structures (scaffolds) Based on Bioactive Glasses

4.1 | Additive Manufacturing of Structures (Scaffolds) Based on Bioactive Glasses

Scaffolds are 3D structures mimicking the extracellular matrix (ECM) of natural tissues [197, 198]. They serve as a platform for cell attachment, proliferation differentiation and tissue formation. Scaffolds of different materials have been devised, in particular, scaffolds made of bioactive glasses have been attracted great attention for bone tissue engineering as they have the ability to promote the growth of bone cells, and to bond strongly with hard and soft tissues [199]. Different techniques to produce scaffolds made of bioactive glass have been devised, for example, polymer foam replication [200], freeze casting [201] or additive manufacturing techniques [202]. Additive manufacturing techniques are preferred to produce scaffolds due to the possibility to produce parts with customizable geometry and pore structure. Among these techniques, laser-based techniques stand out thanks to the flexibility in materials and geometries, efficiency,

21922659, 2026, 20, Downloaded from https://advanced.onlinelibrary.wiley.com/doi/10.1002/adhm.202503610 by Julian Jones - Cochraneitalia , Wiley Online Library on [06/08/2026]. See the Terms and Conditions (https://onlinelibrary.wiley.com/terms-and-conditions) on Wiley Online Library for rules of use; OA articles are governed by the applicable Creative Commons License

TABLE 8 | Processing, structure and biological outcome on laser processed bioactive glasses.

Laser processing route	Key processing parameter(s)	Induced structural / physicochemical modification	Reported biological outcome	Potential risk / limitation	References
Laser cladding	Laser irradiance (power density) and interaction time	Dilution and interdiffusion; Al migration from substrate; modification of glass chemistry	Loss of intrinsic bioactivity when excessive dilution occurs	Risk of alloying rather than true coating; altered dissolution kinetics and impaired apatite formation	[112, 114]
		Strong metallurgical bonding; preservation of coating integrity	Improved bone formation around coated implants (in vivo evidence)	Requires strict control of energy input to avoid compositional deviation	[111]
PLD	Substrate temperature	Excessive temperature (>200°C) → partial crystallization	Reported negative effect on biocompatibility when crystallization occurs	Need to maintain amorphous character for predictable bioactivity	[154]
	Ambient exposure / storage conditions	Moisture-driven ageing; ion leaching; formation of hydrated silica-rich layer; carbonate formation	Altered surface reactivity; potential impact on biological response	Reduced mechanical stability (hydrated vs non-hydrated layers); storage sensitivity	[146, 151]
	Pulse energy and deposition time	Substrate thickness influence on apatite nucleation kinetics	CaP formation promoted above minimum thickness; substrate-dependent bioactivity	Need for thickness control to ensure reliable osteoconductivity	[169]
	Laser deposition preserving amorphous bioactive glass chemistry	Stable coating-implant interface	No inflammatory response; new bone growth observed in vivo	Limited long-term in vivo data beyond early time points	[153, 172]
Laser surface texturing	Pulse duration (ns): thermal processing	Surface melting; heat-affected zone; thermoelastic microcracks	Increased roughness may enhance cell response via surface area effects	Microcracks may compromise long-term mechanical stability	[176, 178, 184]
	Femtosecond pulse duration; high peak intensity	Highly localized modification; minimal thermal damage; cleaner microfeatures	Reduced bacterial adhesion on 45S5; potential multifunctional bioactivity	Scalability and reproducibility require further validation	[182, 184]

21922659, 2026, 20, Downloaded from https://advanced.onlinelibrary.wiley.com/doi/10.1002/adhm.202503610 by Julian Jones - Cochraneltalia , Wiley Online Library on [06/08/2026]. See the Terms and Conditions (https://onlinelibrary.wiley.com/terms-and-conditions) on Wiley Online Library for rules of use; OA articles are governed by the applicable Creative Commons License

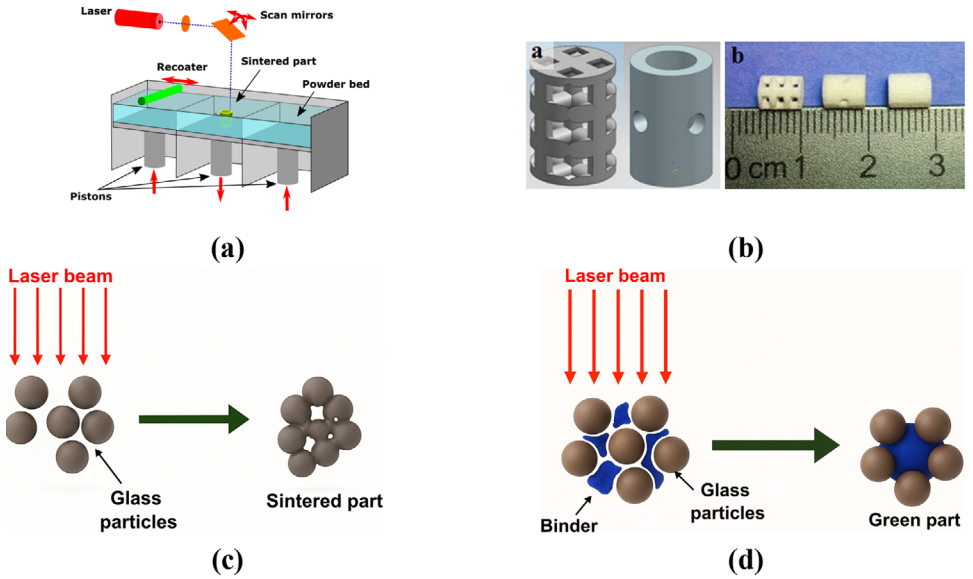


FIGURE 9 | (a) Schematic illustration of the selective laser sintering/melting (SLS/SLM) processes. (b) CAD models and fabricated green scaffolds with different geometry (porous, hollow and solid). Reprinted with kind permission of Elsevier from Ref. [210]. Schematic representations of the (c) direct and (d) indirect (i.e. using a binder) sintering of particles in SLS.

possibilities of customization, and reduced material waste. For the production of bioactive glass scaffolds we should highlight the following additive manufacturing techniques: selective laser sintering (SLS) or laser directed energy deposition (LDED).

4.1.1 | Selective Laser Sintering (SLS)

4.1.1.1 | Description of the Technique. Traditional techniques such as solvent casting, freeze drying, foam replication, etc. [203] have been used to produce scaffolds made of bioactive glass, however, their main disadvantage is that specific-patient geometries or porosities cannot be produced. In this sense, AM techniques, and particularly selective laser sintering (SLS) can overcome these limitations.

Selective laser sintering is a type of AM process based on the consolidation of a powder bed with a focused laser beam. This process was initially developed in the 1980s by The University of Texas at Austin's Mechanical engineering Department [204]. Consolidation of the powder is produced by sintering the particles; alternatively, full melting can be also produced; this process is called Selective laser melting (SLM).

In SLS and SLM, solid components are fabricated by using a laser beam. This is scanned over the powder bed and increases locally its temperature. Particles are bonded by sintering or melting, as illustrated in Figure 9a. The main elements a SLS/SLM machine are: (1) a central build chamber where the final part is formed, (2) two side chambers containing the initial supply of powder, (3) a roller mechanism that evenly distributes a layer of powder onto the build surface, and (4) a laser scanning system responsible for sintering the deposited powder [205, 206]. As each new layer is sintered by the laser, the build platform lowers slightly, while the powder feed pistons rise to deliver a fresh, thin layer of powder using the roller. This cycle repeats layer by layer and a part is produced (see Figure 9b). Additionally, heaters are often positioned near the powder bed to preheat the powder bed material to just below its melting point, helping to reduce thermal distortion and shrinkage during the laser processing stage [207].

Sintering of particles can occur in many ways, but two main categories can be distinguished: *direct* and *indirect* (i.e. a lower melting point material, called binder, is melted by the laser beam and holds the higher melting point particles bonded) way (see Figure 9c,d) (see Ref. [208] for a more detailed explanation of the binding mechanisms). In any case, the unsintered powder must be removed from the final part. This unused powder acts as a support structure during processing. This is interesting to help in the production of intricate geometries, for example: undercuts, or overhanging features. However, this excess powder must be removed as soon as the part is finally produced. Then, some post-processing step, such as cleaning, polishing, surface coating, heat treatment, etc. is always required [209].

4.1.1.2 | SLS-Produced Bioactive Glass Scaffolds. First works demonstrating the possibility of using SLS to produce 3D glass parts focused their attention to the production of bioactive glass-ceramic parts [211–214]. Apatite-mullite (A-M) [211–213] and apatite-wollastonite (A-W) [214] parts were produced in a direct and an indirect way. Direct sintering of glass particles by laser was demonstrated; however, the range of processing conditions to produce this bonding is more restricted than using a binder [211]. Around a 5% by mass of an acrylic powder binder was mixed with powders of these biomaterials (average particle diameter in a range of 45–90 μm). This binder was melted by low power CO_2 laser radiation (5-12 W) to produce a solid part (green part) with enough mechanical strength to be manipulated. The green part is subsequently post-processed to burn off the binder and sinter the powder particles. Notice that it is required to remove the whole binder as this is not biocompatible. Heating cycles up to 1200°C were investigated to reach adequate strength properties. Parts

21922659, 2026, 20, Downloaded from https://advanced.onlinelibrary.wiley.com/doi/10.1002/adhm.202503610 by Julian Jones - Cochraneitalia , Wiley Online Library on [06/08/2026]. See the Terms and Conditions (https://onlinelibrary.wiley.com/terms-and-conditions) on Wiley Online Library for rules of use; OA articles are governed by the applicable Creative Commons License

produced in this way showed a large porosity (40%), excellent in-vitro bioactivity and in-vivo behavior.

Works performed by Kolan et al. [203, 210, 215–218], Velez et al. [219, 220] and other authors [221] demonstrated the potential of SLS to produce scaffolds made of 13–93 bioactive glass (see Figure 9b). Other authors, demonstrated the possibility to produce scaffolds of other glass compositions (such as the 45S5 [222], the borate glass 13–93B3 [218]), composite scaffolds (e.g. β-TCP+silica glass [223], HA+silica glass [224], forsterite+silica glass [225], PDLLA+ silica glass [226, 227]), ion-doped bioactive glass scaffolds (such as Fe-doped [228], Ag-doped [229]) or doped with other drugs (such as bone morphogenetic protein-2 [230]).

Bioactive glass parts produced by SLS were produced directly and indirectly, i.e. using a binder. Best results, as for glass-ceramics, were noticed for the indirect way. Glass particles and the binder are mixed and ball-milled (this last step performed to bond the binder to the surface of the glass particles), and then laser processed during SLS process. If biocompatible binders (e.g. stearic acid particles) are used, their removal is not needed after processing. If non-biocompatible binders are used, these must be removed by a suitable postprocessing technique (debinding+sintering), e.g. burning out the green part. After this, little or no carbon residues remain in the scaffold. If the binder is removed by a suitable heat treatment (typically ~700°C during ~1hr), mechanical properties are greatly improved, but shrinkage is substantial (typically ~20%–25%). Notice also that for stearic acid, a typical binder used in SLS of bioactive glass parts, its decomposition starts at ~240°C and completes at ~520°C. If too much binder is used a large shrinkage is observed; moreover, lower strengths are obtained [31].

When producing parts in an indirect way, lower laser powers can be used as compared to the direct way (as seen in Table 9). Moreover, the bed temperature can be considerably lower (typically around the melting point of the binder, i.e. <100°C) than in the direct way (typically the glass transition temperature, i.e. ~600–700°C). The utilization of bed temperatures quite close to the melting point of the binder explains the low laser powers required for the indirect sintering process. Another advantage of using binders is the reduction of the crystallinity in the samples. Scaffolds produced by the direct sintering of particles show a higher tendency to crystallize (which impacts on the degradation rate and bioactivity of the scaffolds); this tendency increases with the laser power [222].

Scaffolds with different architecture and geometrical complexity were fabricated using SLS from glass particles with a size < 100 μm (best results found for ~20 μm in particle size) [31, 218, 231]. Typically, cylindrical or prismatic geometries, with a complex porous structure were selected to make the testing of the scaffolds easier. The surface of scaffolds produced by SLS are normally rough. This is positive as it improves adhesion and growth of biological tissues over them. Moreover, scaffolds show compressive strengths around 20–40 MPa, which is higher than that of trabecular bone, but non suitable for load-bearing applications [220].

In vitro tests demonstrated the good biocompatibility for SLS produced parts. SBF-soaked scaffolds showed a fast formation

TABLE 9 | Scaffolds made of bioactive glass coatings obtained by SLS.

Glass	Direct (D) / Indirect (I)	Binder	Laser source	Laser power (W)	Scanning speed (mm/s)	Scan spacing (mm)	Layer thickness (mm)	Bed temp. (°C)	References
13-93	I	Stearic acid (40%–50% vol.)	CO_2	2–3	50.8–406.4	0.076– 0.228			[215]
13-93	D	—	CO_2	5–50	304.8	0.229			[203]
13-93	I	Stearic acid (40%–50% vol.)	CO_2	2–3	50.8–406.4	0.076– 0.228	0.076–0.152	60	
13-93	I	Stearic acid (40%–50% vol.)	CO_2	2–3	76.2–304.8	0.229	0.1524	70	[216]
13-93	I	Stearic acid (12%–22% mass.)	CO_2	3–5	305–508	0.23	0,0762	60	[210]
13-93B3	I	Stearic acid (a 15% mass.)	CO_2	5	508	0.23	0,0762		[218]
45S5	D	—	CO_2	6–30	100		0.2		[222]

21922659, 2026, 20, Downloaded from https://advanced.onlinelibrary.wiley.com/doi/10.1002/adhm.202503610 by Julian Jones - Cochraneitalia , Wiley Online Library on [06/08/2026]. See the Terms and Conditions (https://onlinelibrary.wiley.com/terms-and-conditions) on Wiley Online Library for rules of use; OA articles are governed by the applicable Creative Commons License

(1 week) of a crystalline hydroxyapatite layer on the surface of the scaffolds [31, 210, 216]. It was noticed a reduction of the mechanical strength of scaffolds when immersed into SBF [218].

Cells seeded on the scaffold show a good adhesion via lamellipodia a filopodia and proliferation [216, 219]. No adverse effects on the cell morphology were noticed [31]. In vitro tests also show a higher cell proliferation on scaffolds with a geometry similar as the trabecular bone, with high surface curvatures combined with many changes in this parameter (i.e. biomimetic architectures as scaffolds based on gyroid surfaces) [231, 232].

In vivo tests were also performed and scaffolds showed satisfactory results [219, 220]. A progressive bone growth into the porous SLS scaffolds was observed; moreover, no signs of negative effects or inflammation was observed [31]. In different experiments, scaffolds are implanted into critical size defects performed in animal models (typically rats or rabbits). A faster healing rate and the formation of a bridging callus in only some weeks is observed [230]. In conclusion, bioactive glass scaffolds produced by SLS demonstrate their potential application in treating large bone defects, even in load bearing areas.

One of the main limitations detected in SLS for producing scaffolds is the fabrication of pores with a size lower than that of the laser spot [215]. Although such technical limitations could be solved, removal of unsintered powder trapped into the pores can be difficult or even impossible. Pore sizes in a range of 300–800 um are easily produced with current SLS machines. Notice that this is not a problem as ideal scaffolds should have a pore size larger than ∼100 μm to allow for bone in-growth, and preferably larger than ∼300 μm to improve bone formation [233]. Another potential limitation of SLS produced bioactive glass parts is the possibility of crystallization. This process is known to slow down the bioactivity of bioactive glasses. It was demonstrated that glass remains amorphous after performing SLS using a binder. Then, this does not compromise the bioactivity. Another problem of using binders is the necessity of a final thermal step (debinding+sintering) which could also enhance the tendency to crystallization and also produces a shrinkage of the final part. As discussed, the best results are found using binders; however, an excessive amount of binder reduces the final mechanical properties of the scaffold. To avoid using a binder, and improve the processing in a direct way, Chiu et al. experimented using a Fe-doped glass to improve the formability of 3D structures [228]; an optimum percentage of iron was observed to be required (∼5 wt.%). Another possibility to avoid using binders is the full melting, and not only sintering, of the bioactive glass powders, i.e. the utilization of the SLM technique; however, this approach is still under development, and we can find only some preliminary results in the literature [234–236]. The main associated problems are related to the susceptibility of the parts to cracking.

4.1.2 | Laser Directed Energy Deposition (LDED)

4.1.2.1 | Description of the Technique. The Laser Directed Energy Deposition (LDED) technology to produce three-dimensional parts and objects is nothing more than the natural evolution toward three-dimensional objects of the laser cladding technique explained in Section 3.1. In the laser cladding technique, the objective was producing two-dimensional layers because of overlapping simple tracks. To obtain three-dimensional objects, the idea is stacking these tracks following a predetermined 3D profile.

Figure 10a shows an schematic representation of the laser head used for this purpose by R. Comesaña et al. [237, 238]. In this case the configuration used was the off-axis injection of the precursor bioactive glass powder regarding the optical axis of the laser beam.

4.1.2.2 | LDED-Produced Bioactive Glass Parts. An example of the 3D objects that can be produced using this technique is shown in Figure 10b. In this case the precursor material was S520 bioactive glass that shows a wider working window than the 45S5 as commented in Section 3.1. A CO_2 laser delivering a maximum power of 140 W was used as energy source for melting the bioactive glass powder. Moving the substrate by following the defined 3D model allowed the production of the three-dimensional object.

The logic application of the LDED technique is the manufacturing of implants customized for the patient, as depicted in Figure 11. Critical size defects are not expected to heal naturally; therefore, they require the support of a bone substitution material, that in this case will be made of bioactive glass. A medical imaging examination is performed on the patient to identify the bone defect, particularly in the skull area. The defect is then modeled, and the geometry of the implant to be created is designed. The relevant information is entered into the LDED system, which allows for the implant to be manufactured specifically for the patient [239].

A crucial factor in the production of high-quality bioactive glass implants by the LDED technique is the control of the melting pool temperature and the cooling rate of the glass. The molten glass experiences an exponential decline in temperature from its melting point to the glass transition temperature, with the cooling rate progressively decreasing as the glass continues to cool. Del Val et al. implemented a strategy to control these variables tuning the laser intensity, powder mass flow and scanning speed [240]. Following this strategy sound 3D objects were obtained from 45S5 and S520 bioactive glasses. They measured the mechanical properties in terms of hardness, fracture toughness and compressive strength, and compared them with both the parent bulk glasses and the cortical bone. Results obtained with S520 were very promising with values exceeding those of the non-laser treated material and also of the cortical bone [240].

Following these methods of regulating the melting pool temperature and cooling rate, a 3D component composed of bioactive glass S520 was successfully fabricated by Comesaña et al., as illustrated in Figure 12a [239].

In the same work [239], 3D objects produced from 45S5 and S520 were compared. In both cases the laser-treated bioactive glasses exhibit a non-cytotoxic nature when non-direct contact assays are conducted using the pre-osteoblastic cell line MC3T3-E1. MTT quantification indicated a high level of cellular activity. Furthermore, direct seeding of cell cultures on both LDED parts (made of 45S5 and of S520 bioactive glasses) demonstrated

21922659, 2026, 20, Downloaded from https://advanced.onlinelibrary.wiley.com/doi/10.1002/adhm.202503610 by Julian Jones - Cochraneitalia , Wiley Online Library on [06/08/2026]. See the Terms and Conditions (https://onlinelibrary.wiley.com/terms-and-conditions) on Wiley Online Library for rules of use; OA articles are governed by the applicable Creative Commons License

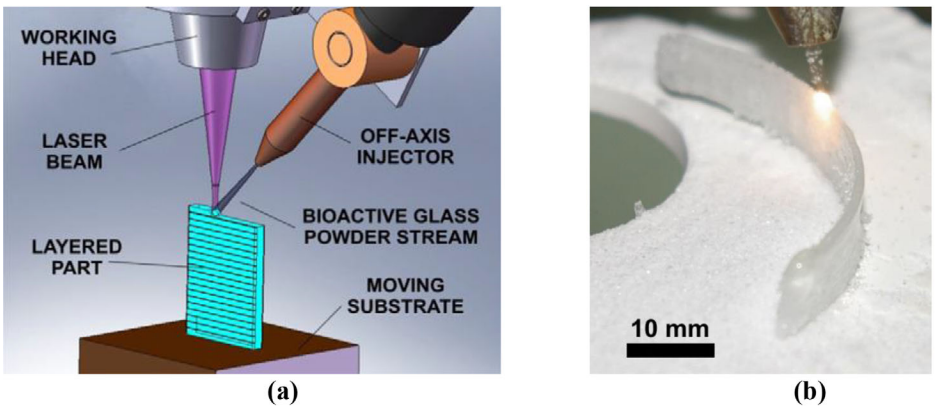


FIGURE 10 | (a) Schematic diagram of the Laser Directed Energy Deposition used for the formation of 3D bioactive glass parts. (b) 3D S520 bioactive glass part produced by LDED using a CO_2 laser as energy source. Reproduced with kind permission of Elsevier from Ref. [238].

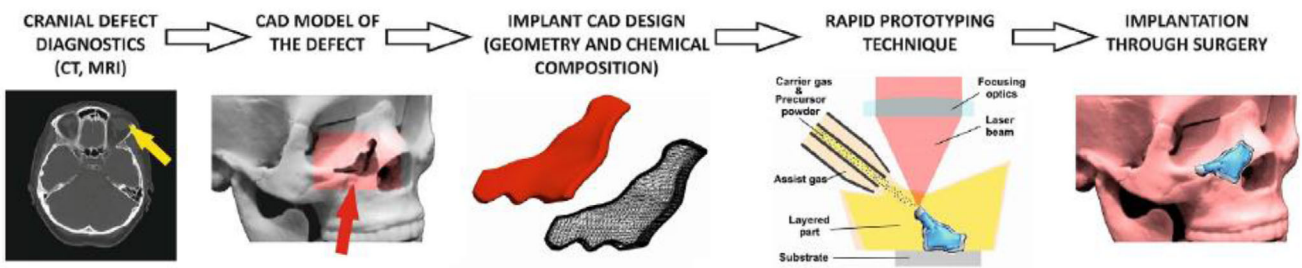


FIGURE 11 | (a) Representation of the strategy to follow for the custom manufacturing of three-dimensional implants from bioactive glass using the LDED technique. Reproduced under the terms of the Creative Commons CC-BY license from [239].

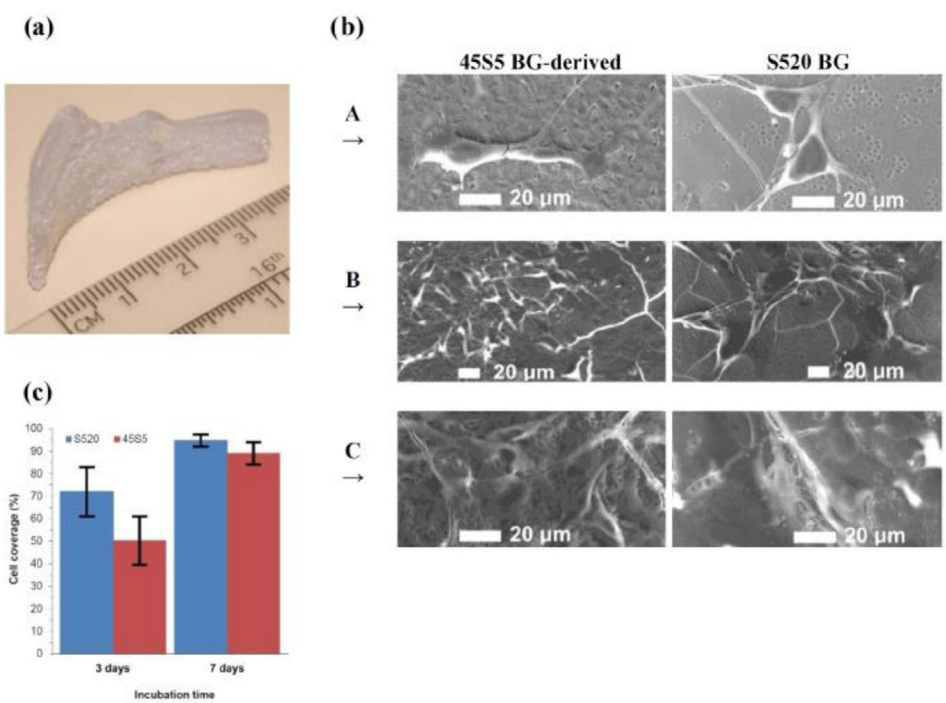


FIGURE 12 | (a) S520 BG part produced by laser direct glass deposition from a three-dimensional CAD model of a left orbital rim implant. (b) SEM morphology and spreading of MC3T3-E1 cell line at one day, three days, and seven days on LDED parts additively made from S520 and 45S5 BG. (c) Cell coverage of the sample surface after three and seven days of incubation time. Reproduced under the terms of the Creative Commons CC-BY license from [239].

21922659, 2026, 20, Downloaded from https://advanced.onlinelibrary.wiley.com/doi/10.1002/adhm.202503610 by Julian Jones - Cochraneitalia , Wiley Online Library on [06/08/2026]. See the Terms and Conditions (https://onlinelibrary.wiley.com/terms-and-conditions) on Wiley Online Library for rules of use; OA articles are governed by the applicable Creative Commons License

TABLE 10 | Comparison of different technologies for producing glass parts.

Feature	Additive manufacturing (laser-based)	Additive manufacturing (non laser-based)	Foam replication	Freeze-Casting
Precision	Excellent	Excellent	Moderate	High
Contact	Non-contact	Non-contact	Templated required	Templated required
Versatility	High	High	Low	Low/Moderate
Speed/Efficiency	Moderate to fast	Moderate	Moderate	Moderate
Material Waste	Minimal	Minimal	Low	Minimal
Cost	High: equipment and raw materials	High: equipment and raw materials	Low: simple equipment	Moderate
Material Limitations	Problem with thermal stress	Material must be printer-compatible	Restricted to foamable materials	Restricted by ice template properties
Specialized Training	High	High	Low	Moderate

that pre-osteoblasts attach and spread effectively, displaying numerous filopodia and a healthy, flattened morphology (see Figure 12b).

Figure 12c illustrates the quantified cell coverage, morphology, and spreading of the MC3T3-E1 cell line on the surface of LDED parts made of both 45S5 and S520 bioactive glasses. The in vitro performance of the LDED bioactive glass parts appears to be quite promising; nevertheless, there have been no reported in vivo studies to date.

4.1.3 | Comparative Analysis of Different AM Techniques for Producing Bioactive Glass Parts

As shown in Table 10, laser-based additive manufacturing techniques offer significant advantages in terms of precision, versatility, and productivity, and they do not require the use of templates or molds. These characteristics make them attractive for the fabrication of complex glass components; however, as in other additive manufacturing processes, the production of bioactive glass parts containing overhangs or unsupported geometries remains challenging and often requires support structures or specific building strategies.

The main drawback of laser-based additive manufacturing, particularly in processes such as Laser Directed Energy Deposition (LDED) and Selective Laser Melting (SLM), is associated with the complex thermal cycles experienced by the material during fabrication. Depending on the scanning strategy and build parameters, bioactive glass components may undergo repeated heating and cooling cycles during layer-by-layer deposition. This effect is further aggravated by heat accumulation as successive layers are deposited. Consequently, steep thermal gradients can develop between the interior of the part and its surface. Given the thermal conductivity and brittle nature of glass, these gradients can generate significant thermal stresses that may lead to crack formation or even the catastrophic fracture of the part. Several strategies have been proposed to mitigate these issues, including the use of preheated build platforms or heated chambers, optimized scanning strategies, and detailed thermal modeling of the process. While these approaches can reduce thermal gradients and residual stresses, their implementation often increases the complexity of the manufacturing system and may require process optimization tailored to the specific geometry, size, and composition of each component. Consequently, further research is still needed to better understand and control the thermal behavior of glass during laser-based additive manufacturing.

In contrast, other additive manufacturing approaches such as indirect selective laser sintering (i.e., binder-assisted processes), stereolithography (SLA), fused deposition modelling (FDM), and two-photon polymerization (2PP) generally avoid the severe thermal gradients associated with direct laser melting of glass. However, these methods present other limitations, including the need for additional post-processing steps such as debinding and sintering to densify the glass structure, which can introduce shrinkage, distortion, or residual porosity. Moreover, the final properties of the parts produced by these routes strongly depend on the effectiveness of these post-processing treatments.

4.2 | Synthesis of Bioactive Glass Nanofibers: Laser Spinning

Laser spinning is a relatively novel technique developed to synthesize glass fibers with diameters ranging from nanometers to micrometers [241–243]. This technique enables the production of large quantities of nanofibers with specific and controllable chemical compositions. The process does not require any chemical additives or post heat treatments. Figure 13 shows a schematic illustration of this technique.

The method is conceptually quite simple: the precursor material, in this case a bioactive glass, should be delivered in the form of a plate or monolith. A laser beam is used as energy source for the formation of the nanofibers. This laser beam is focused within the precursor material with enough intensity to melt the irradiated volume. At the same time a gas jet at supersonic regime is injected into the molten volume. The high momentum of the gas draws the fluid glass obtaining nanometric fibers.

The process of producing nanofibers takes only a few microseconds, as the laser beam delivers a high intensity (laser power

21922659, 2026, 20, Downloaded from https://advanced.onlinelibrary.wiley.com/doi/10.1002/adhm.202503610 by Julian Jones - Cochraneitalia , Wiley Online Library on [06/08/2026]. See the Terms and Conditions (https://onlinelibrary.wiley.com/terms-and-conditions) on Wiley Online Library for rules of use; OA articles are governed by the applicable Creative Commons License

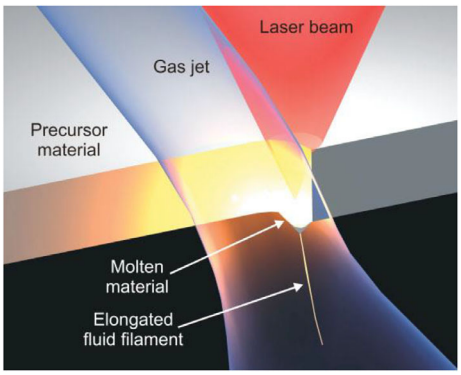


FIGURE 13 | Schematic illustration of the laser spinning technique to produce nanometric bioactive glass fibers. Reproduced with kind permission of John Wiley and Sons from [37].

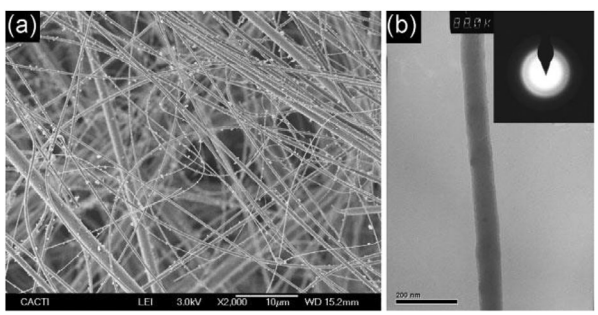


FIGURE 14 | Typical appearance of nanofibers obtained using the laser spinning technique. (a) Scanning electron microscopy image; (b) Transmission electron microscopy image of a single nanofiber; it appears with uniform cylindrical section, solid, and smooth. The inset presents the SAED showing its amorphous structure. Reproduced with kind permission of John Wiley and Sons from [37].

density) that quickly heats a small volume of material from ambient temperature to melting temperature, sometimes exceeding 2000°C. This rapid heating results in the generation of an extremely high temperature gradient, often surpassing 1000°C/mm. Additionally, the supersonic gas jet plays a crucial role in rapidly stretching and cooling the fibers, allowing them to maintain their characteristic cylindrical filament shape. Due to the high cooling speed, the resulting nanofibers are amorphous. First nanofibers of 45S5 bioactive glass were obtained by Quintero et al. using the laser spinning technique [37]. They produced a random web of nanofibers resembling natural cotton. The fibers were not attached to each other as is the case with electrospinning, which opens up the possibility of further processing into ordered arrays. The aspect of the nanofibers obtained is shown in Figure 14

The laser spinning technique is developed under such special working conditions (low glass viscosity working window, extremely fast elongation of the glass filament and the rapid cooling) that it is possible to locally melt the precursor bioactive glass plate and obtain nanofibers without the chemical composition being significantly altered as demonstrated by X-ray Fluorescence spectroscopy (XRF). Furthermore, the structure of the starting glass remains intact in the nanofibers, as demonstrated by the Magic Angle Spinning Nuclear Magnetic Resonance (MAS-NMR) technique [244, 245].

Bioactive glass nanofibers produced by laser spinning have a wide range of applications, spanning from soft to hard tissue engineering. One of the primary potential applications is in serving as scaffolds for bone tissue engineering and drug release systems. They are also utilized in wound healing and in the manufacturing of nanobiocomposites, as detailed in Table 11. While most of the research has focused on silicate glass nanofibers, there have been experiments with phosphate and borosilicate glasses as well.

The enormous surface area-to-volume ratio of these nanofibers makes them highly reactive, much greater than the corresponding bulk starting materials. Quintero et al. [37] demonstrated this excellent reactivity by subjecting S45S5 and 52S4.6 nanofibers to an immersion test in simulated body fluid (SBF) following the ISO 23317:2014 standard. After just 12 h of immersion, an amorphous calcium phosphate layer is formed on the surface the nanofibers, while the glass is being dissolved in the SBF (see Figure 15). After one or two days of immersion, the silicate glass nanofibers undergo complete degradation, resulting in the formation of a kind of hollow nanotube made of calcium phosphate due to the dissolution of the silica network and the precipitation of calcium phosphate. Furthermore, it is observed that the calcium phosphate layer undergoes crystallization after 5 days in SBF, leading to the formation of hydroxyapatite. As a result, these findings indicate the significant biocompatibility and excellent bioresorbability of the bioactive glass nanofibers, as bone-like minerals are rapidly produced on the surface of the fibers. These remarkable characteristics position this material as an outstanding candidate for applications in bone regeneration.

This is example is a clear proof of the potential of the Laser Spinning is technique: it is possible to use glass formulations far away from that of the bioactive glass "gold standard" that represents Hench's Bioglass 45S5, to produce nanofibers that, by having an enormous surface area to volume ratio, will behave like bioactive glass once introduced into the human body.

Several studies have investigated the antibacterial properties of bioactive glass nanofibers. Echezarreta-López et al. [247] conducted a study demonstrating the antibacterial characteristics of ICIE16 bioactive glass nanofibers produced by laser spinning when tested against Staphylococcus aureus (S. aureus) in comparison to bionert glass fibers. The results of the study revealed a significantly greater bactericidal effect of the ICIE16 bioactive glass nanofibers. This enhanced bactericidal effect was attributed to the increase in pH in the proximity of the nanofibers, which was caused by the release of alkaline ions. Another proposed mechanism for the antibacterial behavior of the fibers involves the formation of needle-like structures around the fibers when they are immersed in the culture medium (refer to Figure 16). These needle-like structures are believed to contribute to the physical rupture and subsequent death of bacteria.

One of the most distinctive characteristics of glass is its ability to accommodate different types of ions in its amorphous structure. This has been exploited by various researchers to introduce different types of therapeutic ions into bioactive glass

21922659, 2026, 20, Downloaded from https://advanced.onlinelibrary.wiley.com/doi/10.1002/adhm.202503610 by Julian Jones - Cochraneitalia , Wiley Online Library on [06/08/2026]. See the Terms and Conditions (https://onlinelibrary.wiley.com/terms-and-conditions) on Wiley Online Library for rules of use; OA articles are governed by the applicable Creative Commons License

TABLE 11 | Survey of relevant research works producing bioactive glass nanofibers by laser spinning.

Glass system	Designation	Doping ions	Application	References
Silicate	45S5		Scaffold (bone tissue engineering)	[37]
Silicate	52S4.6		Scaffold (bone tissue engineering)	[37]
Phosphate			Scaffold (bone tissue engineering)	[246]
Silicate	ICIE16		Scaffold (bone tissue engineering & antibacterial)	[247]
Borosilicate		Zn	Composite (antibacterial)	[248]
Silicate	45S5	Zn, Sr	Wound healing (antibacterial)	[249]
Silicate	13-93		Scaffold (bone tissue engineering)	[250]
Silicate	13-93	Li	Composite (cartilage repair)	[22]
Silicate		Co	Wound healing (antibacterial)	[251]

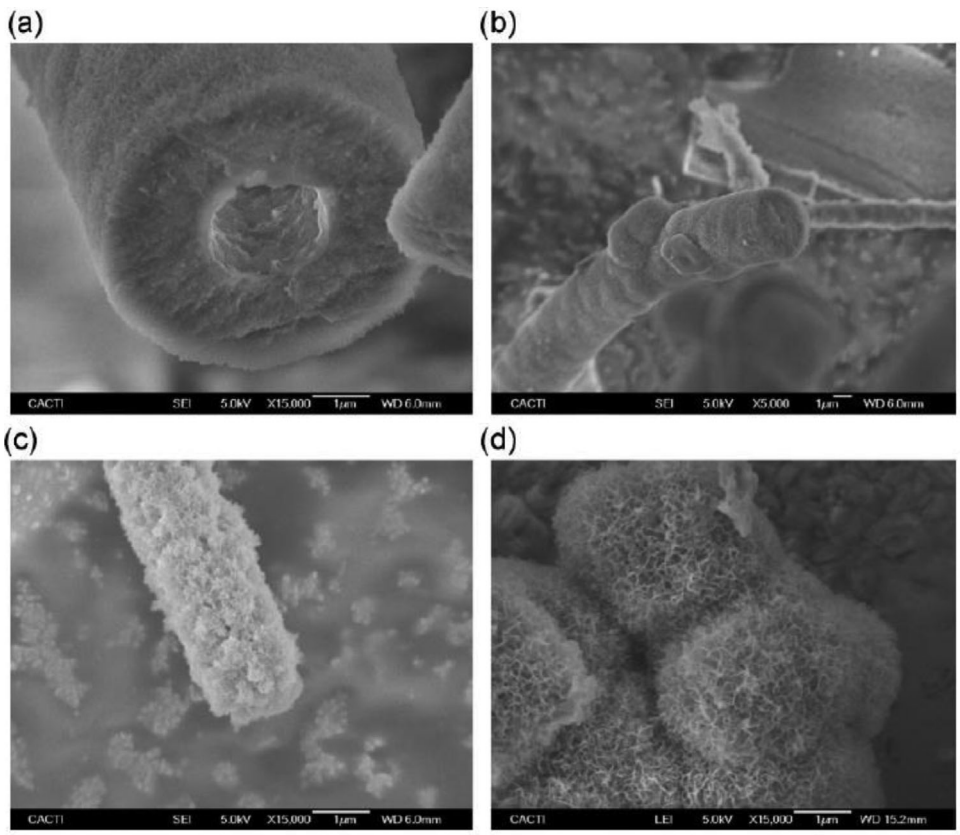


FIGURE 15 | FESEM images of 45S5 bioactive glass nanofibers immersed into SBF for (a,b) 48 h, (c) 12 h and (d) 5 days. Reprinted with kind permission of Wiley from [37].

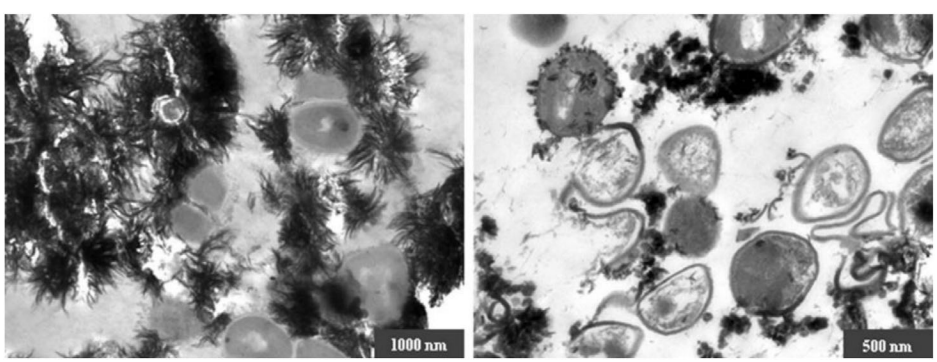


FIGURE 16 | TEM images of ICIE16 glass nanofibers after 4 days in S. Aureus culture. Reprinted with kind permission of Elsevier from [247].

21922659, 2026, 20, Downloaded from https://advanced.onlinelibrary.wiley.com/doi/10.1002/adhm.202503610 by Julian Jones - Cochraneitalia , Wiley Online Library on [06/08/2026]. See the Terms and Conditions (https://onlinelibrary.wiley.com/terms-and-conditions) on Wiley Online Library for rules of use; OA articles are governed by the applicable Creative Commons License

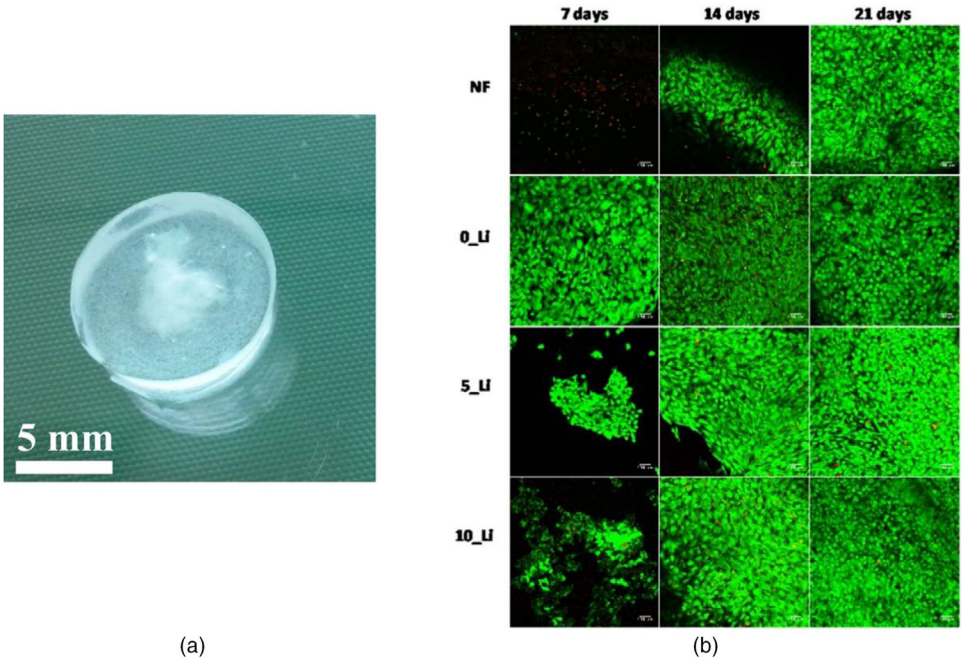


FIGURE 17 | (a) Hyaluronic acid hydrogels cross-linked with divinyl sulfone and reinforced with 13–93 lithium doped bioactive glass fibers. (b) Live/dead assay of ATDC5 seeded on hyaluronic acid hydrogels without fibers (NF) and with 13–93 bioactive glass fibers doped with 0% (0_Li), 5% (5_Li), and 10% (10_Li) of lithium. Reprinted with permission from Elsevier from Ref. [22].

and obtain nanofibers by laser spinning that retain the original glass composition.

The bacteriostatic effect of bioactive glass nanofibers can be even enhanced by the inclusion of antibacterial ions into the glass composition. Esteban-Tejada et al. [248] found a significant enhancement in the bactericidal effect of nanofibers when Zn^{2+} is included in the glass composition. They tested borosilicate glass nanofibers, which included Zn^{2+} ions, against Escherichia coli (E. coli), Streptococcus oralis (S. oralis), Streptococcus mutans (S. mutans), Staphylococcus aureus, and Candida krusei (C. krusei). The presence of E. coli, S. oralis, S. mutans, and C. krusei was reduced to undetectable levels in less than 24 h. When tested against S. aureus, the fibers with Zn^{2+} did not show significantly different results compared to those without Zn^{2+}. Specifically, the nanofibers lacking Zn^{2+} caused a 4-log reduction in S. aureus presence, whereas the zinc-doped nanofibers resulted in a 6-log reduction. Furthermore, the structure and antibacterial properties of the nanofibers were found to remain unchanged even after being immersed in human saliva for 8 days. As a result, these nanofibers demonstrate potential for effective treatment of oral lesions.

In a study by Echezarreta-Lopez et al. [249], it was demonstrated that 45S5 bioactive glass nanofibers produced by Laser Spinning have the capability to be doped with antibacterial ions, including Zn^{2+} and Sr^{2+}. The study also showcased the release of these ions and the antibacterial properties of the fibers when tested against Staphylococcus aureus.

Riveiro et al. [22] doped 13–93 bioactive glass with lithium to produce nanofibers by the Laser Spinning technique. These nanofibers were employed as filler material in hyaluronic acid hydrogels cross-linked with divinyl sulfone, as depicted in Figure 17a. The primary purpose of the fibers is to reinforce the hydrogel and serve as a drug delivery system to supply Li+ ions for promoting the healing of cartilage lesions. The study results showed a significant enhancement in the mechanical properties of the hydrogel with the inclusion of fibers. However, it was observed that the increase in mechanical properties is non-linear, and for larger amounts of fibers (exceeding a 1/10 mass ratio), the Young's modulus does not continue to increase. In fact, it is slightly reduced due to a decrease in the cross-linking density of the hydrogel. Experiments conducted with ATDC5 cells in vitro demonstrated the favorable biocompatibility of fiber-doped hydrogels, as depicted in Figure 17b. Furthermore, the research revealed that the release of lithium from the fibers fosters an optimal microenvironment for the proliferation and differentiation of chondrocytes. As a result, this composite material showcases distinctive chondrogenic properties, making it a promising candidate for treating cartilage injuries.

Wound healing is another promising application of bioactive glass nanofibers produced by Laser Spinning. Wound healing is a complex process that involves a coordinated sequence of phases: inflammation, proliferation, and remodeling. In chronic wounds, the healing process halts at the inflammatory phase, leading to prolonged healing times and increased susceptibility to complications. Patients with vascular disability experience reduced blood flow to the site of injury, which compromises the immune response and creates a worrying high risk of infection. When an infection occurs, the wound microenvironment becomes proinflammatory, preventing the healing process from progressing to the proliferative and remodeling phases. Microbial colonies present in the wound typically lead to the formation of biofilms in the affected area. Around 60% of chronic wounds and 6% of acute wounds contain biofilms, making it extremely challenging to eliminate the resident bacteria. In cases where the body's natural

21922659, 2026, 20, Downloaded from https://advanced.onlinelibrary.wiley.com/doi/10.1002/adhm.202503610 by Julian Jones - Cochraneitalia , Wiley Online Library on [06/08/2026]. See the Terms and Conditions (https://onlinelibrary.wiley.com/terms-and-conditions) on Wiley Online Library for rules of use; OA articles are governed by the applicable Creative Commons License

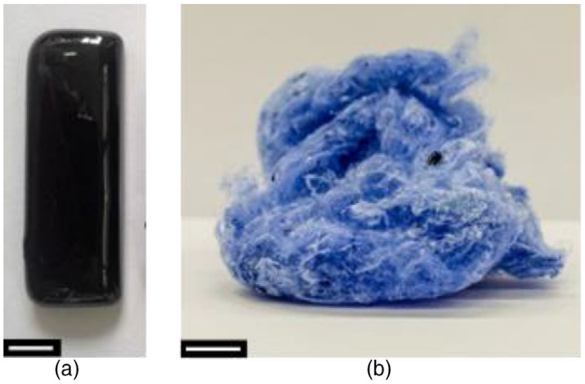


FIGURE 18 | Co-releasing glasses fabricated by laser spinning: (a) Image of a Co-doped glass preform. (b) Mesh of micro and nanofibers produced by laser spinning. Scale bar is 1 cm in both images. Reproduced from Ref. [251] under a CC-BY license.

healing mechanisms are unable to repair a wound, it becomes necessary to stimulate the healing process. The antibacterial properties of bioactive glass nanofibers, together with the ability of hosting therapeutic ions, inspired Solanki et al. to produce cobalt containing silicate based nanofibers by laser spinning [251]. The formulation of the parent glass (55 SiO_2, 20 Na_2O, 10 K_2O, 10 MgO, 5 CoO, mol%) was designed to avoid the formation of a hydroxyapatite layer when immersed into physiologic fluid, since formation of an apatite layer is not required for wound healing applications (see Figure 18). They demonstrated that the release of Cobalt ions can stimulate angiogenesis, by activating the Hypoxia Inducible Factor (HIF-1) pathway.

They found higher amounts of HIF-1α and Vascular Endothelial Growth Factor (VEGF) in keratinocytes exposed to conditioned media from the cobalt-containing glass fibers, as compared to cells exposed to similar amounts of cobalt chloride. This observation was attributed to a synergistic effect resulting from the combination of cobalt and other therapeutic ions released from the glass. The capability of the glass fibers to activate the HIF-1 pathway and promote VEGF expression indicates the potential for using glass fibers in the treatment of chronic wounds.

4.2.1 | Comparative Analysis of Different Techniques for Producing Bioactive Glass Nanofibers

Laser spinning, melt spinning, and electrospinning are among the most explored techniques for producing bioactive glass fibers (see Table 12). Melt spinning is a relatively simple and scalable method that allows the production of continuous glass fibers directly from the melt without the need for solvents or post-processing steps; however, it typically produces fibers in the micrometer range and therefore has limited capability for generating true nanofibrous structures. In contrast, electrospinning enables the fabrication of ultrafine fibers with diameters in the nanometer range and the formation of highly porous fibrous mats that are particularly attractive for tissue engineering or wound healing applications. Nevertheless, this technique requires the use of polymer carriers and solvents; moreover, the resulting composite fibers must undergo calcination to remove any organic components. This post-treatment can induce the crystallization of the fibers. In contrast, laser spinning represents a solvent-free alternative capable of producing glass nanofibers directly from the melt. Despite its potential for high production rates and high-purity fibers, the process must be explored to improve control over the fiber morphology and diameter distribution, and its application to more glass compositions and systems should be explored. In-vivo experiments are also lacking in laser spun fibers.

5 | Limitations and Practical Challenges of Laser Processing of Bioactive Glasses

While laser-based techniques provide unique capabilities for the controlled processing of bioactive glasses, including spatial selectivity, strong coating adhesion, and the ability to tailor surface morphology and chemistry, their practical implementation must be evaluated within a broader technological and translational context. A balanced assessment requires consideration not only of their advantages but also of their limitations relative to conventional processing routes.

5.1 | Process Robustness, Reproducibility, and Scalability

One of the main limitations of many laser-assisted techniques for bioactive glasses lies in the narrow processing window imposed by the thermal sensitivity and brittleness of these materials. Laser processing often involves high thermal gradients that can generate residual stresses and, in some cases, microcracking, particularly in thermally driven regimes such as laser cladding or nanosecond laser surface treatment [64, 66, 164]. These effects may compromise long-term structural stability and require careful control of laser irradiance, scanning strategy, and control of the heat input during the process.

Reproducibility is also a key requirement for practical applications. Laser-material interaction in bioactive glasses is highly sensitive to processing parameters, including laser irradiance (power density), substrate temperature, and interaction time, which can significantly influence crystallization, dilution, and interfacial chemistry. For example, in laser cladding of 45S5 bioactive glass on Ti6Al4V, excessive dilution and interdiffusion were shown to modify glass chemistry and lead to loss of intrinsic bioactivity [101]. These observations emphasize the need for careful control of processing parameters.

In addition, while laser-based additive manufacturing and surface processing techniques have demonstrated feasibility at laboratory scale, scale-up and production efficiency remain key challenges for industrial adoption. The sensitivity of glass processing to thermal history and the need to prevent devitrification or cracking complicate scale-up, particularly for large or complex geometries.

Another critical limitation is the control of crystallization during laser processing. Partial devitrification, observed in several laser-based routes including selective laser sintering and thermal laser treatments, can alter dissolution kinetics and potentially reduce bioactivity [26, 103, 165, 200]. Maintaining the amorphous

21922659, 2026, 20, Downloaded from https://advanced.onlinelibrary.wiley.com/doi/10.1002/adhm.202503610 by Julian Jones - Cochraneitalia , Wiley Online Library on [06/08/2026]. See the Terms and Conditions (https://onlinelibrary.wiley.com/terms-and-conditions) on Wiley Online Library for rules of use; OA articles are governed by the applicable Creative Commons License

TABLE 12 | Comparison of different technologies for producing bioactive glass nanofibers.

Feature	Laser spinning	Melt spinning	Electrospinning
Fiber size	Nano–micro	Mainly micro	Mainly nano
Use of solvents	No	No	Yes
Post-treatment required	No	No	Yes (calcination)
Morphology control	Moderate	Low (for nanoscale)	High
Production rate	Moderate–high	High	Low–moderate

structure is therefore often essential to preserve predictable ion release and biological response.

Furthermore, long-term stability must be considered, particularly for highly reactive bioactive glass coatings. For example, thin bioactive glass films produced by pulsed laser deposition have been shown to be susceptible to moisture-induced ageing, involving ion leaching and formation of hydrated silica-rich surface layers, with associated reductions in mechanical properties [131, 137]. These observations indicate that stability and storage conditions should be regarded as part of the functional performance of laser-processed bioactive glass systems rather than as secondary considerations.

5.2 | Comparison With Conventional Processing Routes

Laser-assisted processing provides valuable capabilities in spatial and microstructural control; however, conventional techniques may be more suitable in some cases. Traditional methods including sol–gel processing, plasma spraying, and electrophoretic deposition, offer alternative approaches with different balances of cost, scalability, and process simplicity. For instance, while laser cladding enables strong metallurgical bonding and localized processing, it requires careful control of thermal input to avoid dilution and compositional deviation [101, 102], whereas some conventional coating routes may operate at lower thermal loads but may present different limitations in adhesion or microstructural control [112].

Therefore, the selection of laser processing versus conventional processing must be done taking into account the specific application, depending on the required balance between adhesion strength, structural control, processing complexity, and the ability to scale up production.

Laser systems involve relatively high equipment and operational costs compared with many conventional processing methods. Process optimization for brittle glass materials may require complex thermal management and parameter control. In addition, certain laser-based approaches, particularly ultrafast processing and laser-assisted additive manufacturing, are still mostly confined to laboratory studies and require further development before reliable industrial use can be achieved.

Taken together, these considerations indicate that laser-assisted processing should be viewed as a powerful enabling technology rather than a universally optimal solution. While lasers provide unmatched capabilities for precise surface modification, controlled microstructuring, and strong coating to substrate adhesion, their successful application in commercial products requires careful control of crystallization, dilution, thermal stress, and process reproducibility. Moreover, comparative evaluation with established non-laser routes is essential to identify applications where laser processing provides a clear functional or clinical advantage.

6 | Summary and Future Prospects

Despite the laser and the bioactive glass are inventions from the same period (1960's), the potential applications of laser in this kind of biomaterial have not been fully exploited yet. The laser is a tool with exceptional characteristics that make it very different from other types of techniques normally used for processing glass, and especially bioactive glasses. The possibility of concentrating a high amount of energy in a very small volume allows the processing of bioactive glasses in a unique way that modifications can be obtained in the same, such as the generation of nanofibers, without compromising its bioactivity.

By properly selecting the processing conditions, especially selecting the appropriate wavelength of the laser source to be used, it is possible to perform highly selective processes in bioactive glasses. Although most bioactive glasses are transparent to most different types of laser radiation, it is possible to modify any type of bioactive glass by selecting the appropriate laser. When the laser radiation is within the UV zone or the mid-IR, this radiation is absorbed by most bioactive glasses. This allows us to heat the glass and produce modifications in it in a very controlled manner. As we have seen in this article, the bioactivity of the treated glasses is not compromised given the very special characteristics of the laser processing. The possibility of very rapid and selective heating and cooling allows the initial amorphous structure of the glasses to be maintained without observing significant vitrification or change of composition due to the release of volatile species during processing.

In this paper, we examined the primary applications of laser technology in the synthesis and processing of bioactive glass products. Initially, we have outlined the optical response of bioactive glasses to laser radiation (in both linear and non-linear regimes) and the key laser-induced phenomena that occur during the laser materials processing of bioactive glasses. Subsequently, we have assessed the most significant research studies focused on the surface engineering of bioactive glasses (including the production of thin and thick coatings via PLD, and laser cladding or the

21922659, 2026, 20, Downloaded from https://advanced.onlinelibrary.wiley.com/doi/10.1002/adhm.202503610 by Julian Jones - Cochraneitalia , Wiley Online Library on [06/08/2026]. See the Terms and Conditions (https://onlinelibrary.wiley.com/terms-and-conditions) on Wiley Online Library for rules of use; OA articles are governed by the applicable Creative Commons License

modification of bioactive glass surfaces by laser texturing), the additive manufacturing of bioactive glass components (created through SLS and other laser-based techniques), as well as the synthesis of bioactive glass-derived nanofibers. However, despite a large research effort was performed in the applications of lasers for the synthesis and processing of bioactive glass materials, potential applications of lasers have not been fully grasped. Further investigations are needed both from the fundamental and applied point of view.

More fundamental research efforts are needed to fully understand the non-linear interactions of lasers with transparent materials and clarify some of the phenomena induced by femtosecond laser processing. Non-linear absorption mechanisms involved in ultrafast laser processing, including the physical and chemical interactions, are still unclear; this makes simulation and prediction of results after processing difficult [252, 253]. Multiscale simulation, combining continuum theories, molecular dynamic simulations, density-functional theory, etc. could improve the understanding of the processes involved during femtosecond laser processing. On the other hand, most of the induced well-known or newly discovered non-linear phenomena observed in transparent materials (e.g. production of nanoporous glass surfaces [254], generation of nanogratings [255], etc.) have still not been explored in bioactive glasses. Their application could open the door to produce new developments such as the 4D bioactive glass scaffolds [256]. Finally, we should mention that applicability of ultrafast laser processing is largely demonstrated in laboratory conditions, but few industrial systems meet industrial standards. New developments to improve the throughput/efficiency are required.

From a more applied point of view, the application of lasers into the realm of bioactive glasses offers new possibilities. Up to now, laser texturing has been applied to the modification of the surface of bioactive glasses. Despite the promising results, more research to determine the impact of the micro- and nanoroughness induced by the laser, as well as the in-vivo characterization of laser treated surfaces must be performed. Laser surface engineering, such as the production of laser-induced periodic surface structures (LIPSS) on the surface of bioactive glasses [257], or the application of direct laser interference patterning (already demonstrated in some bioceramics) [258] could help to study the influence of the nanoroughness on the cell-bioactive glass surfaces or to improve the treatment of large surfaces, respectively.

Regarding the production of bioactive glass parts by laser-based additive manufacturing techniques, new developments are still required. Despite it was demonstrated the possibility of producing glass parts by SLS or LDED, the impact of the geometry and size of the potentially produced parts is not clear. The impact of thermal stresses in complex or large parts cannot be disregarded [259, 260]. These can produce microcracks compromising the mechanical integrity of the final parts. New developments for the current systems, e.g. to control the temperature distribution along the part during processing or the design of new additive manufacturing systems or processes (e.g. laser additive manufacturing following a sol-gel route [261]) are required. On the other hand, laser processing of glass (e.g. during additive manufacturing but also during production of coatings by laser cladding) tends to induce some crystallization. As already discussed along this manuscript, crystallization affects the bioactivity of the bioactive glass parts. Thermal simulations to control the energy deposition and the crystallization is required.

Laser processes can be also used to promote the synthesis and applications of nanomaterials based on bioactive glasses. Laser spinning opened the door to the synthesis of bioactive glass nanofibers in large quantities and with desired composition. These micro- and nanofibers have many potential applications. They can be used as scaffolds, composites or even in more advanced applications. These fibers can be used as an active material, e.g. to transmit laser light [262] or to sense [263]. Different ways can be devised to make them act as degradable optical fibers. In this way, a multifactor approach (optical therapy, ion release) can be exploited to stimulate healing of soft or hard tissues, or to heal but also sense. Other potential application of lasers consist in the production of bioactive glass nanoparticles [264]. Bioactive glasses can benefit from the large advantages (single-step and clean process, control of particle size and morphology, scalability, versatility, etc.) of lasers in the production nanoparticles [265–267]. If particles are produced in liquid, suitable media should be used to avoid their degradation. Moreover, suitable laser sources should be selected to guarantee a high efficiency and production rate. Finally, possibility of producing amorphous or crystalline nanoparticles by laser should be explored.

The quality and efficiency of laser processes have been largely increased by modelling and simulation. Modelling and simulation of laser processing bioactive glass materials and the determination of the impact of the process on the mechanical properties (relevant for load-bearing applications), or bioactivity, among others, must be explored in the future. Very few works have been devoted to the simulation of different laser processes applied on bioactive glasses due to their complexity. Moreover, the potential impact of processing parameters on the bioactivity is not determined by simulations as it is a concept difficult to quantify. Future application of machine learning in this field can be of interest.

6.1 | Concrete Challenges and Future Directions

Further progress in laser processing of bioactive glasses will depend on addressing a number of well-defined scientific, technological, and clinical issues that remain only partly resolved.

A common finding in laser-based processing is the strong influence of processing parameters on the resulting material structure and biological response. In laser cladding, changes in laser irradiance, thermal history, or substrate conditions can modify crystallinity, interfacial chemistry, and microstructure, and therefore affect bioactivity and stability of the coatings produced. Similar challenges have been widely reported in laser-assisted additive manufacturing, where consistent part quality and process repeatability remain difficult to achieve and require improved process monitoring and control. Future work should therefore focus on clearer definition of processing windows and on systematic correlation between processing conditions, structure, and biological performance.

21922659, 2026, 20, Downloaded from https://advanced.onlinelibrary.wiley.com/doi/10.1002/adhm.202503610 by Julian Jones - Cochraneitalia , Wiley Online Library on [06/08/2026]. See the Terms and Conditions (https://onlinelibrary.wiley.com/terms-and-conditions) on Wiley Online Library for rules of use; OA articles are governed by the applicable Creative Commons License

Although short-term in vitro and in vivo studies show promising bioactive and osteoconductive behavior, the long-term performance of laser-processed bioactive glass parts is still insufficiently documented. The biological response to bioactive glasses evolves over extended periods, and their dissolution products are known to influence tissue regeneration. For laser-processed materials, it will be important to evaluate long-term degradation, mechanical integrity, and the biological effects of processing-induced structural changes such as partial crystallization or ageing phenomena previously reported [31, 114, 146, 151].

Despite the existence of numerous medical products based on bioactive glass (at least 25 bioactive glass medical devices), mainly for orthopedic, dental, and wound care applications [268], the use of lasers in their synthesis, modification, or application in conjunction with laser processing has not yet reached the market. Several patents relying on the use of laser sources have been filed (for example, for the production of bioactive porous graft implants [269], bioactive glass scaffolds [270], and bioactive glass coatings [271]); however, none of these technologies, has reached commercialization. The lack of technology transfer is primarily due to their low technology readiness level (TRL), and none of the current or potential manufacturers of bioactive glasses has yet completed the clinical and regulatory approval cycle required for market introduction. In the broader biomedical manufacturing field, issues related to material reliability, manufacturing precision, and regulatory requirements continue to limit clinical adoption [27]. Similar considerations apply to laser processing of bioactive glasses, where reliable control of composition, crystallinity, and biological response is required. For example, in laser cladding of bioactive glass coatings, or in the production of bioactive glass parts by LDED or SLS, it seems required the certification of a processing procedure (including systems and processing parameters) rather than certify only the material to pass regulatory certification compulsory to launch new medical products based on these technologies. Then, resolving these issues is essential for progressing from experimental studies to reliable clinical application.

Despite the challenges outlined above, several directions remain particularly promising. Continued developments in bioactive glass research highlight their potential in tissue regeneration, ion-mediated therapeutic effects, and multifunctional biomaterials. Laser-based approaches provide opportunities for controlled surface functionalization, integration with advanced manufacturing strategies, and fabrication of complex architectures tailored to specific biological functions (as well as others given in the specific sections of this review). At the same time, current clinical challenges, such as improved implant integration, infection-resistant surfaces, and patient-specific regenerative solutions, offer clear motivation for further research.

In this review, we have demonstrated some possibilities of lasers to process and synthesize bioactive glass materials; however, lasers can also be used in conjunction with bioactive glasses in a different way. Laser light can activate bioactive glass materials, allowing them to function as light-triggered drug delivery systems that stimulate various biological processes. There are some experiences on this regard [272, 273], but more research is needed to fully understand the process and take benefit of all the possibilities.

In summary, the application of laser technology for processing bioactive glasses have been demonstrated in multiple works, but only the current potential applications have been explored. Moreover, new developments are expected. Then, glasses can move from being merely a passive element for laser technology (used in different optical elements such as lenses, windows, beamsplitters, etc.) to be a crucial material to be processed for multiple biomedical applications and converging discoveries from the same period.

Acknowledgements

This work was partially supported by the EU research project EVERGLASS (HORIZON EUROPE. Program HORIZON-EIC-2023-PATHFINDEROPEN-01 (PN:101129967), Government of Spain [PID2020-117900RB-I00 (MCI/AEI/FEDER, UE)] and [MCI/AEI/FEDER, UE (PID2022-138763OA-100)], and by Xunta de Galicia (ED431C 2023/25).

Conflicts of Interest

The authors declare no conflicts of interest.

Data Availability Statement

The authors have nothing to report.

References

1. L. L. Hench and J. R. Jones, "Bioactive Glasses: Frontiers and Challenges," *Frontiers in Bioengineering and Biotechnology* 3 (2015): 194, https://doi.org/10.3389/fbioe.2015.00194.

2. J. R. Jones, "Review of Bioactive Glass: from Hench to Hybrids," *Acta Biomaterialia* 9, no. 1 (2013): 4457–4486, https://doi.org/10.1016/j.actbio.2012.08.023.

3. D. S. Brauer, "Bioactive Glasses—Structure and Properties," *Angewandte Chemie International Edition* 54, no. 14 (2015): 4160–4181, https://doi.org/10.1002/anie.201405310.

4. M. N. Rahaman, D. E. Day, B. Sonny Bal, et al., "Bioactive Glass in Tissue Engineering," *Acta Biomaterialia* 7, no. 6 (2011): 2355–2373, https://doi.org/10.1016/j.actbio.2011.03.016.

5. V. Miguez-Pacheco, L. L. Hench, and A. R. Boccaccini, "Bioactive Glasses beyond Bone and Teeth: Emerging Applications in Contact with Soft Tissues," *Acta Biomaterialia* 13 (2015): 1–15, https://doi.org/10.1016/j.actbio.2014.11.004.

6. W. Huang, M. N. Rahaman, D. E. Day, and Y. Li, "Mechanisms for Converting Bioactive Silicate, Borate, and Borosilicate Glasses to Hydroxyapatite in Dilute Phosphate Solution," *Physics and Chemistry of Glasses—European Journal of Glass Science and Technology Part B* 47, no. 6 (2006): 647–658.

7. L. L. Hench, "Bioceramics," *Journal of the American Ceramic Society* 81, no. 7 (1998): 1705–1728.

8. S. Fagerlund, L. Hupa, and M. Hupa, "Dissolution Patterns of Biocompatible Glasses in 2-amino-2-hydroxymethyl-propane-1,3-diol (Tris) Buffer," *Acta Biomaterialia* 9, no. 2 (2013): 5400–5410, https://doi.org/10.1016/j.actbio.2012.08.051.

9. Q. Fu, M. N. Rahaman, H. Fu, and X. Liu, "Silicate, Borosilicate, and Borate Bioactive Glass Scaffolds with Controllable Degradation Rate for Bone Tissue Engineering Applications. I. Preparation and In Vitro Degradation," *Journal of Biomedical Materials Research Part A* 95A, no. 1 (2010): 164–171, https://doi.org/10.1002/jbm.a.32824.

10. G. Kaur, O. P. Pandey, K. Singh, D. Homa, B. Scott, and G. Pickrell, "A Review of Bioactive Glasses: Their Structure, Properties, Fabrication and

21922659, 2026, 20, Downloaded from https://advanced.onlinelibrary.wiley.com/doi/10.1002/adhm.202503610 by Julian Jones - Cochraneitalia , Wiley Online Library on [06/08/2026]. See the Terms and Conditions (https://onlinelibrary.wiley.com/terms-and-conditions) on Wiley Online Library for rules of use; OA articles are governed by the applicable Creative Commons License

Apatite Formation," *Journal of Biomedical Materials Research Part A* 102, no. 1 (2014): 254–274, https://doi.org/10.1002/jbm.a.34690.

11. A. Szcześ, L. Hołysz, and E. Chibowski, "Synthesis of Hydroxyapatite for Biomedical Applications," *Advances in Colloid and Interface Science* 249 (2017): 321–330.

12. S. Ferraris, S. Yamaguchi, N. Barbani, et al., "Bioactive Materials: In Vitro Investigation of Different Mechanisms of Hydroxyapatite Precipitation," *Acta Biomaterialia* 102 (2020): 468–480, https://doi.org/10.1016/j.actbio.2019.11.024.

13. S. Kargozar, F. Baino, S. Hamzehlou, R. G. Hill, and M. Mozafari, "Bioactive Glasses: Sprouting Angiogenesis in Tissue Engineering," *Trends in Biotechnology* 36, no. 4 (2018): 430–444, https://doi.org/10.1016/j.tibtech.2017.12.003.

14. C. Wu and J. Chang, "Multifunctional Mesoporous Bioactive Glasses for Effective Delivery of Therapeutic Ions and Drug/Growth Factors," *Journal of Controlled Release* 193 (2014): 282–295, https://doi.org/10.1016/j.jconrel.2014.04.026.

15. S. Kargozar, M. Montazerian, S. Hamzehlou, H.-W. Kim, and F. Baino, "Mesoporous Bioactive Glasses: Promising Platforms for Antibacterial Strategies," *Acta Biomaterialia* 81 (2018): 1–19, https://doi.org/10.1016/j.actbio.2018.09.052.

16. A. Hoppe, V. Mouriño, and A. R. Boccaccini, "Therapeutic Inorganic Ions in Bioactive Glasses to Enhance Bone Formation and beyond," *Biomaterials Science* 1, no. 3 (2013): 254–256, https://doi.org/10.1039/C2BM00116K.

17. S. M. Rabiee, N. Nazparvar, M. Azizian, D. Vashaee, and L. Tayebi, "Effect of Ion Substitution on Properties of Bioactive Glasses: a Review," *Ceramics International* 41, no. 6 (2015): 7241–7251, https://doi.org/10.1016/j.ceramint.2015.02.140.

18. A. Hoppe, N. S. Güldal, and A. R. Boccaccini, "A Review of the Biological Response to Ionic Dissolution Products from Bioactive Glasses and Glass-Ceramics," *Biomaterials* 32, no. 11 (2011): 2757–2774, https://doi.org/10.1016/j.biomaterials.2011.01.004.

19. M. Cannio, D. Bellucci, J. A. Roether, D. N. Boccaccini, and V. Cannillo, "Bioactive Glass Applications: A Literature Review of Human Clinical Trials," *Materials* 14, no. 18 (2021): 5440, https://doi.org/10.3390/ma14185440.

20. E. Schepers, M. D. Clercq, P. Ducheyne, and R. Kempeneers, "Bioactive Glass Particulate Material as a Filler for Bone Lesions," *Journal of Oral Rehabilitation* 18, no. 5 (1991): 439–452, https://doi.org/10.1111/j.1365-2842.1991.tb01689.x.

21. D. Petrović, D. Galić, D. Seifert, N. Lešić, and M. Smolić, "Evaluation of Bioactive Glass Treatment for Dentin Hypersensitivity: A Systematic Review," *Biomedicines* 11, no. 7 (2023): 1992, https://doi.org/10.3390/biomedicines11071992.

22. A. Riveiro, S. Amorim, A. Solanki, et al., "Hyaluronic Acid Hydrogels Reinforced with Laser Spun Bioactive Glass Micro- and Nanofibres Doped with Lithium," *Materials Science and Engineering: C* 126 (2021): 112124, https://doi.org/10.1016/j.msec.2021.112124.

23. J.-A. N. Oliver, Y. Su, X. Lu, P.-H. Kuo, J. Du, and D. Zhu, "Bioactive Glass Coatings on Metallic Implants for Biomedical Applications," *Bioactive Materials* 4 (2019): 261–270, https://doi.org/10.1016/j.bioactmat.2019.09.002.

24. K. C. R. Kolan, J. A. Semon, B. Bromet, D. E. Day, and M. C. Leu, "Bioprinting with Human Stem Cell-Laden Alginate-Gelatin Bioink and Bioactive Glass for Tissue Engineering," *International Journal of Bioprinting* 5, no. 2 (2019): 204, https://doi.org/10.18063/ijb.v5i2.2.204.

25. J. E. Shelby, *Introduction to Glass Science and Technology*, 3rd. ed (Royal Society of Chemistry, 2020).

26. M. H. Kaou, M. Furkó, K. Balázsi, and C. Balázsi, "Advanced Bioactive Glasses: The Newest Achievements and Breakthroughs in the Area," *Nanomaterials* 13, no. 16 (2023): 2287, https://doi.org/10.3390/nano13162287.

27. Y. Zhu, X. Zhang, G. Chang, S. Deng, and H. F. Chan, "Bioactive Glass in Tissue Regeneration: Unveiling Recent Advances in Regenerative Strategies and Applications," *Advanced Materials* 37, no. 2 (2025): 2312964, https://doi.org/10.1002/adma.202312964.

28. W. M. Steen and J. Mazumder, *Laser Material Processing*, 4th ed. (Springer, 2010), https://doi.org/10.1007/978-1-84996-062-5.

29. L. D'Alessio, D. Ferro, V. Marotta, A. Santagata, R. Teghil, and M. Zaccagnino, "Laser Ablation and Deposition of Bioglass 45S5 Thin Films," *Applied Surface Science* 183, no. 1-2 (2001): 10–17.

30. S. Sinha, "Laser Based Surface Treatment of Bioactive Glass: Dependence on Pulsed Laser Ablation," *Applied Surface Science Advances* 11 (2022): 100295, https://doi.org/10.1016/j.apsadv.2022.100295.

31. R. Gmeiner, U. Deisinger, and J. Schönherr, "Additive Manufacturing of Bioactive Glasses and Silicate Bioceramics," *Journal of Ceramic Science and Technology* 6, no. 2 (2015): 75–86.

32. E. Kannatey-Asibu Jr, *Principles of Laser Materials Processing*, 1st ed. (John Wiley & Sons, 2009).

33. W. Rath and C. Brettschneider, "Industrial Laser Materials Processing," *Laser Technik Journal* 11, no. 4 (2014): 23–27, https://doi.org/10.1002/latj.201400037.

34. W. M. Steen, "Laser Material Processing—An Overview," *Journal of Optics A: Pure and Applied Optics* 5, no. 4 (2003): S3–S7, https://doi.org/10.1088/1464-4258/5/4/351.

35. D. Schuocker, "Laser Cutting," *Materials and Manufacturing Processes* 4, no. 3 (1989): 311–330, https://doi.org/10.1080/10426918908956297.

36. A. Riveiro, F. Quintero, M. Boutinguiza, et al., "Laser Cutting: a Review on the Influence of Assist Gas," *Materials* 12, no. 1 (2019): 157, https://doi.org/10.3390/ma12010157.

37. F. Quintero, J. Pou, R. Comesaña, et al., "Laser Spinning of Bioactive Glass Nanofibers," *Advanced Functional Materials* 19, no. 19 (2009): 3084–3090, https://doi.org/10.1002/adfm.200801922.

38. P. Holmberg, "Laser Processing of Silica Based Glass," in *Department of Applied Physics* (KTH Royal Institute of Technology, 2015).

39. R. Kitamura, L. Pilon, and M. Jonasz, "Optical Constants of Silica Glass from Extreme Ultraviolet to Far Infrared at near Room Temperature," *Applied Optics* 46, no. 33 (2007): 8118–8133, https://doi.org/10.1364/AO.46.008118.

40. D. Bäuerle, *Laser Processing and Chemistry*, 4th ed. (Springer, 2011), https://doi.org/10.1007/978-3-642-17613-5.

41. M. V. Allmen and A. Blatter, "Laser-Beam Interactions with Materials: Physical Principles and Applications," in *Springer Series in Materials Science* (Springer, 2013).

42. L. J. Yang, Y. Wang, Z. G. Tian, and N. Cai, "YAG Laser Cutting Soda-Lime Glass with Controlled Fracture and Volumetric Heat Absorption," *International Journal of Machine Tools and Manufacture* 50, no. 10 (2010): 849–859, https://doi.org/10.1016/j.ijmachtools.2010.07.001.

43. A. D. McLachlan and F. P. Meyer, "Temperature Dependence of the Extinction Coefficient of Fused Silica for CO_2 Laser Wavelengths," *Applied Optics* 26, no. 9 (1987): 1728–1731, https://doi.org/10.1364/AO.26.001728.

44. G. H. Siegel Jr, "Ultraviolet Spectra of Silicate Glasses: A Review of Some Experimental Evidence," *Journal of Non-Crystalline Solids* 13, no. 3 (1974): 372–398.

45. T. Steyer, K. L. Day, and D. R. Huffman, "Infrared Absorption by Small Amorphous Quartz Spheres," *Applied Optics* 13, no. 7 (1974): 1586–1590, https://doi.org/10.1364/AO.13.001586.

46. K. L. Wlodarczyk, "Surface Deformation Mechanisms in Laser Smoothing and Micromachining of Optical Glasses," in *School of Engineering and Physical Sciences* (Heriot-Watt University, 2011).

47. A. M. Efimov, *Optical Constants of Inorganic Glasses*, 1st ed. (CRC Press, 2020), https://doi.org/10.1201/9780367811020.

21922659, 2026, 20, Downloaded from https://advanced.onlinelibrary.wiley.com/doi/10.1002/adhm.202503610 by Julian Jones - Cochraneitalia , Wiley Online Library on [06/08/2026]. See the Terms and Conditions (https://onlinelibrary.wiley.com/terms-and-conditions) on Wiley Online Library for rules of use; OA articles are governed by the applicable Creative Commons License

48. E. W. Van Stryland and D. J. Hagan, *Nonlinear Absorption* (Encyclopedia of Optical Engineering, 2003): 1475–1481.

49. C. Schaffer, A. Brodeur, and E. Mazur, "Laser-Induced Breakdown and Damage in Bulk Transparent Materials Induced by Tightly Focused Femtosecond Laser Pulses," *Measurement Science and Technology* 12, no. 11 (2001): 1784–1794, https://doi.org/10.1088/0957-0233/12/11/305.

50. X. Liu, D. Du, and G. Mourou, "Laser Ablation and Micromachining with Ultrashort Laser Pulses," *IEEE Journal of Quantum Electronics* 33, no. 10 (1997): 1706–1716, https://doi.org/10.1109/3.631270.

51. D. Von der Linde and H. Schüler, "Breakdown Threshold and Plasma Formation in Femtosecond Laser–Solid Interaction," *Journal of the Optical Society of America B* 13, no. 1 (1996): 216–222, https://doi.org/10.1364/JOSAB.13.000216.

52. A. Butkutė and L. Jonušauskas, "3D Manufacturing of Glass Microstructures Using Femtosecond Laser," *Micromachines* 12, no. 5 (2021): 499, https://doi.org/10.3390/mi12050499.

53. W. L. Smith, "Laser-Induced Breakdown in Optical Materials," *Optical Engineering* 17, no. 5 (1978): 489–503, https://doi.org/10.1117/12.7972269.

54. M. Sun, U. Eppelt, W. Schulz, and J. Zhu, "Role of Thermal Ionization in Internal Modification of Bulk Borosilicate Glass with Picosecond Laser Pulses at High Repetition Rates," *Optical Materials Express* 3, no. 10 (2013): 1716–1726, https://doi.org/10.1364/OME.3.001716.

55. C. B. Schaffer, N. Nishimura, E. N. Glezer, A. M.-T. Kim, and E. Mazur, "Dynamics of Femtosecond Laser-Induced Breakdown in Water from Femtoseconds to Microseconds," *Optics Express* 10, no. 3 (2002): 196–203, https://doi.org/10.1364/OE.10.000196.

56. K. Itoh, W. Watanabe, S. Nolte, and C. B. Schaffer, "Ultrafast Processes for Bulk Modification of Transparent Materials," *MRS Bulletin* 31, no. 8 (2006): 620–625.

57. D. Krol, "Femtosecond Laser Modification of Glass," *Journal of Non-Crystalline Solids* 354, no. 2–9 (2008): 416–424, https://doi.org/10.1016/j.jnoncrysol.2007.01.098.

58. R. Osellame, G. Cerullo, and R. Ramponi, "Topics in Applied Physics," *Femtosecond Laser Micromachining*, 1st ed. (Springer Berlin, 2012).

59. L. V. Keldysh, "Ionization in the Field of a Strong Electromagnetic Wave," *Journal of Experimental and Theoretical Physics* 20, no. 5 (1965): 1307–1314.

60. M. V. Allmen and A. Blatter, "Laser-Beam Interactions with Materials: Physical Principles and Applications," *Springer Series in Materials Science* 2nd ed. (Springer-Verlag, 1995).

61. J. Chevalier and L. Gremillard, "Ceramics for Medical Applications: a Picture for the next 20 Years," *Journal of the European Ceramic Society* 29, no. 7 (2009): 1245–1255, https://doi.org/10.1016/j.jeurceramsoc.2008.08.025.

62. M. Plewinski, K. Schickle, M. Lindner, A. Kirsten, M. Weber, and H. Fischer, "The Effect of Crystallization of Bioactive Bioglass 45S5 on Apatite Formation and Degradation," *Dental Materials* 29, no. 12 (2013): 1256–1264, https://doi.org/10.1016/j.dental.2013.09.016.

63. O. P. Filho, G. P. La Torre, and L. L. Hench, "Effect of Crystallization on Apatite-layer Formation of Bioactive Glass 45S5," *Journal of Biomedical Materials Research* 30, no. 4 (1996): 509–514, https://doi.org/10.1002/(SICI)1097-4636(199604)30:4%3c509::AID-JBM9%3e3.0.CO;2-T.

64. L. A. Buchanan and A. El-Ghannam, "Effect of Bioactive Glass Crystallization on the Conformation and Bioactivity of Adsorbed Proteins," *Journal of Biomedical Materials Research Part A* 93A, no. 2 (2010): 537–546.

65. M. Montazerian, A. Shearer, and J. C. Mauro, "Perspectives on the Impact of Crystallization in Bioactive Glasses and Glass-Ceramics," *International Journal of Ceramic Engineering & Science* 6, no. 1 (2024): 10194, https://doi.org/10.1002/ces2.10194.

66. T. Komatsu, R. Ihara, T. Honma, et al., "Patterning of Non-Linear Optical Crystals in Glass by Laser-Induced Crystallization," *Journal of the American Ceramic Society* 90, no. 3 (2007): 699–705, https://doi.org/10.1111/j.1551-2916.2006.01441.x.

67. H. Arstila, E. Vedel, L. Hupa, and M. Hupa, "Factors Affecting Crystallization of Bioactive Glasses," *Journal of the European Ceramic Society* 27, no. 2 (2007): 1543–1546, https://doi.org/10.1016/j.jeurceramsoc.2006.04.017.

68. J. Mazumder and W. M. Steen, "Heat Transfer Model for cw Laser Material Processing," *Journal of Applied Physics* 51, no. 2 (1980): 941–947, https://doi.org/10.1063/1.327672.

69. Y. L. Yao, H. Chen, and W. Zhang, "Time Scale Effects in Laser Material Removal: A Review," *International Journal of Advanced Manufacturing Technology* 26, no. 5 (2005): 598–608, https://doi.org/10.1007/s00170-003-2026-y.

70. J. Cao, M. Lancry, F. Brisset, L. Mazerolles, R. Saint-Martin, and B. Poumellec, "Femtosecond Laser-Induced Crystallization in Glasses: Growth Dynamics for Orientable Nanostructure and Nanocrystallization," *Crystal Growth & Design* 19, no. 4 (2019): 2189–2205, https://doi.org/10.1021/acs.cgd.8b01802.

71. I. H. Chowdhury and X. Xu, "Heat Transfer in Femtosecond Laser Processing of Metal," *Numerical Heat Transfer, Part A: Applications* 44, no. 3 (2003): 219–232, https://doi.org/10.1080/716100504.

72. Y. Teng, J. Zhou, K. Sharafudeen, S. Zhou, K. Miura, and J. Qiu, "Space-Selective Crystallization of Glass Induced by Femtosecond Laser Irradiation," *Journal of Non-Crystalline Solids* 383 (2014): 91–96, https://doi.org/10.1016/j.jnoncrysol.2013.04.015.

73. P. Kongsuwan, G. Brandal, and Y. L. Yao, "Laser Induced Porosity and Crystallinity Modification of a Bioactive Glass Coating on Titanium Substrates," *Journal of Manufacturing Science and Engineering* 137, no. 3 (2015): 031004, https://doi.org/10.1115/1.4029566.

74. K. P. O'Flynn and K. T. Stanton, "Laser Sintering and Crystallization of a Bioactive Glass-Ceramic," *Journal of Non-Crystalline Solids* 360 (2013): 49–56, https://doi.org/10.1016/j.jnoncrysol.2012.10.021.

75. R. Comesaña, F. Quintero, F. Lusquiños, et al., "Laser Cladding of Bioactive Glass Coatings," *Acta Biomaterialia* 6, no. 3 (2010): 953–961, https://doi.org/10.1016/j.actbio.2009.08.010.

76. H. Y. Zheng and T. Lee, "Studies of CO_2 Laser Peeling of Glass Substrates," *Journal of Micromechanics and Microengineering* 15, no. 11 (2005): 2093–2097, https://doi.org/10.1088/0960-1317/15/11/014.

77. L. G. Hector and R. B. Hetnarski, "Thermal Stresses in Materials due to Laser Heating," in *Thermal Stresses IV*, ed. R. B. Hetnarski (Amsterdam, 1996): 453–531.

78. K. Dai and L. Shaw, "Distortion Minimization of Laser-Processed Components through Control of Laser Scanning Patterns," *Rapid Prototyping Journal* 8, no. 5 (2002): 270–276, https://doi.org/10.1108/13552540210451732.

79. K. Yamamoto, N. Hasaka, H. Morita, and E. Ohmura, "Thermal Stress Analysis on Laser Scribing of Glass," *Journal of Laser Applications* 20, no. 4 (2008): 193–200, https://doi.org/10.2351/1.2995761.

80. J. M. Dowden, *The Mathematics of Thermal Modeling: An Introduction to the Theory of Laser Material Processing*, 2nd ed. (CRC Press, 2024), https://doi.org/10.1201/9781032684758.

81. M. Feit and A. Rubenchik, "Mechanisms of CO_2 Laser Mitigation of Laser Damage Growth in Fused Silica," in *XXXIV Annual Symposium on Optical Materials for High Power Lasers: Boulder Damage Symposium* (SPIE, 2003).

82. C. Wei, H. He, Z. Deng, J. Shao, and Z. Fan, "Study of Thermal Behaviors in CO_2 Laser Irradiated Glass," *Optical Engineering* 44, no. 4 (2005): 044202, https://doi.org/10.1117/1.1882374.

83. F. Baino and E. Fiume, "Elastic Mechanical Properties of 45S5-Based Bioactive Glass–Ceramic Scaffolds," *Materials* 12, no. 19 (2019): 3244, https://doi.org/10.3390/ma12193244.

84. D. Bellucci, V. Cannillo, and A. Sola, "Coefficient of Thermal Expansion of Bioactive Glasses: Available Literature Data and Analytical

21922659, 2026, 20, Downloaded from https://advanced.onlinelibrary.wiley.com/doi/10.1002/adhm.202503610 by Julian Jones - Cochraneltalia , Wiley Online Library on [06/08/2026]. See the Terms and Conditions (https://onlinelibrary.wiley.com/terms-and-conditions) on Wiley Online Library for rules of use; OA articles are governed by the applicable Creative Commons License

Equation Estimates," *Ceramics International* 37, no. 8 (2011): 2963–2972, https://doi.org/10.1016/j.ceramint.2011.05.048.

85. M. A. De Diego, N. J. Coleman, and L. L. Hench, "Tensile Properties of Bioactive Fibers for Tissue Engineering Applications," *Journal of Biomedical Materials Research* 53, no. 3 (2000): 199–203, https://doi.org/10.1002/(SICI)1097-4636(2000)53:3%3c199::AID-JBM2%3e3.0.CO;2-J.

86. D. C. Clupper, J. E. Gough, P. M. Embanga, I. Notingher, and L. L. Hench, "Bioactive Evaluation of 45S5 Bioactive Glass Fibres and Preliminary Study of Human Osteoblast Attachment," *Journal of Materials Science: Materials in Medicine* 15, no. 7 (2004): 803–808.

87. J. Wu, A. Rezikyan, M. R. Ross, P. J. Lezzi, and J. Luo, "Temperature and Thermal Stress Analysis of Ultrashort Laser Processed Glass," *Journal of Non-Crystalline Solids: X* 16 (2022): 100124.

88. X.-Z. Shi, M. Zhu, L. Liu, et al., "Effect of Different Contents of WO_3 and B_2O_3 on the Structure and Thermal, Mechanical, Corrosion Properties of Phosphate Glass," *Ceramics International* 49, no. 9 (2023): 14035–14045, https://doi.org/10.1016/j.ceramint.2022.12.285.

89. S. Nisar, L. Li, and M. Sheikh, "Laser Glass Cutting Techniques—A Review," *Journal of Laser Applications* 25, no. 4 (2013): 042010, https://doi.org/10.2351/1.4807895.

90. M. S. Giridhar, K. Seong, A. Schülzgen, P. Khulbe, N. Peyghambarian, and M. Mansuripur, "Femtosecond Pulsed Laser Micromachining of Glass Substrates with Application to Microfluidic Devices," *Applied Optics* 43, no. 23 (2004): 4584–4589, https://doi.org/10.1364/AO.43.004584.

91. K. Sugioka, J. Xu, D. Wu, et al., "Femtosecond Laser 3D Micromachining: A Powerful Tool for the Fabrication of Microfluidic, Optofluidic, and Electrofluidic Devices Based on Glass," *Lab on A Chip* 14, no. 18 (2014): 3447–3458, https://doi.org/10.1039/C4LC00548A.

92. J. Qiu, K. Miura, and K. Hirao, "Femtosecond Laser-induced Microfeatures in Glasses and Their Applications," *Journal of Non-Crystalline Solids* 354, no. 12-13 (2008): 1100–1111, https://doi.org/10.1016/j.jnoncrysol.2007.02.092.

93. F. L. Pedrotti, L. M. Pedrotti, and L. S. Pedrotti, *Introduction to Optics*, 3rd ed. (Cambridge University Press, 2017), https://doi.org/10.1017/9781108552493.

94. J. Hecht, *Understanding Lasers: An Entry-Level Guide*, 4th ed. (Wiley-IEEE Press, 2018), https://doi.org/10.1002/9781119310693.

95. C. Chang, K. Tzankov, L. Xu, D. Stockwell, and J. Wojtkiewicz, "Highly Efficient 3rd Harmonic Generation in Nd:YAG Laser," in *Conference on Lasers and Electro-Optics 2012* (Optica Publishing Group, 2012).

96. S. K. Sharma, P. K. Mukhopadhyay, A. Singh, R. Kandasamy, and S. M. Oak, "A Simple, Compact, and Efficient Diode-Side-Pumped Linear Intracavity Frequency Doubled Nd:YAG Rod Laser with 50 Ns Pulse Width and 124 W Green Output Power," *Review of Scientific Instruments* 81, no. 7 (2010): 073104.

97. A. A. Manshina, I. I. Tumkin, E. M. Khairullina, et al., "The Second Laser Revolution in Chemistry: Emerging Laser Technologies for Precise Fabrication of Multifunctional Nanomaterials and Nanostructures," *Advanced Functional Materials* 34, no. 40 (2024): 2405457, https://doi.org/10.1002/adfm.202405457.

98. T. S. Rose, J. S. Swenson, D. A. Hinkley, and R. A. Fields, "Efficient Laser Performance Using a Micro-Optic Based Pump Source," in *Advanced Solid State Lasers* (Optica Publishing Group, 1994).

99. K. Shimizu, M. Taniwaki, S. Sato, M. Kumagai, Y. Takashima, and Y. Naito, "High-Power Room-Temperature-Operated CO Laser," in *Advanced High-Power Lasers and Applications* (SPIE, 2000).

100. W. McNaught and G. Wlodarczyk, "kW Industrial CO Laser Operating at Room Temperature," in XI International Symposium on Gas Flow and Chemical Lasers and High Power Laser Conference (SPIE, 1997).

101. J. Schrooten and J. A. Helsen, "Adhesion of Bioactive Glass Coating to Ti6Al4V Oral Implant," *Biomaterials* 21, no. 14 (2000): 1461–1469, https://doi.org/10.1016/S0142-9612(00)00027-2.

102. S. Bajda, K. Cholewa-Kowalska, M. Krzyzanowski, et al., "Laser-Directed Energy Deposition of Bioactive Glass on Ti-6Al-7Nb Titanium Alloy Substrate with Highly Refined Grain Structure," *Surface and Coatings Technology* 485 (2024): 130904, https://doi.org/10.1016/j.surfcoat.2024.130904.

103. C. X. Wang, Z. Q. Chen, and M. Wang, "Fabrication and Characterization of Bioactive Glass Coatings Produced by the Ion Beam Sputter Deposition Technique," *Journal of Materials Science: Materials in Medicine* 13, no. 3 (2002): 247–251.

104. A. Pazo, E. Saiz, and A. P. Tomsia, "Silicate Glass Coatings on Ti-Based Implants," *Acta Materialia* 46, no. 7 (1998): 2551–2558, https://doi.org/10.1016/S1359-6454(98)80039-6.

105. M. Mehdipour, A. Afshar, and M. Mohebali, "Electrophoretic Deposition of Bioactive Glass Coating on 316L Stainless Steel and Electrochemical Behavior Study," *Applied Surface Science* 258, no. 24 (2012): 9832–9839, https://doi.org/10.1016/j.apsusc.2012.06.038.

106. P. Galliano, J. J. De Damborenea, M. J. Pascual, and A. Durán, "Sol-Gel Coatings on 316L Steel for Clinical Applications," *Journal of Sol-Gel Science and Technology* 13, no. 1–3 (1999): 723–727, https://doi.org/10.1023/A:1008653208083.

107. J. Schrooten, H. Van Oosterwyck, J. Vander Sloten, and J. A. Helsen, "Adhesion of New Bioactive Glass Coating," *Journal of Biomedical Materials Research* 44, no. 3 (1999): 243–252, https://doi.org/10.1002/(SICI)1097-4636(19990305)44:3%3c243::AID-JBM2%3e3.0.CO;2-O.

108. V. M. Weerasinghe, "Laser Cladding of Flat Plates," in *Department of MetalIurgy* (Imperial College London, University of London, 1984).

109. V. Weerasinghe and W. Steen, "Laser Cladding with Pneumatic Powder Delivery," in *Applied Laser Tooling* (Springer, 1987): 183–211, https://doi.org/10.1007/978-94-009-3569-3.

110. N. Moritz, E. Vedel, H. Ylänen, M. Jokinen, and M. Hupa, "Characterisation of Bioactive Glass Coatings on Titanium Substrates Produced Using a CO_2 Laser," *Journal of Materials Science: Materials in Medicine* 15, no. 7 (2004): 787–794.

111. N. Moritz, S. Rossi, E. Vedel, T. Tirri, H. Ylänen, and H. Aro, "Implants Coated with Bioactive Glass by CO_2-Laser, an In Vivo Study," *Journal of Materials Science: Materials in Medicine* 15 (2004): 795–802.

112. P.-H. Kuo, S. S. Joshi, X. Lu, et al., "Laser Coating of Bioactive Glasses on Bioimplant Titanium Alloys," *International Journal of Applied Glass Science* 10, no. 3 (2019): 307–320, https://doi.org/10.1111/ijag.12642.

113. F. Lusquinos, "Bioceramic-Glass Coatings Produced by Laser Cladding Technique," in *Proceedings of the Fourth International WLT-Conference on Laser in Manufacturing (LIM 2007)* (2007): 393–396.

114. F. Lusquiños, "Production of Bioactive Glass Coatings by Nd:YAG Laser Cladding," in *21st European Conference on Biomaterials (ESB 2007)* (Nantes, 2007).

115. J. Pou, F. Lusquiños, F. Quintero, et al., "Laser Processing and Synthesis of Ceramic Biomaterials for Osseointegrable Applications," in *26th International Congress on Applications of Lasers and Electro-Optics (ICALEO 2007)* (AIP Publishing, 2007), https://doi.org/10.2351/1.5061069.

116. F. Lusquiños, J. Pou, J. L. Arias, M. Boutinguiza, B. León, and M. Pérez-Amo, "Alloying of Hydroxyapatite onto Ti6Al–4 V by High Power Laser Irradiation," *Journal of Materials Science: Materials in Medicine* 13, no. 6 (2002): 601–605.

117. M. Brink, "The Influence of Alkali and Alkaline Earths on the Working Range for Bioactive Glasses," *Journal of Biomedical Materials Research* 36, no. 1 (1997): 109–117, https://doi.org/10.1002/(SICI)1097-4636(199707)36:1%3c109::AID-JBM13%3e3.0.CO;2-D.

118. F. Baino, M. Marshall, N. Kirk, and C. Vitale-Brovarone, "Design, Selection and Characterization of Novel Glasses and Glass-ceramics for Use in Prosthetic Applications," *Ceramics International* 42, no. 1 (2016): 1482–1491, https://doi.org/10.1016/j.ceramint.2015.09.094.

119. A. Hrubý, "Evaluation of Glass-forming Tendency by Means of DTA," *Czechoslovak Journal of Physics B* 22, no. 11 (1972): 1187–1193.

21922659, 2026, 20, Downloaded from https://advanced.onlinelibrary.wiley.com/doi/10.1002/adhm.202503610 by Julian Jones - Cochraneltalia , Wiley Online Library on [06/08/2026]. See the Terms and Conditions (https://onlinelibrary.wiley.com/terms-and-conditions) on Wiley Online Library for rules of use; OA articles are governed by the applicable Creative Commons License

120. S. Bajda, Y. Liu, R. Tosi, et al., "Laser Cladding of Bioactive Glass Coating on Pure Titanium Substrate with Highly Refined Grain Structure," *Journal of the Mechanical Behavior of Biomedical Materials* 119 (2021): 104519, https://doi.org/10.1016/j.jmbbm.2021.104519.

121. F. Baino, M. A. Montealegre, G. Orlygsson, G. Novajra, and C. Vitale-Brovarone, "Bioactive Glass Coatings Fabricated by Laser Cladding on Ceramic Acetabular Cups: A Proof-of-Concept Study," *Journal of Materials Science* 52 (2017): 9115–9128, https://doi.org/10.1007/s10853-017-0837-8.

122. F. Baino, J. Minguella-Canela, F. Korkusuz, et al., "In Vitro Assessment of Bioactive Glass Coatings on Alumina/Zirconia Composite Implants for Potential Use in Prosthetic Applications," *International Journal of Molecular Sciences* 20, no. 3 (2019): 722, https://doi.org/10.3390/ijms20030722.

123. F. Lusquiños, "Biocompatible Material Processing with High Power Lasers," *Department of Applied Physics* (University of Vigo, 2001).

124. M. Krzyzanowski, S. Bajda, Y. Liu, A. Triantaphyllou, W. Mark Rainforth, and M. Glendenning, "3D analysis of Thermal and Stress Evolution during Laser Cladding of Bioactive Glass Coatings," *Journal of the Mechanical Behavior of Biomedical Materials* 59 (2016): 404–417, https://doi.org/10.1016/j.jmbbm.2016.02.023.

125. M. Sathish, N. Radhika, and B. Saleh, "A Critical Review on Functionally Graded Coatings: Methods, Properties, and Challenges," *Composites Part B: Engineering* 225 (2021): 109278, https://doi.org/10.1016/j.compositesb.2021.109278.

126. V. Cannillo and A. Sola, "Different Approaches to Produce Coatings with Bioactive Glasses: Enamelling vs Plasma Spraying," *Journal of the European Ceramic Society* 30, no. 10 (2010): 2031–2039, https://doi.org/10.1016/j.jeurceramsoc.2010.04.021.

127. A. Sola, D. Bellucci, V. Cannillo, and A. Cattini, "Bioactive Glass Coatings: A Review," *Surface Engineering* 27, no. 8 (2011): 560–572, https://doi.org/10.1179/1743294410Y.0000000008.

128. N. A. Shepelin, Z. P. Tehrani, N. Ohannessian, C. W. Schneider, D. Pergolesi, and T. Lippert, "A Practical Guide to Pulsed Laser Deposition," *Chemical Society Reviews* 52, no. 7 (2023): 2294–2321, https://doi.org/10.1039/D2CS00938B.

129. J. Yu, W. Han, A. A. Suleiman, S. Han, N. Miao, and F. C.-C. Ling, "Recent Advances on Pulsed Laser Deposition of Large-Scale Thin Films," *Small Methods* 8, no. 7 (2024): 2301282, https://doi.org/10.1002/smtd.202301282.

130. M. N. R. Ashfold, F. Claeyssens, G. M. Fuge, and S. J. Henley, "Pulsed Laser Ablation and Deposition of Thin Films," *Chemical Society Reviews* 33, no. 1 (2004): 23–31, https://doi.org/10.1039/b207644f.

131. A. Ojeda-G-P, M. Döbeli, and T. Lippert, "Influence of Plume Properties on Thin Film Composition in Pulsed Laser Deposition," *Advanced Materials Interfaces* 5, no. 18 (2018): 1701062, https://doi.org/10.1002/admi.201701062.

132. H.-U. Krebs, M. Weisheit, J. Faupel, E. Süske, and T. Scharf, "Pulsed Laser Deposition (PLD)—A Versatile Thin Film Technique," in *Advances in Solid State Physics*, ed. B. Kramer (Springer, 2003), 505–518.

133. P. R. Willmott and J. R. Huber, "Pulsed Laser Vaporization and Deposition," *Reviews of Modern Physics* 72, no. 1 (2000): 315–328, https://doi.org/10.1103/RevModPhys.72.315.

134. J. A. Greer, "History and Current Status of Commercial Pulsed Laser Deposition Equipment," *Journal of Physics D: Applied Physics* 47, no. 3 (2013): 034005, https://doi.org/10.1088/0022-3727/47/3/034005.

135. J. Cheung and J. Horwitz, "Pulsed Laser Deposition History and Laser-Target Interactions," *MRS Bulletin* 17, no. 02 (1992): 30–36, https://doi.org/10.1557/S0883769400040598.

136. A. J. Haider, T. Alawsi, M. J. Haider, B. A. Taha, and H. A. Marhoon, "A Comprehensive Review on Pulsed Laser Deposition Technique to Effective Nanostructure Production: Trends and Challenges," *Optical and Quantum Electronics* 54, no. 8 (2022): 488, https://doi.org/10.1007/s11082-022-03786-6.

137. J. Ma, C. Z. Wang, C. L. Ban, C. Z. Chen, and H. M. Zhang, "Pulsed Laser Deposition of Magnesium-Containing Bioactive Glass Film on Porous Ti–6Al–4V Substrate Pretreated by Micro-Arc Oxidation," *Vacuum* 125 (2016): 48–55, https://doi.org/10.1016/j.vacuum.2015.12.005.

138. Y. Zhao, C. Chen, and D. Wang, "The Application of Pulsed Laser Deposition in Producing Bioactive Ceramic Films," *Surface Review and Letters* 12, no. 3 (2005): 401–408, https://doi.org/10.1142/S0218625X05007177.

139. T. Kitsugi, T. Nakamura, M. Oka, Y. Senaha, T. Goto, and T. Shibuya, "Bone-Bonding Behavior of Plasma-Sprayed Coatings of BioglassR, AW-Glass Ceramic, and Tricalcium Phosphate on Titanium Alloy," *Journal of Biomedical Materials Research* 30, no. 2 (1996): 261–269, https://doi.org/10.1002/(SICI)1097-4636(199602)30:2%3c261::AID-JBM17%3e3.0.CO;2-P.

140. X. Shiwei and H. Jintao, "Ion Beam Enhanced Deposit Technology," *Atomic Energy Science and Technology* 36 (2002): 458–461.

141. X. Li, "Preparation of CaO-P_2O_5-SiO_2 System Bioactive Glass by Sol-Gel Process and Research of Bioactive Mechanism," *Glass and Enamel-China* 31, no. 1 (2003): 37–39.

142. R. Drevet, J. Fauré, and H. Benhayoune, "Electrophoretic Deposition of Bioactive Glass Coatings for Bone Implant Applications: A Review," *Coatings* 14, no. 9 (2024): 1084.

143. S. Liste, P. González, J. Serra, J. P. Borrajo, and S. Chiussi, "Study of the Stoichiometry Transfer in Pulsed Laser Deposition of Bioactive Silica-Based Glasses," *Thin Solid Films* 453–454 (2004): 219–223.

144. D. Tanaskovic, B. Jokic, G. Socol, et al., "Synthesis of Functionally Graded Bioactive Glass-Apatite Multistructures on Ti Substrates by Pulsed Laser Deposition," *Applied Surface Science* 254, no. 4 (2007): 1279–1282, https://doi.org/10.1016/j.apsusc.2007.08.009.

145. L. D'Alessio, R. Teghil, M. Zaccagnino, I. Zaccardo, D. Ferro, and V. Marotta, "Pulsed Laser Ablation and Deposition of Bioactive Glass as Coating Material for Biomedical Applications," *Applied Surface Science* 138-139 (1999): 527–532, https://doi.org/10.1016/S0169-4332(98)00610-2.

146. R. Teghil, L. D'Alessio, D. Ferro, and S. M. Barinov, "Hardness of Bioactive Glass Film Deposited on Titanium Alloy by Pulsed Laser Ablation," *Journal of Materials Science Letters* 21, no. 5 (2002): 379–382, https://doi.org/10.1023/A:1014903117057.

147. G. Czél, R. Teghil, and D. Janovszky, "Pulsed Laser Deposition of Bioglass Coatings on Dental Implants," in *3rd Hungarian Conference on Materials Science, Testing and Informatics*, ed. J. Gyulai, (Balatonfured, 2003): 9–14.

148. J. Serra, S. Liste, P. González, et al., "The Role of the Temperature and Laser Fluence on the Properties of PLD Bioactive Glass Films," *Applied Physics A* 79, no. 4-6 (2004): 983–986, https://doi.org/10.1007/s00339-004-2610-5.

149. J. C. Miller and R. F. E. Haglund, *Laser Ablation and Desorption* (Academic Press, 1998).

150. J. Serra, P. González, S. Chiussi, B. León, and M. Perez-Amor, "Processing of Bioglass Coatings by Excimer Laser Ablation," in *13th international Symposium on Ceramics in Medicine (BIOCERAMICS)* (2001), 635–638.

151. P. González, J. Serra, S. Liste, S. Chiussi, B. León, and M. Pérez-Amor, "Ageing of Pulsed-Laser-Deposited Bioactive Glass Films," *Vacuum* 67, no. 3-4 (2002): 647–651, https://doi.org/10.1016/S0042-207X(02)00256-7.

152. J. P. Borrajo, P. González, S. Liste, et al., "Pulsed Laser Deposition of Bioactive Glass Films in Ammonia and Disilane Atmospheres," *Applied Surface Science* 248, no. 1-4 (2005): 369–375, https://doi.org/10.1016/j.apsusc.2005.03.084.

153. J. P. Borrajo, J. Serra, P. González, B. León, and F. M. Munoz, "In Vivo Evaluation of Titanium Implants Coated with Bioactive Glass by Pulsed

21922659, 2026, 20, Downloaded from https://advanced.onlinelibrary.wiley.com/doi/10.1002/adhm.202503610 by Julian Jones - Cochraneitalia , Wiley Online Library on [06/08/2026]. See the Terms and Conditions (https://onlinelibrary.wiley.com/terms-and-conditions) on Wiley Online Library for rules of use; OA articles are governed by the applicable Creative Commons License

Laser Deposition," *Journal of Materials Science: Materials in Medicine* 18, no. 12 (2007): 2371–2376.

154. E. Gyorgy, S. Grigorescu, G. Socol, et al., "Bioactive Glass and Hydroxyapatite Thin Films Obtained by Pulsed Laser Deposition," *Applied Surface Science* 253, no. 19 (2007): 7981–7986, https://doi.org/10.1016/j.apsusc.2007.02.146.

155. Y. Zhao, M. Song, C. Chen, and J. Liu, "Effects of the Substrate Temperature on the Bioglass Films Deposited by Pulsed Laser," *Applied Surface Science* 254, no. 21 (2008): 6897–6901, https://doi.org/10.1016/j.apsusc.2008.04.092.

156. C. Berbecaru, H. V. Alexandru, A. Ianculescu, et al., "Bioglass Thin Films for Biomimetic Implants," *Applied Surface Science* 255, no. 10 (2009): 5476–5479, https://doi.org/10.1016/j.apsusc.2008.08.020.

157. C. K. Sanz, A. R. dos Santos, M. H. P. da Silva, et al., "Niobo-Phosphate Bioactive Glass Films Produced by Pulsed Laser Deposition on Titanium Surfaces for Improved Cell Adhesion," *Ceramics International* 45, no. 14 (2019): 18052–18058, https://doi.org/10.1016/j.ceramint.2019.06.025.

158. J. V. Rau, A. De Bonis, M. Curcio, et al., "Borate and Silicate Bioactive Glass Coatings Prepared by Nanosecond Pulsed Laser Deposition," *Coatings* 10, no. 11 (2020): 1105, https://doi.org/10.3390/coatings10111105.

159. Y. Zhao, M. Song, C. Chen, and J. Liu, "The Role of the Pressure in Pulsed Laser Deposition of Bioactive Glass Films," *Journal of Non-Crystalline Solids* 354, no. 33 (2008): 4000–4004, https://doi.org/10.1016/j.jnoncrysol.2008.05.019.

160. S. Liste, J. Serra, P. González, et al., "The Role of the Reactive Atmosphere in Pulsed Laser Deposition of Bioactive Glass Films," *Thin Solid Films* 453 (2004): 224–228.

161. J. V. Rau, M. Curcio, M. G. Raucci, et al., "Cu-Releasing Bioactive Glass Coatings and Their in Vitro Properties," *ACS Applied Materials & Interfaces* 11, no. 6 (2019): 5812–5820, https://doi.org/10.1021/acsami.8b19082.

162. M. Curcio, B. Bochicchio, A. Pepe, et al., "Mn-Doped Glass–Ceramic Bioactive (Mn-BG) Thin Film to Selectively Enhance the Bioactivity of Electrospun Fibrous Polymeric Scaffolds," *Coatings* 12, no. 10 (2022): 1427.

163. D.-A. Draghici, A.-A. Mihai, M.-O. Aioanei, et al., "Strontium-Substituted Bioactive Glass-Ceramic Films for Tissue Engineering," *Boletín de la Sociedad Española de Cerámica y Vidrio* 61, no. 3 (2022): 184–190, https://doi.org/10.1016/j.bsecv.2020.09.006.

164. A. N. Trandaș, A. Trifan, A. D. Ungureanu, A. Dusciuc, and M. Opriș, "Properties of Europium and Silver Doped Bioglass Thin Films Obtained by Two Deposition Methods: Biointerfaces for Bioinert Implants," *Materials Chemistry and Physics* 309 (2023): 128396.

165. D. Tanaskovic, D. Veljovic, R. Petrović, et al., "Double-Layer Bioactive Glass Coatings Obtained by Pulsed Laser Deposition," *Key Engineering Materials* 361 (2008): 277–280.

166. A. de Carlos, J. P. Borrajo, J. Serra, P. Gonzalez, and B. Leon, "Behaviour of MG-63 Osteoblast-Like Cells on Wood-Based Biomorphic SiC Ceramics Coated with Bioactive Glass," *Journal of Materials Science: Materials in Medicine* 17 (2006): 523–529.

167. G. M. Oliveira, M. P. Ferraz, P. G. González, J. Serra, B. Leon, and M. Perez-Amor, "PLD Bioactive Ceramic Films: the Influence of $CaO\text{-}P_2O_5$ Glass Additions to Hydroxyapatite on the Proliferation and Morphology of Osteblastic Like-Cells," *Journal of Materials Science: Materials in Medicine* 19, no. 4 (2008): 1775–1785.

168. S. Shaikh, S. Kedia, A. G. Majumdar, M. Subramanian, and S. Sinha, "45S5 bioactive Glass Coating on Ti6Al4V Alloy Using Pulsed Laser Deposition Technique," *Materials Research Express* 6, no. 12 (2019): 125428, https://doi.org/10.1088/2053-1591/ab7568.

169. J. P. Borrajo, P. González, S. Liste, et al., "The Role of the Thickness and the Substrate on the In Vitro Bioactivity of Silica-Based Glass Coatings," *Materials Science and Engineering: C* 25, no. 2 (2005): 187–193, https://doi.org/10.1016/j.msec.2005.01.015.

170. L. Floroian, B. Savu, G. Stanciu, et al., "Nanostructured Bioglass Thin Films Synthesized by Pulsed Laser Deposition: CSLM, FTIR Investigations and In Vitro Biotests," *Applied Surface Science* 255, no. 5 PART 2 (2008): 3056–3062, https://doi.org/10.1016/j.apsusc.2008.08.105.

171. A. C. Popescu, F. Sima, L. Duta, et al., "Biocompatible and Bioactive Nanostructured Glass Coatings Synthesized by Pulsed Laser Deposition: In Vitro Biological Tests," *Applied Surface Science* 255, no. 10 (2009): 5486–5490, https://doi.org/10.1016/j.apsusc.2008.10.031.

172. D. G. Wang, C. Z. Chen, Q. S. Ma, Q. P. Jin, and H. C. Li, "A Study on In Vitro and In Vivo Bioactivity of HA/45S5 Composite Films by Pulsed Laser Deposition," *Applied Surface Science* 270 (2013): 667–674, https://doi.org/10.1016/j.apsusc.2013.01.117.

173. P. I. Zyrianova, M. M. Eltantawy, D. V. Silin, et al., "Biomimetic Materials Based on Hydroxyapatite Patterns for Studying Extracellular Cell Communication," *Materials & Design* 238 (2024): 112718, https://doi.org/10.1016/j.matdes.2024.112718.

174. T. Ekblad and B. Liedberg, "Protein Adsorption and Surface Patterning," *Current Opinion in Colloid & Interface Science* 15, no. 6 (2010): 499–509, https://doi.org/10.1016/j.cocis.2010.07.008.

175. R. Sergi, D. Bellucci, and V. Cannillo, "A Comprehensive Review of Bioactive Glass Coatings: State of the Art, Challenges and Future Perspectives," *Coatings* 10, no. 8 (2020): 757.

176. B. Lei, X. Chen, Y. Wang, N. Zhao, C. Du, and L. Fang, "Surface Nanoscale Patterning of Bioactive Glass to Support Cellular Growth and Differentiation," *Journal of Biomedical Materials Research Part A* 94A, no. 4 (2010): 1091–1099, https://doi.org/10.1002/jbm.a.32776.

177. L. L. Hench and J. Wilson, "Surface-Active Biomaterials," *Science* 226, no. 4675 (1984): 630–636.

178. E. A. B. E. Kaufmann, P. Ducheyne, S. Radin, D. A. Bonnell, and R. Composto, "Initial Events at the Bioactive Glass Surface in Contact with Protein-Containing Solutions," *Journal of Biomedical Materials Research* 52, no. 4 (2000): 825–830, https://doi.org/10.1002/1097-4636(20001215)52:4%3c825::AID-JBM28%3e3.0.CO;2-M.

179. J. E. Gough, I. Notingher, and L. L. Hench, "Osteoblast Attachment and Mineralized Nodule Formation on Rough and Smooth 45S5 Bioactive Glass Monoliths," *Journal of Biomedical Materials Research Part A* 68A, no. 4 (2004): 640–650, https://doi.org/10.1002/jbm.a.20075.

180. A. Itala, E. G. Nordstram, H. Ylanen, H. T. Aro, and M. Hupa, "Creation of Microrough Surface on Sintered Bioactive Glass Microspheres," *Journal of Biomedical Materials Research* 56, no. 2 (2001): 282–288, https://doi.org/10.1002/1097-4636(200108)56:2%3c282::AID-JBM1096%3e3.0.CO;2-5.

181. A. Itälä, H. O. Ylänen, J. Yrjans, et al., "Characterization of Microrough Bioactive Glass Surface: Surface Reactions and Osteoblast Responses In Vitro," *Journal of Biomedical Materials Research* 62, no. 3 (2002): 404–411, https://doi.org/10.1002/jbm.10273.

182. S. Shaikh, D. Singh, M. Subramanian, et al., "Femtosecond Laser Induced Surface Modification for Prevention of Bacterial Adhesion on 45S5 Bioactive Glass," *Journal of Non-Crystalline Solids* 482 (2018): 63–72, https://doi.org/10.1016/j.jnoncrysol.2017.12.019.

183. D. M. N. Menon, D. Pugliese, and D. Janner, "Infrared Nanosecond Laser Texturing of Cu-Doped Bioresorbable Calcium Phosphate Glasses," *Applied Sciences* 12, no. 7 (2022): 3516.

184. M. González-Quintas, B. Gago-Vidal, E. Calvo-García, et al., "Surface Modification of Bioactive Glasses by Femtosecond and CO_2 Lasers," *Coatings* 15, no. 2 (2025): 195.

185. E. Marin, S. Horiguchi, M. Zanocco, et al., "Bioglass Functionalization of Laser-Patterned Bioceramic Surfaces and Their Enhanced Bioactivity," *Heliyon* 4, no. 12 (2018): 01016.

186. A. Riveiro, A. L. B. Maçon, J. del Val, R. Comesaña, and J. Pou, "Laser Surface Texturing of Polymers for Biomedical Applications," *Frontiers in Physics* 6 (2018): 16, https://doi.org/10.3389/fphy.2018.00016.

187. A. Riveiro, R. Soto, J. del Val, et al., "Texturing of Polypropylene (PP) with Nanosecond Lasers," *Applied Surface Science* 374 (2016): 379–386, https://doi.org/10.1016/j.apsusc.2016.01.206.

21922659, 2026, 20, Downloaded from https://advanced.onlinelibrary.wiley.com/doi/10.1002/adhm.202503610 by Julian Jones - Cochraneitalia , Wiley Online Library on [06/08/2026]. See the Terms and Conditions (https://onlinelibrary.wiley.com/terms-and-conditions) on Wiley Online Library for rules of use; OA articles are governed by the applicable Creative Commons License

188. P. Pou, J. del Val, A. Riveiro, et al., "Laser Texturing of Stainless Steel under Different Processing Atmospheres: From Superhydrophilic to Superhydrophobic Surfaces," *Applied Surface Science* 475 (2019): 896–905, https://doi.org/10.1016/j.apsusc.2018.12.248.

189. A. Riveiro, T. Abalde, P. Pou, et al., "Influence of Laser Texturing on the Wettability of PTFE," *Applied Surface Science* 515 (2020): 145984.

190. A. Riveiro, R. Soto, R. Comesaña, et al., "Laser Surface Modification of PEEK," *Applied Surface Science* 258 (2012): 9437–9442.

191. A. Riveiro, R. Soto, J. del Val, et al., "Laser Surface Modification of Ultra-High-Molecular-Weight Polyethylene (UHMWPE) for Biomedical Applications," *Applied Surface Science* 302 (2014): 236–242.

192. B. N. Chichkov, C. Momma, S. Nolte, F. Alvensleben, and A. Tünnermann, "Femtosecond, Picosecond and Nanosecond Laser Ablation of Solids," *Applied Physics A Materials Science & Processing* 63, no. 2 (1996): 109–115, https://doi.org/10.1007/BF01567637.

193. A. O. Ijaola, E. A. Bamidele, C. J. Akisin, et al., "Wettability Transition for Laser Textured Surfaces: A Comprehensive Review," *Surfaces and Interfaces* 21 (2020): 100802, https://doi.org/10.1016/j.surfin.2020.100802.

194. A. Riveiro, P. Pou, J. del Val, et al., "Laser Texturing to Control the Wettability of Materials," *Procedia CIRP* 94 (2020): 879–884, https://doi.org/10.1016/j.procir.2020.09.065.

195. K. R. Rust, G. T. Singleton, J. Wilson, and P. J. Antonelli, "Bioglass Middle Ear Prosthesis: Long-Term Results," *Otology & Neurotology* 17, no. 3 (1996): 371–374.

196. M. Montazerian, E. D. Zanotto, and J. C. Mauro, "Model-Driven Design of Bioactive Glasses: From Molecular Dynamics through Machine Learning," *International Materials Reviews* 65, no. 5 (2020): 297–321, https://doi.org/10.1080/09506608.2019.1694779.

197. P. X. Ma, "Scaffolds for Tissue Fabrication," *Materials Today* 7, no. 5 (2004): 30–40, https://doi.org/10.1016/S1369-7021(04)00233-0.

198. F. J. O'Brien, "Biomaterials & Scaffolds for Tissue Engineering," *Materials Today* 14, no. 3 (2011): 88–95.

199. Q. Fu, E. Saiz, M. N. Rahaman, and A. P. Tomsia, "Bioactive Glass Scaffolds for Bone Tissue Engineering: State of the Art and Future Perspectives," *Materials Science and Engineering: C* 31, no. 7 (2011): 1245–1256, https://doi.org/10.1016/j.msec.2011.04.022.

200. Q. Z. Chen, I. D. Thompson, and A. R. Boccaccini, "45S5 Bioglass-Derived Glass–Ceramic Scaffolds for Bone Tissue Engineering," *Biomaterials* 27, no. 11 (2006): 2414–2425, https://doi.org/10.1016/j.biomaterials.2005.11.025.

201. H. Zhang, I. Hussain, M. Brust, M. F. Butler, S. P. Rannard, and A. I. Cooper, "Aligned Two- and Three-Dimensional Structures by Directional Freezing of Polymers and Nanoparticles," *Nature Materials* 4, no. 10 (2005): 787–793, https://doi.org/10.1038/nmat1487.

202. S. J. Hollister, "Porous Scaffold Design for Tissue Engineering," *Nature Materials* 4, no. 7 (2005): 518–524, https://doi.org/10.1038/nmat1421.

203. K. C. R. Kolan, "Selective Laser Sintering of 13–93 Bioactive Glass," in *21st Annual International Solid Freeform Fabrication Symposium—An Additive Manufacturing Conference, SFF 2010* (University of Texas, 2010).

204. M. Shellabear and O. Nyrhilä, "DMLS-Development History and state of the Art," paper presented at *Proceedings of the 4th LANE Conference*, Erlangen, Germany, September 21–24 (2004).

205. S. Das, "Physical Aspects of Process Control in Selective Laser Sintering of Metals," *Advanced Engineering Materials* 5, no. 10 (2003): 701–711, https://doi.org/10.1002/adem.200310099.

206. S. Singh, V. Sharma, and A. Sachdeva, "Progress in Selective Laser Sintering Using Metallic Powders: A Review," *Materials Science and Technology* 32, no. 8 (2016): 760–772, https://doi.org/10.1179/1743284715Y.0000000136.

207. H.-J. Yang, P.-J. Hwang, and S.-H. Lee, "A Study on Shrinkage Compensation of the SLS Process by Using the Taguchi Method," *International Journal of Machine Tools and Manufacture* 42, no. 11 (2002): 1203–1212, https://doi.org/10.1016/S0890-6955(02)00070-6.

208. J.-P. Kruth, P. Mercelis, J. Van Vaerenbergh, L. Froyen, and M. Rombouts, "Binding Mechanisms in Selective Laser Sintering and Selective Laser Melting," *Rapid Prototyping Journal* 11, no. 1 (2005): 26–36, https://doi.org/10.1108/13552540510573365.

209. M. Agarwala, D. Bourell, J. Beaman, H. Marcus, and J. Barlow, "Post-Processing of Selective Laser Sintered Metal Parts," *Rapid Prototyping Journal* 1, no. 2 (1995): 36–44, https://doi.org/10.1108/13552549510086853.

210. K. C. R. Kolan, M. C. Leu, G. E. Hilmas, and M. Velez, "Effect of Material, Process Parameters, and Simulated Body Fluids on Mechanical Properties of 13-93 Bioactive Glass Porous Constructs Made by Selective Laser Sintering," *Journal of the Mechanical Behavior of Biomedical Materials* 13 (2012): 14–24, https://doi.org/10.1016/j.jmbbm.2012.04.001.

211. J. Lorrison, R. D. Goodridge, K. W. Daigarno, and D. J. Wood, "Selective Laser Sintering of Bioactive Glass-Ceramics," in *American Society for Engineering Education (ASEE) Gulf-Southwest Section Annual Meeting 2018* (University of Texas, 2002).

212. K. W. Dalgarno, D. J. Wood, and R. D. Goodridge, "Mechanical Properties and Biological Responses of Bioactive Glass Ceramics Processed Using Indirect SLS," in *16th Solid Freeform Fabrication Symposium, SFF 2005* (University of Texas, 2005).

213. R. D. Goodridge, K. W. Dalgarno, and D. J. Wood, "Indirect Selective Laser Sintering of an Apatite-Mullite Glass-Ceramic for Potential Use in Bone Replacement Applications," *Proceedings of the Institution of Mechanical Engineers, Part H: Journal of Engineering in Medicine* 220, no. 1 (2006): 57–68, https://doi.org/10.1243/095441105X69051.

214. D. J. Wood, J. Dyson, K. Xiao, K. W. Dalgarno, and P. Genever, "Processing and Characterization of Apatite-Wollastonite Porous Scaffolds for Bone Tissue Engineering," *Key Engineering Materials* 361–363 (2008): 923–926.

215. K. C. R. Kolan, N. D. Doiphode, and M. C. Leu, "Selective Laser Sintering and Freeze Extrusion Fabrication of Scaffolds for Bone Repair Using 13–93 Bioactive Glass: A Comparison," in *21st Annual International Solid Freeform Fabrication Symposium—An Additive Manufacturing Conference, SFF 2010* (University of Texas, 2010).

216. K. C. R. Kolan, M. C. Leu, G. E. Hilmas, R. F. Brown, and M. Velez, "Fabrication of 13-93 Bioactive Glass Scaffolds for Bone Tissue Engineering Using Indirect Selective Laser Sintering," *Biofabrication* 3, no. 2 (2011): 025004, https://doi.org/10.1088/1758-5082/3/2/025004.

217. K. C. R. Kolan, M.-C. Leu, and G. Hilmas, "Effect of Particle Size, Binder Content and Heat Treatment on Mechanical Properties of 13–93 Bioactive Glass Scaffolds," in *22nd Annual International Solid Freeform Fabrication Symposium—An Additive Manufacturing Conference, SFF 2011* (University of Texas, 2011).

218. K. C. R. Kolan, M.-C. Leu, and G. Hilmas, "Effect of Architecture and Porosity on Mechanical Properties of Borate Glass Scaffolds Made by Selective Laser Sintering," in *24th International Solid Freeform Fabrication Symposium—An Additive Manufacturing Conference, SFF 2013* (University of Texas, 2013).

219. M. Velez, K. C. R. Kolan, M.-C. Leu, G. Hilmas, and R. F. Brown, "Selective Laser Sintering Fabrication of 13–93 Bioactive Glass Bone Scaffolds," in *Biomaterials Science-Processing, Properties, and Applications—Materials Science and Technology 2010 Conference and Exhibition, MS and T'10* (Wiley, 2011): 185–193.

220. M. Velez, S. Jung, K. C. R. Kolan, M. C. Leu, D. E. Day, and, T. Chu, "In Vivo Evaluation of 13–93 Bioactive Glass Scaffolds Made by Selective Laser Sintering (SLS)," in *Next Generation Biomaterials and Surface Properties of Biomaterials Symposia—Materials Science and Technology 2011 Conference and Exhibition, MS and T 2011*, Columbus, OH (2012): 91–99.

221. Y. Cao, B. Yang, C. Gao, P. Feng, and C. Shuai, "Laser Sintering of Nano 13-93 Glass Scaffolds: Microstructure, Mechanical Properties and

21922659, 2026, 20, Downloaded from https://advanced.onlinelibrary.wiley.com/doi/10.1002/adhm.202503610 by Julian Jones - Cochraneitalia , Wiley Online Library on [06/08/2026]. See the Terms and Conditions (https://onlinelibrary.wiley.com/terms-and-conditions) on Wiley Online Library for rules of use; OA articles are governed by the applicable Creative Commons License

Bioactivity," *Science of Sintering* 47, no. 1 (2015): 31–39, https://doi.org/10.2298/SOS1501031C.

222. J. Liu, H. Hu, P. Li, C. Shuai, and S. Peng, "Fabrication and Characterization of Porous 45S5 Glass Scaffolds via Direct Selective Laser Sintering," *Materials and Manufacturing Processes* 28, no. 6 (2013): 610–615.

223. J. Liu, C. Gao, P. Feng, S. Peng, and C. Shuai, "Selective Laser Sintering of β-TCP/Nano-58S Composite Scaffolds with Improved Mechanical Properties," *Materials & Design* 84 (2015): 395–401, https://doi.org/10.1016/j.matdes.2015.06.161.

224. C. Shuai, Y. Cao, C. Gao, P. Feng, T. Xiao, and S. Peng, "Hydroxyapatite Whisker Reinforced 63s Glass Scaffolds for Bone Tissue Engineering," *BioMed Research International* 2015 (2015): 1–8, https://doi.org/10.1155/2015/379294.

225. J. Deng, P. Li, C. Gao, P. Feng, C. Shuai, and S. Peng, "Bioactivity Improvement of Forsterite-Based Scaffolds with Nano-58s Bioactive Glass," *Materials and Manufacturing Processes* 29, no. 7 (2014): 877–884, https://doi.org/10.1080/10426914.2014.921712.

226. R. V. Pereira, G. V. Salmoria, M. O. C. Moura, and Á. Aragones, "Scaffolds of PDLLA/Bioglass 58S Produced via Selective Laser Sintering," *Materials Research* 17 (2014): 33–38, https://doi.org/10.1590/S1516-14392014005000075.

227. G. V. Salmoria, R. do Vale Pereira, and A. Aragones, "Preparation of PDLLA/Bioglass58S Scaffolds by Selective Laser Sintering," in *6th International Conference on Advanced Research in Virtual and Physical Prototyping* (Leira, 2014).

228. K.-Y. Chiu, K.-K. Chen, Y.-H. Wang, F.-H. Lin, and J.-Y. Huang, "Formability of Fe-Doped Bioglass Scaffold via Selective Laser Sintering," *Ceramics International* 46, no. 10 (2020): 16510–16517, https://doi.org/10.1016/j.ceramint.2020.03.216.

229. G. Qian, L. Zhang, X. Liu, S. Wu, S. Peng, and C. Shuai, "Silver-Doped Bioglass Modified Scaffolds: A Sustained Antibacterial Efficacy," *Materials Science and Engineering: C* 129 (2021): 112425.

230. W.-C. Liu, I. S. Robu, R. Patel, M. C. Leu, M. Velez, and T.-M. Gabriel Chu, "The Effects of 3D Bioactive Glass Scaffolds and BMP-2 on Bone Formation in Rat Femoral Critical Size Defects and Adjacent Bones," *Biomedical Materials* 9, no. 4 (2014): 045013.

231. K. C. R. Kolan, A. Thomas, M. C. Leu, and G. Hilmas, "In Vitro Assessment of Laser Sintered Bioactive Glass Scaffolds with Different Pore Geometries," *Rapid Prototyping Journal* 21, no. 2 (2015): 152–158, https://doi.org/10.1108/RPJ-12-2014-0175.

232. K. C. R. Kolan, Y. W. Huang, J. A. Semon, and M. C. Leu, "3D-Printed Biomimetic Bioactive Glass Scaffolds for Bone Regeneration in Rat Calvarial Defects," *International Journal of Bioprinting* 6, no. 2 (2020): 1–17.

233. V. Karageorgiou and D. Kaplan, "Porosity of 3D Biomaterial Scaffolds and Osteogenesis," *Biomaterials* 26, no. 27 (2005): 5474–5491, https://doi.org/10.1016/j.biomaterials.2005.02.002.

234. C. S. Rodrigo-Vázquez, N. Kamboj, M. Aghayan, et al., "Manufacturing of Silicon – Bioactive Glass Scaffolds by Selective Laser Melting for Bone Tissue Engineering," *Ceramics International* 46, no. 17 (2020): 26936–26944, https://doi.org/10.1016/j.ceramint.2020.07.171.

235. D. Svyetlichnyy, "Simulation of the Selective Laser Sintering/Melting Process of Bioactive Glass 45S5," *Simulation Modelling Practice and Theory* 136 (2024): 103009.

236. Y. Yin, Q. Huang, L. Liang, et al., "In Vitro Degradation Behavior and Cytocompatibility of ZK30/Bioactive Glass Composites Fabricated by Selective Laser Melting for Biomedical Applications," *Journal of Alloys and Compounds* 785 (2019): 38–45, https://doi.org/10.1016/j.jallcom.2019.01.165.

237. R. Comesaña Piñeiro, "Application of Rapid Prototyping Based on Laser Cladding to the Production of Bone Functional Implants," in *Department of Applied Physics* (University of Vigo, 2010).

238. R. Comesaña, F. Lusquiños, J. del Val, et al., "Three-Dimensional Bioactive Glass Implants Fabricated by Rapid Prototyping Based on CO_2 Laser Cladding," *Acta Biomaterialia* 7, no. 9 (2011): 3476–3487, https://doi.org/10.1016/j.actbio.2011.05.023.

239. R. Comesaña, F. Lusquiños, J. del Val, et al., "Toward Smart Implant Synthesis: Bonding Bioceramics of Different Resorbability to Match Bone Growth Rates," *Scientific Reports* 5, no. 1 (2015): 10677, https://doi.org/10.1038/srep10677.

240. J. del Val, R. López-Cancelos, A. Riveiro, et al., "On the Fabrication of Bioactive Glass Implants for Bone Regeneration by Laser Assisted Rapid Prototyping Based on Laser Cladding," *Ceramics International* 42, no. 1 (2016): 2021–2035, https://doi.org/10.1016/j.ceramint.2015.10.009.

241. F. Quintero, A. B. Mann, J. Pou, F. Lusquiños, and A. Riveiro, "Rapid Production of Ultralong Amorphous Ceramic Nanofibers by Laser Spinning," *Applied Physics Letters* 90, no. 15 (2007): 153109.

242. F. Quintero, J. Pou, F. Lusquiños, and A. Riveiro, "Experimental Analysis of the Production of Micro- and Nanofibres by Laser Spinning," *Applied Surface Science* 254, no. 4 (2007): 1042–1047, https://doi.org/10.1016/j.apsusc.2007.07.190.

243. F. Quintero, O. Dieste, J. Pou, F. Lusquiños, and A. Riveiro, "On the Conditions to Produce Micro-and Nanofibres by Laser Spinning," *Journal of Physics D: Applied Physics* 42, no. 6 (2009): 065501, https://doi.org/10.1088/0022-3727/42/6/065501.

244. O. Dieste, F. Quintero, J. Pou, F. Lusquiños, and A. Riveiro, "Influence of the Working Conditions on Nanofiber Diameters Obtained by Laser Spinning," *Applied Physics A* 104, no. 4 (2011): 1217–1222, https://doi.org/10.1007/s00339-011-6415-z.

245. F. Quintero, Ó. Dieste, J. Penide, F. Lusquiños, A. Riveiro, and J. Pou, "Nonconventional Production of Glass Nanofibers by Laser Spinning," *Journal of the American Ceramic Society* 97, no. 10 (2014): 3116–3121, https://doi.org/10.1111/jace.13127.

246. F. Quintero, R. Comesaña, F. Lusquiños et al., "Nanofibers of Phosphate Based Bioactive Glass by Laser Spinning," paper presented at *25th European Conference on Biomaterials—Annual Conference of the European Society for Biomaterials, ESB 2013*, Madrid, Spain, September 8–12 (2013).

247. M. M. Echezarreta-López, T. De Miguel, F. Quintero, J. Pou, and M. Landin, "Antibacterial Properties of Laser Spinning Glass Nanofibers," *International Journal of Pharmaceutics* 477, no. 1-2 (2014): 113–121, https://doi.org/10.1016/j.ijpharm.2014.09.050.

248. L. Esteban-Tejeda, B. Cabal, R. Torrecillas, et al., "Antimicrobial Activity of Submicron Glass Fibres Incorporated as a Filler to a Dental Sealer," *Biomedical Materials* 11, no. 4 (2016): 045014.

249. M. M. Echezarreta-López, T. de Miguel, F. Quintero, J. Pou, and M. Landín, "Fabrication of Zn-Sr–Doped Laser-Spinning Glass Nanofibers with Antibacterial Properties," *Journal of Biomaterials Applications* 31, no. 6 (2017): 819–831, https://doi.org/10.1177/0885328216684652.

250. A. Riveiro, F. Quintero, J. del Val, R. Comesaña, F. Lusquiños, and J. Pou, "Laser Spinning of 13–93 Bioactive Glass Nanofibers," paper presented at MS and T 2019 – Materials Science and Technology 2019, Portland, Oregon, USA, September 29–October 3, (2019).

251. A. K. Solanki, H. Autefage, A. R. Rodriguez, et al., "Cobalt Containing Glass Fibres and Their Synergistic Effect on the HIF-1 Pathway for Wound Healing Applications," *Frontiers in Bioengineering and Biotechnology* 11 (2023): 1125060.

252. L. Gao, Q. Zhang, and M. Gu, "Femtosecond Laser Micro/Nano Processing: From Fundamental to Applications," *International Journal of Extreme Manufacturing* 7, no. 2 (2024): 022010, https://doi.org/10.1088/2631-7990/ad943e.

253. J. Feng, J. Wang, H. Liu, et al., "A Review of an Investigation of the Ultrafast Laser Processing of Brittle and Hard Materials," *Materials* 17, no. 15 (2024): 3657, https://doi.org/10.3390/ma17153657.

21922659, 2026, 20, Downloaded from https://advanced.onlinelibrary.wiley.com/doi/10.1002/adhm.202503610 by Julian Jones - Cochraneltalia , Wiley Online Library on [06/08/2026]. See the Terms and Conditions (https://onlinelibrary.wiley.com/terms-and-conditions) on Wiley Online Library for rules of use; OA articles are governed by the applicable Creative Commons License

254. M. Lancry, B. Poumellec, J. Canning, K. Cook, J.-C. Poulin, and F. Brisset, "Ultrafast Nanoporous Silica Formation Driven by Femtosecond Laser Irradiation," *Laser & Photonics Reviews* 7, no. 6 (2013): 953–962, https://doi.org/10.1002/lpor.201300043.

255. Q. Xie, N. Shchedrina, M. Cavillon, B. Poumellec, and M. Lancry, "Nanoscale Investigations of Femtosecond Laser Induced Nanogratings in Optical Glasses," *Nanoscale Advances* 6, no. 2 (2024): 489–498, https://doi.org/10.1039/D3NA00748K.

256. S. Weng, X. Kuang, Q. Zhang, et al., "4D Printing of Glass Fiber-Regulated Shape Shifting Structures with High Stiffness," *ACS Applied Materials & Interfaces* 13, no. 11 (2021): 12797–12804, https://doi.org/10.1021/acsami.0c18988.

257. J. Bonse, S. V. Kirner, and J. Krüger, "Laser-Induced Periodic Surface Structures (LIPSS)," in *Handbook of Laser Micro- and Nano-Engineering*, ed. K. Sugioka (Springer Nature, 2021): 879–936, https://doi.org/10.1007/978-3-030-63647-0.

258. D. Fabris, A. F. Lasagni, M. C. Fredel, and B. Henriques, "Direct Laser Interference Patterning of Bioceramics: A Short Review," *Ceramics* 2, no. 4 (2019): 578–586, https://doi.org/10.3390/ceramics2040045.

259. C. Xin, Z. Li, L. Hao, and Y. Li, "A Comprehensive Review on Additive Manufacturing of Glass: Recent Progress and Future Outlook," *Materials & Design* 227 (2023): 111736, https://doi.org/10.1016/j.matdes.2023.111736.

260. M. Lang, X. Ruan, G. Chen, C. He, R. Hu, and Y. Cheng, "Numerical Analysis of the Temperature Field during Single-Pass Two-Layers Laser Additive Manufacturing of Fused Silica Glass," *Journal of Physics: Conference Series* 2174, no. 1 (2022): 012017.

261. M. Murthi and J. F. Destino, "Sol-Gel Technologies for Additive Manufacturing Glass Materials," *Journal of Sol-Gel Science and Technology* 116 (2025): 2257–2271.

262. P. Lopez-Iscoa, N. Ojha, D. Pugliese, et al., "Design, Processing, and Characterization of an Optical Core-Bioactive Clad Phosphate Fiber for Biomedical Applications," *Journal of the American Ceramic Society* 102, no. 11 (2019): 6882–6892, https://doi.org/10.1111/jace.16553.

263. G. Keiser, F. Xiong, Y. Cui, and P. P. Shum, "Review of Diverse Optical Fibers Used in Biomedical Research and Clinical Practice," *Journal of Biomedical Optics* 19, no. 8 (2014): 080902, https://doi.org/10.1117/1.JBO.19.8.080902.

264. K. Hiromatsu, D. Hwang, and C. Grigoropoulos, "Active Glass Nanoparticles by Ultrafast Laser Pulses," *Micro & Nano Letters* 3, no. 4 (2008): 121–124, https://doi.org/10.1049/mnl:20080028.

265. H. Zeng, X.-W. Du, S. C. Singh, et al., "Nanomaterials via Laser Ablation/Irradiation in Liquid: A Review," *Advanced Functional Materials* 22, no. 7 (2012): 1333–1353, https://doi.org/10.1002/adfm.201102295.

266. N. Semaltianos, "Nanoparticles by Laser Ablation," *Critical Reviews in Solid State and Materials Sciences* 35, no. 2 (2010): 105–124, https://doi.org/10.1080/10408431003788233.

267. S. I. Dolgaev, A. V. Simakin, V. V. Voronov, G. A. Shafeev, and F. Bozon-Verduraz, "Nanoparticles Produced by Laser Ablation of Solids in Liquid Environment," *Applied Surface Science* 186, no. 1-4 (2002): 546–551, https://doi.org/10.1016/S0169-4332(01)00634-1.

268. A. Shearer, M. Montazerian, J. J. Sly, R. G. Hill, and J. C. Mauro, "Trends and Perspectives on the Commercialization of Bioactive Glasses," *Acta Biomaterialia* 160 (2023): 14–31, https://doi.org/10.1016/j.actbio.2023.02.020.

269. C. S. Bagga, S. B. Jung, and H. W. Bae, *Bioactive Porous Composite Bone Graft implants*, EP2968658B1 (Prosidyan. Inc, 2021).

270. V. G. Varanasi, A. Ilyas, P. R. Kramer, and T. Azimaie, "In Vivo Live 3d Printing of Regenerative Bone Healing Scaffolds for Rapid Fracture Healing," in *The Texas A&M University System*, US20170143831A1 (2017).

271. J. Martinez Fernandez, "Biocompatible Material," in *Universidad de Sevilla*, EP1609441A1 (Universidade de Vigo, 2005).

272. N. S. AboElsaad, M. Soory, L. M. A. Gadalla, et al., "Effect of Soft Laser and Bioactive Glass on Bone Regeneration in the Treatment of Infrabony Defects (a clinical study)," *Lasers in Medical Science* 24, no. 3 (2009): 387–395, https://doi.org/10.1007/s10103-008-0576-9.

273. N. S. AboElsaad, M. Soory, L. M. A. Gadalla, et al., "Effect of Soft Laser and Bioactive Glass on Bone Regeneration in the Treatment of Bone Defects (an experimental study)," *Lasers in Medical Science* 24, no. 4 (2009): 527–533, https://doi.org/10.1007/s10103-008-0590-y.

21922659, 2026, 20, Downloaded from https://advanced.onlinelibrary.wiley.com/doi/10.1002/adhm.202503610 by Julian Jones - Cochraneitalia , Wiley Online Library on [06/08/2026]. See the Terms and Conditions (https://onlinelibrary.wiley.com/terms-and-conditions) on Wiley Online Library for rules of use; OA articles are governed by the applicable Creative Commons License